*Journal of the Mississippi*
# Academy of Sciences

Volume 69, Numbers 2-3

April/July, 2024

Journal of the Mississippi Academy of Sciences
ISSN 0076-9436

**Editorial policy**:
**General**. The Editorial Board publishes articles on all aspects of science that are of general interest to the Mississippi scientific community. General articles include short reviews of general interest, reports of recent advances in a particular area of science, current events of interest to researchers and science educators, etc. Research papers of sufficiently broad scope to be of interest to many Academy members are also considered. Articles of particular interest in Mississippi are especially encouraged. Research papers are reports of original research. Descriptions of laboratory or field exercises suitable for high school or college teaching laboratories are accepted. Brief communications not exceeding two pages are accepted. Submission of any manuscript implies that the paper has not been published and is not being considered for publication elsewhere.
**Copyright**. Copyright protection is secured automatically for contributing authors through publication of this journal. The Board of the Mississippi Academy of Sciences recognizes ownership of this published material belongs solely to the author(s) of individual articles.
**Review**. All papers submitted for publication will be peer-reviewed. You are encouraged to have one or more of your colleagues review the manuscript before submitting it for formal review.
**Proofs and reprints**. When a manuscript is accepted for publication the author of correspondence will receive a PDF file in lieu of reprints.
**Page charges**. Authors or their institutions must pay a charge of $150.00 for manuscript. For individuals that can not pay for their manuscript please let us know in advance and we will work to help to find a sponsor.
**Letters policy**. We welcome reader's opinions and comments about the journal and about science in general. Send you letters to the editor. Include full name, address, and daytime telephone number. Letters may be edited.

All correspondence concerning publication should be directed to:

Dr. Michelle Tucci
Mississippi Academy of Sciences
Post Office Box 55907
Jackson, MS 39296-5907

msacademyofscience@gmail.com
601-760-0073

**Administrative policy:**
**Membership**. Membership is open to anyone interested in science in Mississippi. The basic annual membership fee is $50; students may join for $20. Information about other membership categories is available through the MAS office.
**Advertising**. The Journal of the Mississippi Academy of Sciences accepts paid advertising. Contact the editor or the MAS Office for current rates.

Direct correspondence concerning administration of the Mississippi Academy of Sciences and its journal to:

Dr. Michelle Tucci
Mississippi Academy of Sciences
Post Office Box 55907
Jackson, MS 39296-5907

msacademyofscience@gmail.com
601-760-0073
The Mississippi Academy of Sciences operates a web site: http://www.msacad.org/

Saskatoon, Canadian province of Saskatchewan
City of Bridges, The picture was taken on the bridge overlooking the river in River Park close to the University of Saskatchewan
Picture was taken on June 6, 2024.
Photographed by M. Tucci

# Journal of the Mississippi Academy of Sciences

Volume 69 April-July Number 2-3



*The Journal of the Mississippi Academy of Sciences* (ISSN 0076-9436) is published in January (annual meeting abstracts), April, July, and October, by the Mississippi Academy of Sciences. Members of the Academy receive the journal as part of their regular (nonstudent) membership. Inquiries regarding subscriptions, availability of back issues, and address changes should be addressed to The Mississippi Academy of Sciences, Post Office Box 55709, Jackson, MS 39296-5709, telephone 601-977-0627, or email msacademyofscience@comcast.net.

# TABLE OF CONTENTS

# OUTSTANDING STUDENT AWARD WINNER

## Gut Microbiome Shifts Exacerbated by High-Fat Diet Consumption in a Juvenile Rat

**Allie M. Smith, Lavanya Challagundla, Ian G. McGee, Zyra J. Warfield, Christiano Dos Santos E. Santos, Michael R. Garrett, Bernadette E. Grayson**

University of Mississippi Medical Center, Jackson, MS

**Corresponding Author:** Bernadette E. Grayson, Ph.D
**Email:** Bgrayson@umc.edu
Published in Physiol Genomics 2024 Apr 1;56(4):301-316.
**doi:** 10.1152/physiolgenomics.00113.2023

## ABSTRACT

The gut-brain axis interconnects the central nervous system (CNS) and the commensal bacteria of the gastrointestinal tract. The composition of the diet consumed by the host influences the richness of the microbial populations. Traumatic brain injury (TBI) produces profound neurocognitive damage, but it is unknown how diet influences the microbiome following TBI. The present work investigates the impact of a chow diet versus a 60% fat diet (HFD) on fecal microbiome populations in juvenile rats following TBI. Twenty-day-old male rats were placed on one of two diets for 9 days before sustaining either a Sham or TBI via the Closed Head Injury Model of Engineered Rotational Acceleration (CHIMERA). Fecal samples were collected at both 1- and 9-days postinjury. Animals were cognitively assessed in the novel object recognition tests at 8 days postinjury. Fecal microbiota DNA was isolated and sequenced. Twenty days of HFD feeding did not alter body weight, but fat mass was elevated in HFD compared with Chow rats. TBI animals had a greater percentage of entries to the novel object quadrant than Sham counterparts, $P < 0.05$. The Firmicutes/Bacteroidetes ratio was significantly higher in TBI than in the Sham, $P < 0.05$. Microbiota of the Firmicutes lineage exhibited perturbations by both injury and diet that were sustained at both time points. Linear regression analyses were performed to associate bacteria with metabolic and neurocognitive endpoints. For example, counts of Lachnospiraceae were negatively associated with percent entries into the novel object quadrant. Taken together, these data suggest that both diet and injury produce robust shifts in microbiota, which may have long-term implications for chronic health.NEW & NOTEWORTHY Traumatic brain injury (TBI) produces memory and learning difficulties. Diet profoundly influences the populations of gut microbiota. Following traumatic brain injury in a pediatric model consuming either a healthy or high-fat diet (HFD), significant shifts in bacterial populations occur, of which, some are associated with diet, whereas others are associated with neurocognitive performance. More work is needed to determine whether these microbes can therapeutically improve learning following trauma to the brain.

**KEYWORDS:** adrenocorticotropic hormone; corticosterone; stress; traumatic brain injury

Full Article can be found at the following doi link: Published in Physiol Genomics 2024 Apr 1;56(4):301-316. **doi:** 10.1152/physiolgenomics.00113.2023

# Melatonin Agonist Agomelatine Ameliorates Lipopolysaccharide-Induced Brain Injury, Inflammation, Lipid Peroxidation, and Pre-Social Interaction Impairments in Neonatal Rats

**Rachel T Palmer[1], Jonathan W Lee[1], Selby A Ireland[1], Madison Klim[1], Nilesh Dankhara[1], Michelle A Tucci[2], Norma B Ojeda[3], Mary A Kosek[1], Shuying Lin[4], Lu-Tai Tien[5], Lir-Wan Fan[1]**

[1]Department of Pediatrics, Division of Newborn Medicine, University of Mississippi Medical Center, Jackson, MS 39216, USA, [2] Department of Anesthesiology, University of Mississippi Medical Center, Jackson, MS 39216, USA, [3]Department of Advanced Biomedical Education, University of Mississippi Medical Center, Jackson, MS 39216, USA,[4]Department of Physical Therapy, University of Mississippi Medical Center, Jackson, MS 39216, USA, [5]School of Medicine, Fu Jen Catholic University, Xinzhuang Dist New Taipei City 24205, Taiwan

**Address of Corresponding Author:** Lir-Wan Fan, PhD
**Email:** lwfan@umc.edu
**Doi:** 10.34107/CTJP1687

## ABSTRACT

Inflammation and oxidative stress play important roles in brain injury in neonatal human and animal models. Our previous studies showed that systemic administration of endotoxin lipopolysaccharide (LPS) induces brain damage and neurobehavioral dysfunction in neonatal rats, which is associated with producing pro-inflammatory cytokines and oxidative stress. Recent studies suggest that agomelatine treatment could be a neuroprotective agent in adult animals by reducing inflammation and microglia polarization. The objective of the current study was to determine whether agomelatine, a melatonergic agonist with anti-inflammatory and antioxidative effects, ameliorates LPS-induced brain inflammation and neurobehavioral dysfunction in neonatal rats. Intraperitoneal (i.p.) injections of LPS (2 mg/kg) were administered in postnatal day 5 (P5) Sprague Dawley rat pups, and agomelatine (20 mg/kg) or vehicle was administered (i.p.) 5 min after LPS injection. Control rats were injected (i.p.) with sterile saline. Neurobehavioral tests were performed, and brain inflammation was examined on P6 24 hours after LPS exposure. Our results showed that agomelatine reduced LPS-induced reduction in pre- social interaction (ultrasonic vocalization) and sensorimotor disturbances at P6. Agomelatine also reduced LPS-induced brain injury, including a reduction in white matter oligodendrocyte numbers, increases in microglia numbers, and an increase in levels of IL-1β and thiobarbituric acid reactive substances (TBARS) contents, suggesting anti-inflammatory and antioxidative effects. These results indicate that agomelatine may protect against systemic LPS exposure- induced brain injury, inflammation, lipid peroxidation, and neurobehavioral disturbances, and that the protective effects are associated with its ability to attenuate LPS-induced inflammation and oxidative stress.

**KEY WORDS:** Lipopolysaccharide, Agomelatine, Brain inflammation, Lipid peroxidation, Pre- social interaction impairments, Interleukin-1β

## INTRODUCTION

Increasing evidence has shown that neonatal or perinatal inflammation and hypoxia- ischemia contributes to the development of periventricular leukomalacia (PVL), a white matter disease of premature infants, and eventual impaired neurodevelopmental outcomes (Harden et al., 1996; Rezaie and Dean, 2002; Falahati et al, 2015; Lee, 2017). With these neurodevelopmental outcomes comes an increased risk for developing disorders such as Attention-deficit/hyperactivity disorder (ADHD) (Taylor and O'Shea, 2022). Discovering treatments of the underlying inflammatory processes is paramount to the prevention of these disorders that extend well into adulthood.

In previous studies, we found that intracerebral and systemic injection of lipopolysaccharide (LPS) endotoxin in neonatal P5 rats caused an influx of pro-inflammatory cytokines and resulted in brain inflammation and white matter and neuronal injury (Cai et al., 2013; Fan et al, 2008; Wong et al., 2014; Yeh et al., 2021). Following LPS injection, there was increased oxidative and nitrosative stress and the inflammation that ensued became another source of reactive oxygen and nitrogen species (ROS/RNS) (Fan et al., 2008). Prior studies have shown that oxidative/nitrosative injury to premyelinated oligodendrocytes (OLs) is present in infants with PVL (Haynes et al, 2003). Neonatal rats that were injected with LPS were found to have acute and long-term deficits including decreased social interaction and impairments of acoustic startle, object recognition, and spatial learning (Barhoornori et al, 2012).

Melatonin treatment was found to decrease these effects, including decreased oxidative stress, decreased proinflammatory cytokines and microglial activation, with improved behavior findings (both acute and long-term) (Brzozowska et al., 2009; Wong et al., 2014). Agomelatine is a potent melatonin receptor agonist (MT1/MT2) and moderate affinity serotonin receptor antagonist (5-HT2B, 5-HT2C), used in current antidepressant therapy (Guardiola-Lemaitre et al., 2014) in Australia and across Europe. There is current interest in FDA approval for agomelatine in the United States. In our present study, we used agomelatine treatment to assess the reduction of LPS-induced brain damage and inflammation and behavioral disturbances in the neonatal rat.

## MATERIAL AND METHODS

*Chemicals:* Unless otherwise stated, all chemicals used in this study were purchased from Sigma (St. Louis, MO., USA). Monoclonal mouse antibodies against O4 and adenomatous polyposis coli (clone CC1, APC-CC1), and polyclonal rabbit antibodies against oligodendrocyte transcription factor 2 (Olig2) were purchased from Millipore (Billerica, MA, USA). Polyclonal rabbit antibodies against ionized calcium-binding adapter molecule 1 (Iba1) were obtained from Wako Chemicals USA (Irvine, CA, USA). Enzyme-linked immunosorbent assay (ELISA) kits for immunoassays of rat IL-1□ were purchased from R&D Systems (Minneapolis, MN, USA).

*Animals*

Timed pregnant Sprague-Dawley rats were delivered to the laboratory on day 19 of gestation where they were maintained in a room with a 12-h light/dark cycle at constant temperature (22 ± 2°C). Day of birth for the rat pups was defined as postnatal day 0. After birth, the litter size was adjusted to twelve pups per litter to minimize the effect of litter size on body weight and brain size. All procedures for animal care were conducted in accordance with the National Institutes of Health Guide for the Care and Use of Laboratory Animals and were approved by the Institutional Animal Care and Use Committee at the University of Mississippi Medical Center or Fu Jen Catholic University. Every effort was made to minimize the number of animals used and their suffering.

*Animal Treatment :*A total of 64 rats from eight litters were used in the present study. One pup from each litter was assigned to each group to obtain an n number of eight for each group while maintaining a male to female ratio of 1:1 in each group (8 males and 8 females). Pups were randomly divided into four groups: Saline+Vehicle; Saline+Agomelatine; LPS+Vehicle; LPS+Agomelatine. An intraperitoneal (i.p.) injection of LPS (2 mg/kg, from *Escherichia coli*, serotype 055:B5) was administered to 5-day-old (P5) Sprague–Dawley rat pups of both sexes. The control rats were injected with the same volume of sterile saline (0.1 mL). All animals survived the injection. Both LPS- and saline-injected animals were further divided into two groups: one received i.p. injections of a dose of 20 mg/kg agomelatine dissolved in PBS and the other received the vehicle.

*Behavioral Testing :*Behavioral tests were performed as described previously with modifications (Kaizaki et al, 2013; Fan et al, 2013; Yeh et al, 2021). The developmental test battery was based on previously well-established tests for neurobehavioral toxicity (Altman and Sudarshan, 1975; Hermans et al, 1992). Righting reflex tests, negative geotaxis, hind-limb suspension, wire-hanging maneuver, tail-flick test, and von Frey filament test, were performed on all rat pups at P6 to observe indicators of neurological function at early developmental stages. Pre-social

interaction was determined by isolation-induced ultrasonic vocalization test on P6. Body weights of rats were also recorded on P6. All animals were tested in the same order.

*Pre-social interaction (Isolation-induced ultrasonic vocalization),* this test is used to determine prosocial behavior (Baharnoori et al., 2012; Boulanger-Bertolus and Mouly, 2021; Kirsten et al., 2012). Individual pups were gently lowered into the glass beakers within the testing chambers making sure not to roll them. Pups were recorded for 300 seconds and then placed in a clean cage with littermates that were run simultaneously. Alternatively, in the maternal potentiation paradigm after the first 300 seconds of ultrasonic vocalization (USV) recording, pups were then returned to the home cage with littermates and dam for 300 seconds, and then recorded for a second 300 seconds.

*Righting reflex,* used as a test for muscle strength and subcortical maturation (Altman and Sudarshan, 1975; Yeh et al, 2021). Pups are placed on their backs and the time required to roll back onto all four feet touching the platform is measured. Every P6 pup is given three trials and the time for rollover is recorded. The cut off time is 60 seconds.

*Negative geotaxis,* test used for reflex development, vestibular labyrinth, motor skills and cerebellar integration (Altman and Sudarshan, 1975; Yeh et al, 2021). Rats are initially placed on a 15 degree incline head down and should naturally turn around and crawl upwards. Each P6 pup is given three trials and the time required to turn 180 degrees and crawl upward is recorded. 60 seconds was the cut off time for each trial.

*Wire hanging maneuver,* tests neuromuscular and locomotor development (Altman and Sudarshan, 1975; Yeh et al, 2021). A horizontal rod (35cm long, 5x5 mm2 in cross-sectional area between two 50 cm high poles) is suspended over an open space and the suspension latency is recorded. Falls are protected by placing a sawdust base underneath the pups while testing. The pup should support themselves with their hind limbs to prevent falling and aid in their advance down the horizontal rod. Each P6 pup is given three trials and the cut off time to is 120 seconds.

*Hind-limb suspension test,* used to monitor and record proximal hind-limb strength, fatigue and weakness in neonatal rats (Garrett-Cox et al, 2003). A plastic cylinder (4cm internal diameter, 16cm height) is placed vertically on a flat surface and rat pups are positioned with hind limbs suspended by the lip of the container and heads down. Falls are protected by cotton placed at the bottom of the container. Each P6 pup is given three trials and suspension latencies are recorded. During each trial, the cut off time is 120 seconds.

*von Frey Filaments Test,* this test assesses the mechanical nociception (cutaneous mechanical sensitivity) of rats. Each rat was placed individually inside an elevated acrylic box with a wire mesh floor (Dynamic Plantar Anesthesiometer, UGO BASILE, Italy) and was allotted 5 min to acclimatize to the new environment. Mechanical thresholds for flexion withdrawal reflexes in response to punctuate mechanical stimulation of the plantar surface of the rat's hind paw was tested using von Frey filaments that exert a reproducible stimulus strength in grams ranging from 0.236 to 0.384 mm in diameter with marking forces of 0.02–0.60 g. Response threshold is defined as the von Frey filament which produces reflex paw withdrawal in three out of five applications (Hsieh et al., 2020). Filaments were applied to the plantar surface of one hind paw five times at 10 s intervals alternately, and five times at 10 s intervals alternately to the other hind paw after 3 min of rest.

*Tail-flick test,* the test uses an infrared source to assess the thermal nociceptive threshold in rats. The tail-flick test was performed as described by our previous study with modifications at 24 h after LPS injection (Hsieh et al., 2020). Rats were first habituated to experimenter handling and to being placed into a plastic cylindrical tube. A shallow groove in the Plexiglas plate immobilized the rat's tail during the trials of tests. Half of the rat's tail from the tip to the base of tail was placed under radiant heat (Analgesia Test Tail-Flick Type 812, Columbus Instruments, Columbus, OH, USA). Pain sensitivity was measured by tail flick latency defined as the time from the onset of radiant heat to tail withdrawal. A mandatory cut-off time of 10 s was set to prevent thermal injury to the rats. Tail-flick latency was then calculated as the average of 3 tail- flick latencies.

*Measurement of Lipid Peroxidation:* Lipid

peroxidation was determined in brain samples by measuring malondialdehyde (MDA) levels as thiobarbituric acid-reactive substances (TBARS) (Wong et al, 2014; Hsieh et al, 2020; Rosa et al, 2015). Brain tissues were homogenized in cell extraction buffer (~5 mg/200 µl) containing 2 µl of 5% butylated hydroxytoluene (BHT) on ice, and precipitated proteins were removed by centrifugation at 12,000× *g* for 10 minutes. 200 µl of brain supernatant were mixed with 300 µl 20% trichloroacetic acid (TCA) and incubated for 1 minute. Then 300 µl 0.67% thiobarbituric acid (TBA) was added to the mixture. The reaction was heated to 100 oC for 60 minutes. After cooling, the mixture was centrifuged at 12,000× *g* for 10 minutes, and the absorbance of the supernatant was determined. The number of resulting pink-stained TBARS were determined spectrophotometrically at 532 nm in a 96-well plate reader (µQuant, Bio-Tek instruments Inc., VT, USA). A calibration curve was generated using 1,1,3,3- tetramethoxypropane (malondialdehyde, MDA, ACROS Organic) as the standard, which was subjected to the same treatment as the samples. The results were expressed as nanomoles of TBARS (MDA equivalents) per milligram of protein (nmol MDA / mg protein).

*Determination of IL-1β and COX-2 protein levels by ELISA:* Protein expression of IL-1β in the P6 rat brain and spinal cord was determined by ELISA kits as described previously (Hsieh et al., 2020; Yeh et al. 2021). Brain and spinal cord tissues from each pup were collected 24 h after LPS injection. Tissues were homogenized by sonication in 1 mL ice-cold PBS (pH 7.2) and centrifuged at 12,000 × *g* for 20 min at 4 oC. The supernatant was collected, and the protein concentration was determined by the Bradford method. ELISA was performed according to the manufacturer's instructions, and data were acquired using a 96- well plate reader (Bio-Tek Instruments, Inc., VT, USA). The IL-1□ contents were expressed as picogram of cytokines per milligram of protein.

*Immunohistochemistry:* Brain injury was estimated based on the results of immunohistochemistry in consecutive brain sections prepared from rats sacrificed 1 day (P6) after LPS injection (P5) (Yeh et al, 2021). For immunohistochemistry staining, primary antibodies were used with the following dilutions: O4, 1 µg/ml; APC-CC1, 1:200; Olig2, 1:500; or Iba1, 1:500. O4, APC-CC1 and Olig2 were used to detect late, mature oligodendrocyte progenitor cells, and total oligodendrocytes in the white matter, respectively. Microglia were detected using Iba1 immunostaining, which recognizes both the resting and activated microglia. Sections were incubated with primary antibodies at 4°C overnight and further incubated with secondary antibodies conjugated with fluorescent dyes (Alexa Fluor 488, 1:300, or Alexa Fluor 555, 1:500, Invitrogen, Carlsbad, CA, USA) for 1 h in the dark at room temperature. 4', 6-Diamidino-2-phenylindole (DAPI) (100 ng/ml) was used simultaneously to identify nuclei in the final visualization. Sections incubated in the absence of primary antibody were used as negative controls. The resulting sections were examined under a fluorescent microscope (Nikon Ni-E, Melville, NY, USA) at appropriate wavelengths.

*Quantification of Data and Statistics:* Our previous studies indicate that neonatal i.p. LPS injection induces white matter injury primarily in the cingulum of the forebrain (Yeh et al, 2021; Wong et al, 2014; Hsieh et al, 2020; Fan et al, 2013). Therefore, brain sections at the bregma level were used to assess all pathological changes caused by systemic LPS injection. Immunostaining data were quantified by counting positive stained cells. When the cellular boundary was not distinct, numbers of DAPI-stained nuclei from the superimposed images were counted. Three digital microscopic images were randomly captured in each of three brain sections, and the number of positively stained cells in the three images was counted and averaged (cells/mm2). From the three brain sections, the mean value of cells were taken to represent each brain. Results were standardized as the average number of cells/mm2, to ease comparisons among the different groups. In response to an LPS systemic injection, Iba1+ microglia cells increase, and the soma of these cells become larger. Iba1 immunoreactivity was also quantified by calculating the percentage area of the whole image that contains Iba1 immunostaining using NIH software Image J (Fan et al, 2013).

Data from behavioral testing, TBARS, immunostaining, and ELISA assay were presented as the mean±SEM and analyzed by two-way analysis of variance (ANOVA) followed by the Student–Newman–Keuls test. Results with $p<0.05$ were

considered statistically significant.

## RESULTS AND DISCUSSION

*Agomelatine improved LPS-induced body weight reduction:* Body weight was taken at P5 prior to administration as shown in Fig 1A with LPS+Saline or LPS+Agomelatine vs Saline+Vehicle group. Fig 1B shows P6 body weight with significant LPS-induced reduction in the LPS+Vehicle group ($p< 0.05$). Agomelatine treatment significantly reduced the LPS-induced body weight reduction seen in Fig 1B ($p < 0.05$).

*Agomelatine improved LPS-induced neurobehavioral deficits:* Compared with saline, P6 rats that received LPS i.p. injections at P5 showed a marked increase in neurobehavioral deficits (Fig 2-5). The LPS+Agomelatine group showed a significant improvement in neurobehavioral outcomes whencompared to the LPS+vehicle group (Fig 2-5).

*Pre-social interaction (Isolation-induced ultrasonic vocalization),* testing for rates of ultrasonic vocalization (USV) at approximately 40-50 kHz. Rates of USV are higher in P6 pups in response to cold stress (Brunelli et al, 2009). P6 rats that received systemic LPS injection had significant slowing of their USV total duration in isolation and maternal exposure ($p < 0.05$, Fig 2A) and change in duration from isolation to maternal exposure ($p <0.05$, Fig 2B). Agomelatine treatment after LPS injection ameliorated this reduction in USV that was produced by LPS ($p <0.05$, Fig 2A/1B).

*Righting Reflex:* Significant differences were seen in the LPS-injected group compared to the saline control group with longer mean latency times ($p <0.05$, Fig 3A). When treated with agomelatine, there was a marked shortening of the LPS-induced increased righting reflex latency in P6 rats ($p <0.05$, Fig 3A).

*Negative Geotaxis:* Test is used in evaluating reflex development, vestibular labryinth, motor skills and cerebellar integration. In P6 rats, those that were injected at P5 with LPS showed significantly longer mean latency times along a 15 degree incline compared with the control (saline) group ($p < 0.05$, Fig 3B). In the group treated with agomelatine, the latency times were significantly reduced ($p < 0.05$, Fig 3B).

*Wire Hanging Maneuver:* Mean latency times of the P6 group injected with LPS were significantly less than the control group ($p < 0.05$, Fig 4A). Those P6 rats that were treated with agomelatine showed a significant reduction in the LPS-induced reduction of the mean latency time, almost similar to the control group ($p <0.05$, Fig 4A).

*Hind-Limb Suspension:* During this test which evaluates strength, fatigue and weakness in neonatal rats, the LPS-injected group at P6 showed a significant decrease in mean latency times compared to the control group ($p <0.05$, Fig 4B). This was reversed in the agomelatine treated group as shown in Fig 4B ($p <0.05$).

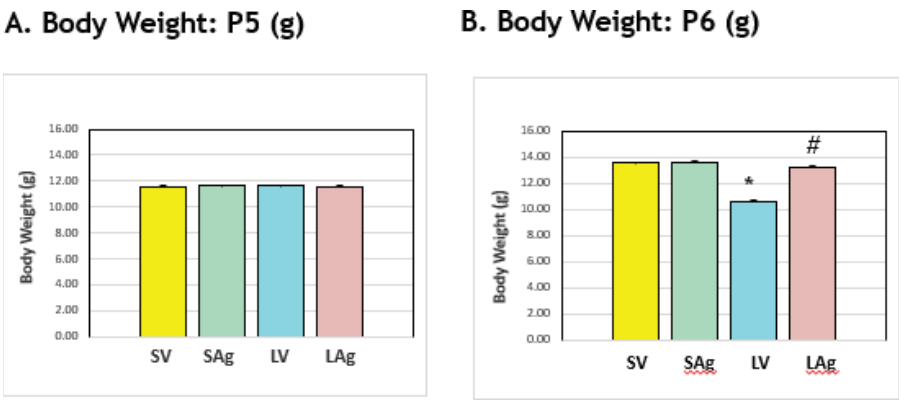


**Figure 1.** Agomelatine reduced LPS-induced reduction of body weight in the P6 rats. *P<0.05, LPS+Vehicle group vs Saline+Vehicle group. # P<0.05, LPS+Agomelatine group vs LPS+Vehicle group. (n = 8M + 8F)

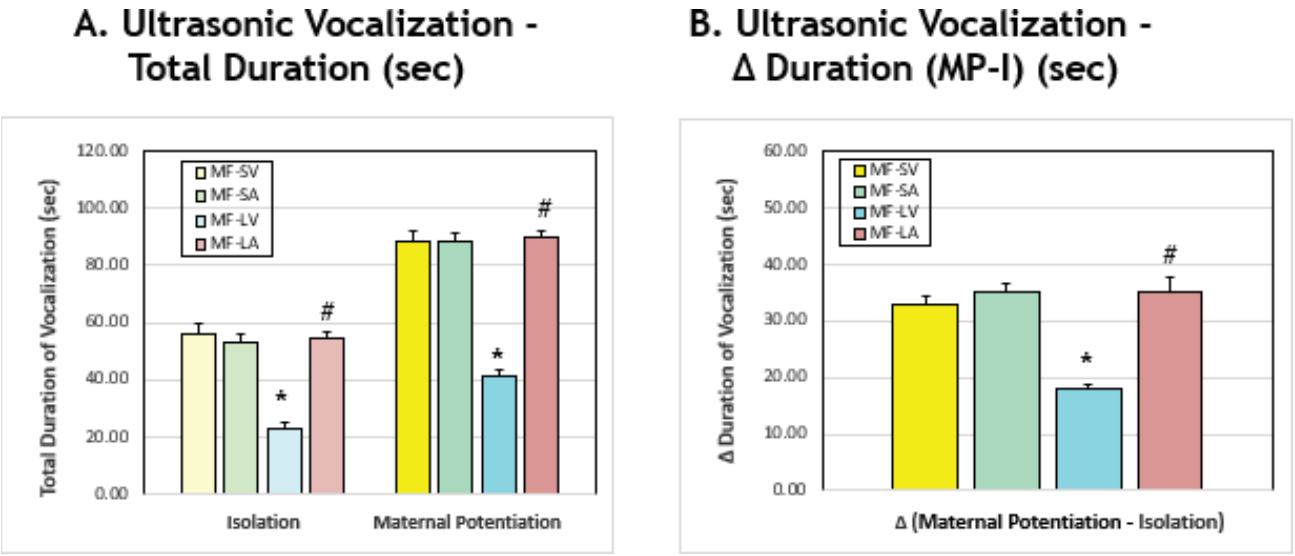


**Figure 2.** Agomelatine reduced systemic LPS-induced reduction in isolation-induced ultrasonic vocalization in (A) total duration of vocalizations (sec), and (B) the differences of total vocalization duration between first and second isolation after 5 min maternal contact in the P6 rat. *P<0.05, LPS+Vehicle group vs Saline+Vehicle group. #P<0.05, LPS+Agomelatine group vs LPS+Vehicle group. (n = 8M + 8F)

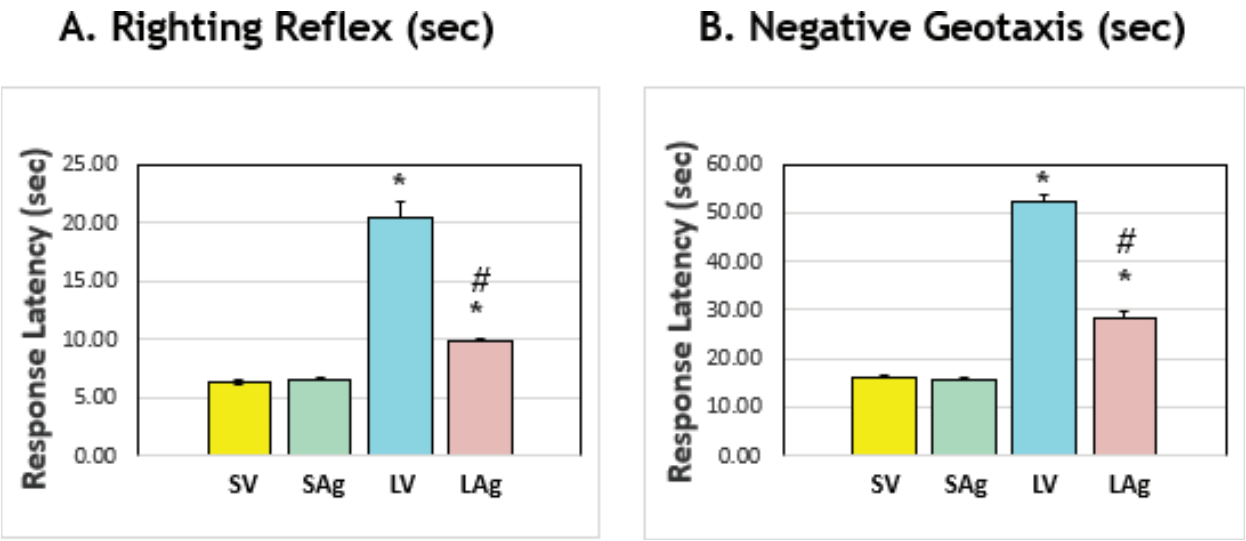


**Figure 3.** Agomelatine reduced systemic LPS-induced elongation of mean latency times in (A) righting reflex, and (B) negative geotaxis in the P6 rat. *P<0.05, LPS+Vehicle or LPS+Agomelatine group vs Saline+Vehicle group. #P<0.05, LPS+Agomelatine group vs LPS+Vehicle group. (n = 8M + 8F)

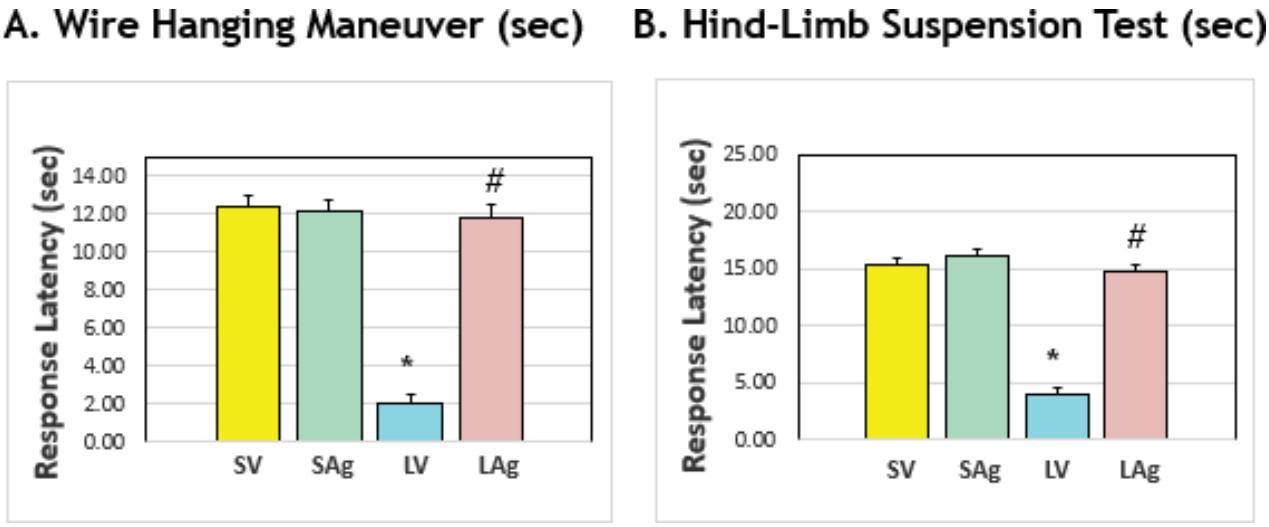


**Figure 4**. Agomelatine reduced systemic LPS-induced reduction of mean latency times in (A) wire hanging maneuver and (B) hind-limb suspension in the P6 rat. *P<0.05, LPS+Vehicle groupvs Saline+Vehicle group. #P<0.05, LPS+Agomelatine group vs LPS+Vehicle group. (n = 8M +8F)

*Von Frey Filament Test:* Test used to evaluate allodynia or nociception response to a "filament" testing the P6 rat's response to having the hind limb stroked with the filament, then recording the reaction. The force of the filament applied to elicit a response was recorded as seen below (Fig 5A). LPS-injected P6 rats showed a significant increased response to light pressure by the filament compared to the control group ($p < 0.05$, Fig 5A). Agomelatine treatment helped significantly to reduce the systemic LPS-induced allodynia ($p < 0.05$, Fig 5A).

*Tail Flick Test:* test is used to monitor hyperalgesia response (held over heat, and their response is measured). LPS injected P6 rats showed significantly decreased response latency ($p<0.05$, Fig 5B). Agomelatine treatment showed significant improvement in latency response times in P6 rats ($p < 0.05$, Fig 5B).

*Agomelatine attenuated LPS-induced loss of oligodendrocytes:* Total oligodendrocytes were evaluated using oligodendrocyte lineage transcription factor 2 (Olig2+) which were seen throughout the white matter in control P6 rats (see Fig 6A-red, 6D). Systemic LPS via i.p. injection was shown to significantly reduce Olig2+ cells throughout the white matter (Fig 6A-red, 6D). Agomelatine treatment did show a reduction in the effect of LPS (Fig 6A-red, 6D).

Mature oligodendrocytes were evaluated by using APC-CC1 antibody and were observed in the cingulum, the white matter subcortical tracts, the internal capsule, and the corpus callosum (Fig 6A-green, 6F). Systemic LPS significantly reduced the number of APC-CC1+ cells ($p< 0.05$, Fig 6F). Agomelatine treatment was shown to significantly reduce LPS's effect on the mature oligodendrocytes with higher levels of APC-CC1+ cells detected (Fig 6F).

In control P6 rat brains, abundant late oligodendrocyte progenitor cells (O4+ staining in cell membranes) were found at the bregma level in the cingulum white matter (see Fig 6E). Systemic LPS injection significantly reduced the number of cells present ($p<0.05$, Fig 6E). Agomelatine treatment showed a significant reduction in this effect by LPS in P6 rats ($p< 0.05$, Fig 6E).

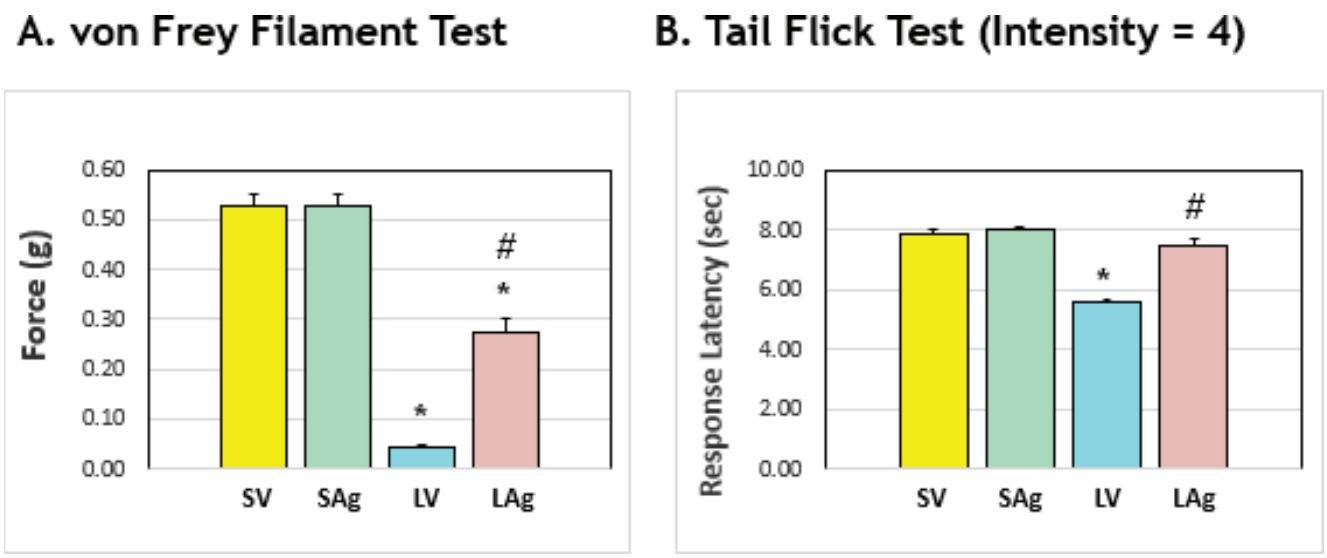


**Figure 5.** Agomelatine reduced systemic LPS-induced (A) allodynia in the von Frey filament test and (B) hyperalgesia in the tail-flick test (intensity = 4) in the P6 rat. *P<0.05, LPS+Vehicle or LPS+Agomelatine group vs Saline+Vehicle group. #P<0.05, LPS+Agomelatine group vs LPS+Vehicle group. (n = 8M + 8F)

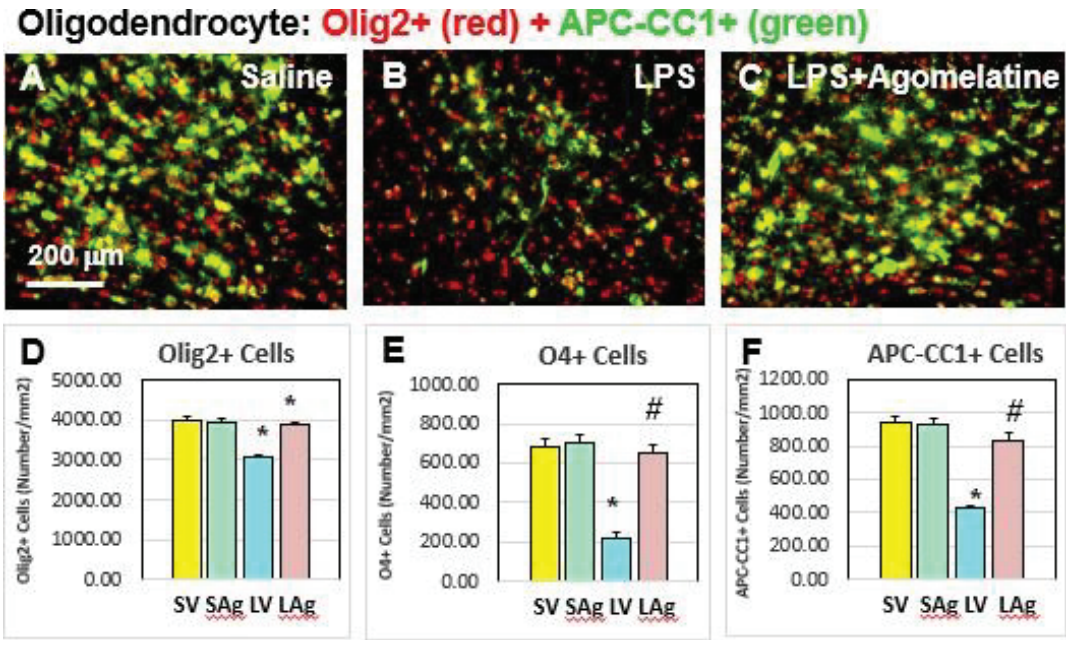


**Figure 6.** Agomelatine attenuated systemic LPS-induced reduction in oligodendrocyte cells in P6 rat brain. A, Saline+Vehicle. B, LPS+Vehicle. C, LPS+Agomelatine. Quantitation of the number of total oligodendrocyte cells (Olig2+, red) (D), oligodendrocyte progenitor cells (O4+/O1-) (E), and mature oligodendrocyte cells (APC-CC1+, green) (F) *P<0.05, LPS+Vehicle or LPS+Agomelatine group vs Saline+Vehicle group. #P<0.05, LPS+Agomelatine group vs LPS+Vehicle group. (n = 4M +4F)

*Agomelatine reduced LPS-induced increases in thiobarbituric acid-reactive substances (TBARS) content:* To investigate the effects of LPS and/or pioglitazone administration on oxidative stress, lipid peroxidation was assessed in brain tissues by measuring thiobarbituric acid-reactive substances (TBARS), as previously established (Wong et al., 2014; Hsieh et al., 2020; Rosa et al., 2015). The levels of TBARS in brain samples from the LPS group were remarkably elevated compared with the control group ($p < 0.05$) twenty-four hours following LPS injection ($p < 0.05$; Fig 7). Agomelatine treatment was shown to reduce LPS-induced increases in the levels of TBARS present in P6 neonatal rats in both the brain and spinal cord ($p<0.05$, Fig 7).

*Agomelatine decreased the LPS-induced increase in microglial activation and inflammatory responses:* In the control group of P6 rats, few microglia are noted by the red immunohistochemical staining of ionized calcium binding adapter molecule 1 (Iba1) (Fig 8A, red, 8D). When given systemic LPS injection, microglia were significantly activated and increased in the cingulum area of the P6 rat brain white matter ($p<0.05$; Figs 8B, D-E). The cells also were larger, with elongated cell bodies, vs the resting, inactive state in the control group. Agomelatine treatment significantly reduced LPS's effects on 1ba1 staining, both the decreased cell concentration and the cells returned to a smaller, resting state compared to the active, larger size with LPS ($p<0.05$, Figs 8C, D-E).

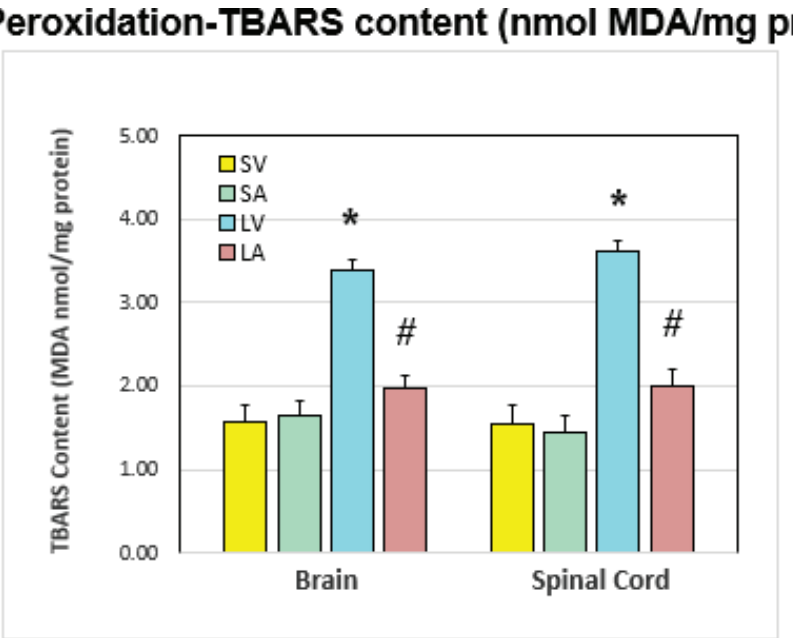


**Figure 7.** Agomelatine reduced systemic LPS-induced increases in thiobarbituric acid-reactive substances (TBARS) content in rat brain and spinal cord 24 h after LPS injection (P6). *P<0.05, LPS+Vehicle group vs Saline+Vehicle group. #P<0.05, LPS+Agomelatine group vs LPS+Vehicle group. (n = 4M +4F)

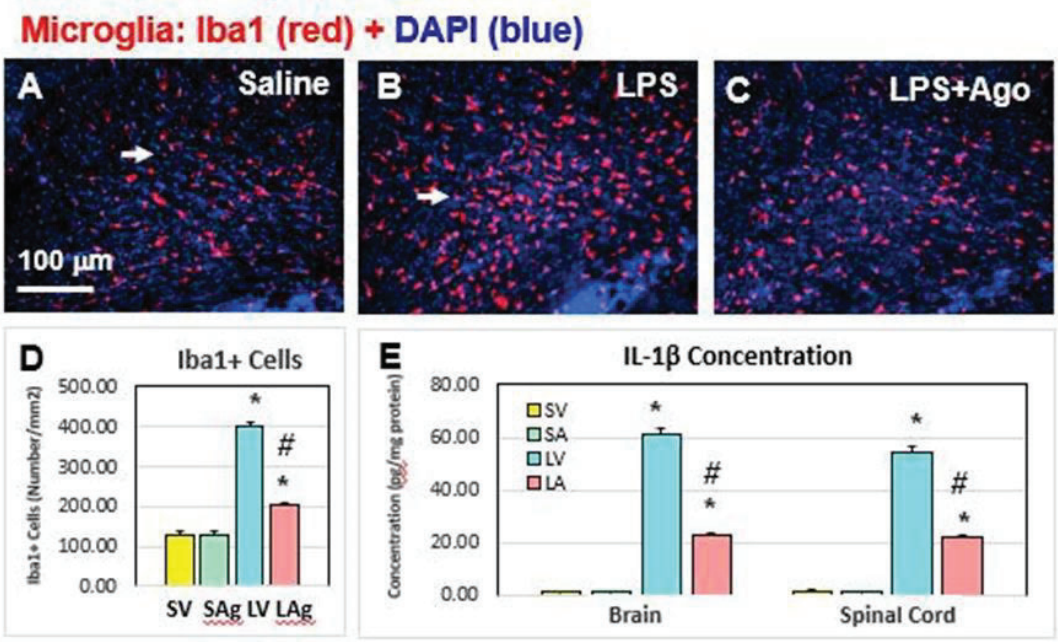


**Figure 8.** Agomelatine attenuated systemic LPS-induced increases in brain microglia (Iba1+ cells, red) (A-C), and inflammatory cytokine IL-1β in the rat brain and spinal cord 24 h after LPS injection (P6). A, Saline+Vehicle. B, LPS+Vehicle. C, LPS+ Agomelatine. Quantitation of the number of Iba1+ cells (D), and the contents of IL-1β (E). *P<0.05, LPS+Vehicle or LPS+Agomelatine group vs Saline+Vehicle group. #P<0.05, LPS+ Agomelatine group vs LPS+Vehicle group. ((n = 4M +4F)

Results from our present study showed that i.p. LPS injection induced systemic oxidative stress and inflammation in neonatal P6 rats, resulting in abnormal neurobehavioral outcomes. Our study was derived from prior melatonin studies, which showed that melatonin treatment significantly decreased LPS-induced brain damage and neurobehavioral disturbances through direct and indirect antioxidant roles by detoxifying reactive oxygen and nitric species (ROS/RNS) and by supporting superoxide dismutase and glutathione peroxidase (Bonnefort-Rousselot and Colin, 2010). Our previous studies with melatonin showed that melatonin decreased the expression of NT and 4-HNE (markers for RNS) in the rat brain and prevented LPS-induced decrease in mitochondrial complex 1 activity in the P6 neonatal rat brain (Wong et al., 2014).

In our present study, we used agomelatine, a potent melatonergic MT1/MT2 receptor agonist and antagonist of serotonergic 5-HT receptors, as its anti-inflammatory and antioxidative actions mimic those of melatonin. In prior studies with agomelatine in adult rats, agomelatine was found to be protective of cerebral ischemic/reperfusion injury by decreasing apoptosis, with decreased Bax and cleaved caspase-3, and significant increase in HO-1 (antioxidative enzyme) and superoxide dismutase (SOD) (Chumboatong et al., 2017). Agomelatine was found to reduce LPS-induced inflammation in adult rats by blocking the NF-kB signaling pathway and ameliorating hyperema, degenerative changes and edema histopathologically (Savran et al., 2020). Also, agomelatine was shown to ameliorate prenatal valproic acid-induced autism spectrum disorder in animal studies (Kumar et al., 2015). Our study results corroborate the previous studies above and expand our knowledge in the premature neonatal population in which inflammation and hypoxemia-ischemia play a critical role in PVL development and neurobehavioral outcomes.

As neonatal rat models with agomelatine are lacking, avenues for continued research are expected given our preliminary data results. Future studies include a plan to expand our studies from P5 to P21, following attention deficit hyperactivity disorder-like behaviors in juvenile rats after LPS injection and agomelatine

treatment as ADHD-like animal models are lacking and further research is ongoing.

## SUMMARY

In summary, our data support previous studies that neonatal systemic LPS exposure in P6 rats produces systemic effects, including decreased body weight, brain inflammation and injury, increases in lipid peroxidation, microglial activation. This results in neurobehavioral disturbances seen in pre-social behavior and strength and reflex testing. Our data collected on treatment with agomelatine following LPS injection show that agomelatine may provide anti- inflammatory and anti-oxidative protection against systemic LPS effects (Figure 9).

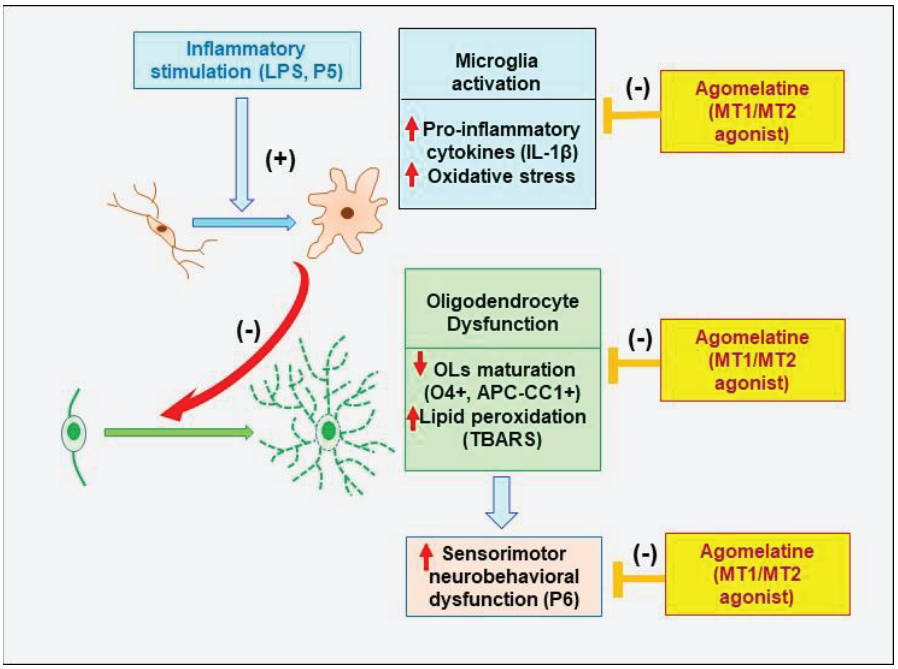


**Figure 9.** Schematic illustration of microglia-oligodendrocytes interaction in the brain white matter in neonatal systemic inflammation-induced sensorimotor neurobehavioral dysfunction. Systemic lipopolysaccharide (LPS) exposure led to stimulation of microglia activation, induction of pro-inflammatory cytokine interleukin-1β (IL-1β), loss of oligodendrocyte lineage cells (O4+/APC-CC1+), and upregulation of lipid peroxidation which caused brain white matter injury and related sensorimotor neurobehavioral dysfunction in neonatal rats. Treatment with melatonin agonist agomelatine reduced LPS-induced loss of oligodendrocytes and sensorimotor neurobehavioral dysfunction, which is associated with attenuation of LPS-induced increment of thiobarbituric acid reactive substances (TBARS) contents, IL-1β levels and number of activated microglia in neonatal rats. These findings suggest that melatonin agonist agomelatine may be useful for therapeutic effects in neonatal white matter disease with its properties of anti- inflammation, anti-oxidation, and promoting of oligodendrocyte progenitor cell differentiation. (Schematic adapted from Yeh et al, 2021).


## ACKNOWLEDGMENTS

This work was supported by Newborn Medicine Funds from the Department of Pediatrics, University of Mississippi Medical Center.

**Conflict of Interest Statement:** All authors declare that there are no conflicts of interest.


## REFERENCES


Altman J, Sudarshan K. 1975. Postnatal development of locomotion in the laboratory rat. Anim Behav 23:896–920. doi:10.1016/0003-3472(75)90114-1.

Altman J, Sudarshan K, Das GD, McCormick N, Barnes D. 1971. The influence of nutrition on

neural and behavioral development. 3. Development of some motor, particularly locomotor patterns during infancy. Dev Psychobiol 4:97-114.

Baharnoori M, Bhardwaj SK, Srivastava LK. 2012. Neonatal behavioral changes in rats with gestational exposure to lipopolysaccharide: a prenatal infection model for developmental neuropsychiatric disorders. Schizophr Bull 38:444-456. doi: 10.1093/schbul/sbq098.

Bonnefont-Rousselot D. and Collin F. 2010. Melatonin: Action as antioxidant and potential applications in human disease and aging. Toxicology. 278:55-67. ISSN 0300-483X. doi.org/10.1016/j.tox.2010.04.008.

Boulanger-Bertolus J, Mouly AM. 2021. Ultrasonic Vocalizations Emission across Development in Rats: Coordination with Respiration and Impact on Brain Neural Dynamics. Brain Sci 11:616. doi: 10.3390/brainsci11050616.

Brunelli SA, Aviles JA, Gannon KS, Branscomb A, Shacham S. 2009. PRX-00023, a selective serotonin 1A receptor agonist, reduces ultrasonic vocalizations in infant rats bred for high infantile anxiety. Pharmacol Biochem Behav 94:8-15. doi: 10.1016/j.pbb.2009.06.014.

Brzozowska I, Ptak-Belowska A, Pawlik M, Pajdo R, Drozdowicz D, Konturek SJ, Pawlik WW, Brzozowski T. 2009. Mucosal strengthening activity of central and peripheral melatonin in the mechanism of gastric defense. J Physiol Pharmacol 60:47–56.

Cai Z, Fan LW, Kaizaki A, Tien LT, Ma T, Pang Y, Lin S, Lin RCS, Simpson KL. 2013. Neonatal systemic exposure to lipopolysaccharide enhances vulnerability of nigrostriatal dopaminergic neurons to rotenone neurotoxicity in later life. Dev Neurosci DOI:10.1159/000346156.

Chumboatong W, Thummayot S, Govitrapong P, Tocharus C, Jittiwat J, Tocharus J. 2017. Neuroprotection of agomelatine against cerebral ischemia/reperfusion injury through an antiapoptotic pathway in rat. Neurochemistry international 102:114–122.

Falahati S, Breu M, Waickman AT, Phillips AW, Arauz EJ, Snyder S, Porambo M, Goeral K, Comi AM, Wilson MA, et al. 2013. Ischemia-induced neuroinflammation is associated with disrupted development of oligodendrocyte progenitors in a model of periventricular leukomalacia. Dev Neurosci 35:182–196. doi:10.1159/000346682.

Fan LW, Kaizaki A, Tien LT, Pang Y, Tanaka S, Numazawa S, Bhatt AJ, Cai Z. 2013. Celecoxib attenuates systemic lipopolysaccharide-induced brain inflammation and white matter injury in the neonatal rats. Neuroscience 240:27-38.

Fan LW, Tien LT, Mitchell HJ, Rhodes PG, Cai Z. 2008. □-Phenyl-*n*-*tert*-butyl-nitrone ameliorates hippocampal injury and improves learning and memory in juvenile rats following neonatal exposure to lipopolysaccharide. Eup J Neurosci 27:1475-1484.

Garrett-Cox RG, Pierro A, Spitz L, Eaton S. (2003. Body temperature and heat production in suckling rat endotoxaemia: beneficial effects of glutamine. J Pediatr Surg 38:37–44.

Guardiola-Lemaitre B, De Bodinat C, Delagrange P, Millan M., Munoz C, Mocaër E. 2014. Agomelatine: Mechanism of Action and Pharmacological Profile in Relation to Antidepressant Properties. Br J Pharm 171:3604–3619. doi: 10.1111/bph.12720.

Haynes RL, Folkerth RD, Keefe RJ, Sung I, Swzeda LI, Rosenberg PA, Volpe JJ, Kinney HC. 2003. Nitrosative and oxidative injury to premyelinating oligodendrocytes in periventricular leukomalacia. J Neuropathol Exp Neurol 62:441-450. doi: 10.1093/jnen/62.5.441.

Hermans RH, Hunter DE, McGivern RF, Cain CD, Longo LD. 1992. Behavioral sequelae in young rats of acute intermittent antenatal hypoxia. Neurotoxicol Teratol 14:119–129. doi:10.1016/0892-0362(92)90060-n.

Hsieh CT, Lee YJ, Lee JW, Lu S, Tucci M, Dai X, Ojeda NB, Lee HJ, Fan LW, Tien LT. 2020. Interleukin-1 receptor antagonist ameliorates the pain sensitivity, spinal inflammation and oxidative stress induced by systemic lipopolysaccharide in neonatal rats. Neurochem Int 104686. doi: 10.1016/j.neuint.2020.104686.

Kaizaki A, Tien LT, Pang Y, Cai Z, Tanaka S, Numazawa S, Bhatt AJ, Fan LW. 2013. Celecoxib reduces brain dopaminergic neuronal

dysfunction, and improves sensorimotor behavioral performance in neonatal rats exposed to systemic lipopolysaccharide. J Neuroinflammation 10:45, DOI:10.1186/1742-2094-10-45.

Kirsten TB, Chaves-Kirsten GP, Chaible LM, Silva AC, Martins DO, Britto LR, Dagli ML, Torrão AS, Palermo-Neto J, Bernardi MM. 2012. Hypoactivity of the central dopaminergic system and autistic-like behavior induced by a single early prenatal exposure to lipopolysaccharide. J Neurosci Res 90:1903-1912. doi: 10.1002/jnr.23089.

Kumar H, Sharma BM, Sharma B. 2015. Benefits of agomelatine in behavioral, neurochemical and blood brain barrier alterations in prenatal valproic acid induced autism spectrum disorder. Neurochemistry international 91:34–45. doi.org/10.1016/j.neuint.2015.10.007

Lee YA. 2017. White matter injury of prematurity: Its mechanisms and clinical features. J. Pathol Transl Med 51:449–455. doi:10.4132/jptm.2017.07.25.

Rezaie P, Dean A. 2002. Periventricular leukomalacia, inflammation and white matter lesions within the developing nervous system. Neuropathology 22:106–132.

Savran M, Aslankoc R, Ozmen O, Erzurumlu Y, Savas HB, Temel EN, Kosar PA, Boztepe S. 2020. Agomelatine could prevent brain and cerebellum injury against LPS-induced neuroinflammation in rats. Cytokine 127:154957. doi.org/10.1016/j.cyto.2019.154957.

Taylor GL, O'Shea TM. Extreme prematurity: Risk and resiliency. 2022. Curr Probl Pediatr Adolesc Health Care 52:101132. doi: 10.1016/j.cppeds.2022.101132.

Wong CS, Jow GM, Kaizaki A, Fan LW, Tien LT. 2014. Melatonin ameliorates brain injury induced by systemic lipopolysaccharide in neonatal rats. Neuroscience 267:147-156.

Yeh JH, Wang KC, Kaizaki A, Lee JW, Wei HC, Tucci MA, Ojeda NB, Fan LW, Tien LT. 2021. Pioglitazone ameliorates lipopolysaccharide-induced behavioral impairment, brain inflammation, white matter injury and mitochondrial dysfunction in neonatal rats. IJMS 22:6306. doi.org/10.3390/ijms22126306.

# Grandparenting in the Digital Age: Loneliness and Computer Usage Trends Among Children in Grandfamilies

**Laura Ann Chapman, Acacia R. Lopez, Danielle K. Nadorff**

Mississippi State University, Mississippi State, MS 39762

**Corresponding Author**: Danielle Nadorff

**Email:** Danielle.Nadorff@msstate.edu.
Doi: 10.34107/CTJP1687

## ABSTRACT

The United States Census Bureau estimates there were 5,793,873 children living in "grandfamilies" in 2021. Children reside with a grandparent caregiver when a parent is unwilling or unable to care for their child, which often overlaps with traumatic experiences. These children are also at risk of developing disrupted attachment due to the separation. Increased exposure to traumatic events and disrupted attachment are linked with emotional issues in children, including feelings of loneliness. Increased traumatic experiences in childhood were linked with problematic internet use in emerging adulthood to cope with feelings of loneliness. Data from the second wave in the national Health Behavior in School-aged Children (HBSC) study was used to explore this hypothesis ($N$= 12638; 1.9% grandchildren; $M$ age = 12.95). Moderation analyses indicated the overall model was significant and accounted for 9% of the variance ($R^2$=0.09, $p < 0.01$.). The moderation of household type was not significant, but the relation between loneliness and the number of hours spent on the computer was significant ($b$ = 5.1, $t(237)$ = 2.38, $p < 0.01$). The results show that while there is a significant relation between the children's feelings of loneliness and the number of hours they spend on the computer daily, there was no significant difference between types of family units. Children with feelings of loneliness may use computers as a coping mechanism broadly, regardless of their family system. Targeted interventions to provide safe internet usage for children experiencing loneliness should be explored. Grandparents may benefit from psychoeducation on problematic internet usage for their grandchildren.

**KEYWORDS:** grandfamilies, children, loneliness, computer usage, coping mechanism, family structure, attachment, traumatic experiences, psychoeducation, intervention.

## INTRODUCTION

Loneliness has been described as a national epidemic in the United States and has been linked with various mental health issues, including depression and generally lower life satisfaction (Holt-Lunstad et al., 2015; Zipes, 2023). Extant literature suggests that although loneliness impacts individuals across the lifespan and various strata, including race and socioeconomic status, children and adolescents are at a heightened risk of experiencing loneliness compared to other age groups (Prizeman et al., 2023). Youth who experience loneliness are also susceptible to social isolation, potentially exacerbating depressive symptoms and low life satisfaction during this developmental stage (Achterbergh et al., 2020). Youth who suffer from loneliness and depression are likely to have poor academic performance, fewer social supports, and are at an increased risk of endorsing depression in their adulthood (Almeida et al., 2022). These potential outcomes underscore the importance of elucidating risk factors and coping mechanisms within this population.

Given the proliferation of the internet in modern society, there have been findings that suggest internet usage may be an appropriate and accessible coping mechanism for many psychological symptoms, including loneliness (Angane et al., 2020; Demirtepe-Saygılı & Metin- Orta, 2021; Shillair et al., 2015). Loneliness is most likely to occur when an individual feels their social needs are not met, and the internet may provide an outlet for individuals to "connect" with others virtually. For example, individuals who play video games use online

multiplayer games may be seeking a substitute for in-person social interactions (Maroney et al., 2019). In another study, adolescents experiencing loneliness due to the COVID-19 lockdown were more likely use the internet as a coping mechanism than their peers who were struggling with anxiety (Cauberghe et al., 2021). These findings suggest that although there is heterogeneity in the types of internet usage, some methods of usage may be beneficial to explore as coping mechanisms for loneliness while others may represent problematic internet usage which exacerbate loneliness (Skues et al., 2016).

There are several known risk factors for loneliness amongst children and adolescents including limited social support, low socioeconomic status, and a history of abuse and neglect (Dahlberg et al., 2022; de Heer et al., 2022). Foster children often represent an amalgamation of these risk factors and as such, have been shown to have a higher propensity for loneliness (Lalayants & Prince, 2015). Another population who may be at a heightened risk of loneliness are children raised by their grandparents (those in "grandfamilies"), when the biological parent is unwilling or unable to continue care. Due to the traumatic events that commonly cause grandchildren to be placed in the care of their grandparents, including incarceration of or abandonment by the biological parent, these children are often exposed to adverse childhood experiences which have been correlated to an increased risk to various mental health issues (Lopez et al., 2023; Xu et al., 2022). Further, children in grandfamilies are often lacking in resources, particularly social support and financial means (Kelly, 2019). The culmination of these risk factors indicate that grandchildren raised by grandparents may be particularly disposed to feelings of loneliness. These grandchildren represent a significant population in the US, with most recent Census data indicating that there were approximately 5.8 million grandchildren being raised by their grandparents (United States Census Bureau, 2022). Despite the large population, these grandchildren continue to be an underrepresented group in psychological research. To date, although there have been several studies examining outcomes for grandparents, there have been no studies to explore how grandchildren raised in a grandfamily cope with feelings of loneliness.

In exploring the patterns of computer and internet usage among children living in grandfamilies, it is essential to consider the unique dynamics of their family structure, distinguishing them from their non-grandparent peers. Grandfamilies, characterized by the presence of grandparents as primary caregivers, introduce a distinctive familial context that may influence children's digital behaviors (Pilkauskas & Dunifon, 2016). Thus, the intergenerational nature of grandfamilies, coupled with potential variations in socioeconomic circumstances and parenting styles, may shape children's access to and utilization of technology. It is plausible that the supportive roles assumed by grandparents could impact the digital environment within these households, potentially influencing the amount and purpose of computer or internet engagement among the grandchildren. Understanding these nuanced family dynamics is crucial for unraveling the complexities of technology use in grandfamilies and shedding light on how this population may differ from their peers in non-grandparental caregiving arrangements. This investigation aims to contribute valuable insights into the intersection of family structure and digital behaviors, offering a nuanced understanding of the factors shaping children's computer and internet usage within the context of grandfamilies.

## Current Study

The purpose of the current study was to investigate the relation between family structure, feelings of loneliness, and computer usage among school-aged children. This study aims to understand the nuanced connections between family structure, feelings of loneliness, and computer usage among school-aged children, thereby filling a critical gap in the existing literature and contributing valuable insights to the broader understanding of children's well-being in the context of contemporary family dynamics. Three hypotheses were formulated and explored using data from the second wave of the national

Health Behavior in School-aged Children (HBSC) study.

Hypothesis 1 (H1): Children reporting increased feelings of loneliness will spend more time on the computer compared to their non-lonely peers.

Hypothesis 2 (H2): Children in grandfamilies will report higher levels of loneliness compared to children living with their biological parents.

Hypothesis 3 (H3): The relation between children experiencing feelings of loneliness and the amount of time they spend on the computer will be moderated by the family status of grandfamilies.

## MATERIALS AND METHODS

**Participants:** Data from the second wave in the national Health Behavior in School-aged Children (HBSC) study was used to explore hypotheses (N= 12638; 220 grandchildren; M age = 12.95). Participants were 12,638 children in grades 5th-10th (M age = 12.95, SD = 9.52). The data collection process involved the administration of self-report surveys, which were carried out within classroom settings by school personnel.

**Family Status:** Family status was determined based on participants' responses to a multiple-choice question about who lives in their primary home. This variable was not assessed through a formal questionnaire but ascertained by participants checking what adult is responsible for their care at their primary residency.

**Loneliness:** Loneliness was assessed using a single-item self-report measure in which participants were asked, “Thinking about last week, have you felt lonely?” to rate how often they felt lonely during the previous week. Responses were measured on a 5-point Likert **scale, ranging from "Never" to "Always."**

**Daily Computer Usage**: Daily computer usage was assessed through a single-item self-report measure, where participants estimated the number of hours, they spent on a computer at home each day. Participants estimated the number of hours they spent using a computer at home each day (0 to 7 or more).

**Procedure:** The HSBC dataset is a free and publicly accessible data set. The data collection questionnaires were given out in the classroom and were self-completed by students to evaluate health-related behavior of children in grades 5 – 10, including questions about bullying, diet, physical health, peer and family relationships, and drug and alcohol use (Iannotti, 2013). All analyses were completed using SPSS Process Macro v3.15.

## RESULTS

As shown in Figure 1, the relation between loneliness and the number of hours spent on the computer daily was also found to be significant ($b$ = 5.1, $t(237) = 2.38$, $p < .01$).

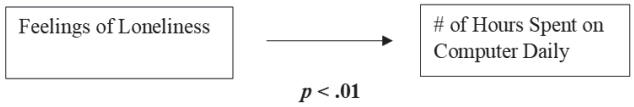


Figure 1

This result provided support for the first hypothesis, indicating that children who reported feeling lonely spent more time on the computer on average compared to their non-lonely peers. In Figure 2 it is shown that the relation between children living in grandfamilies and experiencing more loneliness in comparison to their peers was significant ($t(12641) = 15.57$, $p < .001$).

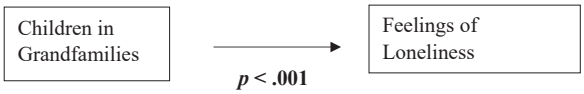


Figure 2

This finding supported the second hypothesis, indicating that children in grandfamilies reported higher levels of loneliness than those living with their biological parents.

A moderation analysis was conducted to investigate the role of household type as a moderating variable in the relation between children's feelings of loneliness and their daily computer usage (Figure 3). The results indicated that the overall model was significant and accounted for 9% of the variance ($R^2 = .09$, $p <$ .01). However, moderation by household type was found to be not significant, indicating that the

type of family structure did not have a moderating impact on the relation between loneliness and daily computer usage in contradiction to the third hypothesis. An exploratory independent samples t-test was conducted to investigate potential factors contributing to this discrepancy. Specifically, this t-test examined the number of computers in the homes of children raised by their grandparents. The results indicated that there significantly fewer computers in the homes of children raised by their grandparents, $t(238) = .02$, $p < .001$.

This difference could explain why the interaction of family status is not significant, as children may be engaging in internet use less often as a direct result of not having physical access to a computer, rather than a preference for a different coping modality. This investigation underscores the importance of considering various factors that may influence the study's outcomes and offers a more refined perspective on the intricate interplay of variables within the research framework for this population.

**Figure 3:**

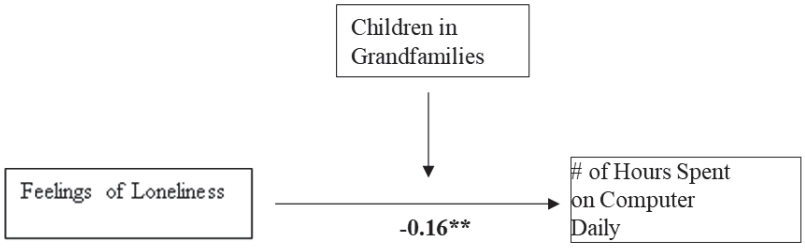


## DISCUSSION

The purpose of the current study was to investigate the relation between family structure, feelings of loneliness, and computer usage among school-aged children. Three hypotheses were formulated and explored using data from the second wave of the national Health Behavior in School-aged Children (HBSC) study.

Hypothesis 1 (H1) predicted that children reporting feelings of loneliness would spend more time on the computer, on average, compared to their non-lonely peers. The analysis confirmed this hypothesis, demonstrating that children who reported being lonely did spend more time on the computer. This suggests that loneliness may drive increased computer usage as a potential coping mechanism among children.

The second hypothesis (H2) posited that children in grandfamilies would report higher levels of loneliness compared to children living with their biological parents. The results of the analysis indicated a significant difference in reported loneliness between these two groups, supporting H1. Children in grandfamilies were indeed more likely to report feelings of loneliness. This finding suggests that the family structure may have a significant impact on a child's emotional well-being.

Hypothesis 3 (H3) proposed that children in grandfamilies who reported more feelings of loneliness would spend more hours per day on the computer than their peers living with their biological parents. In fact, children in grandfamilies experiencing loneliness did not spend more time on the computer. This may be related to the potential lack of resources experienced by grandparent caregivers, including limited access to technology in

their homes.

Findings from this study suggest that broadly, children who experience loneliness are more likely to engage in computer usage than their non-lonely peers. Further, this study demonstrated that children raised by their grandparents reported more loneliness than their same- age peers. However, children raised by grandparents were not more likely to engage in computer usage. This may be explained, in part, by the fact that grandparent-headed households had significantly fewer computers than non-grandparent headed households, $t(238) = .02$, $p < .001$.

Thus, this study suggests that an exploration of the internet as a coping mechanism is necessary to determine if the way that children use the internet impacts their levels of loneliness. If used properly, there is a growing body of literature that supports the use of internet-based platforms to address symptoms of anger, depression, and anxiety (Editorial Team, 2022). For example, recent technological innovations have also given rise to mobile applications that target psychopathology symptoms, such as anger, and the grandfamilies population may benefit from engaging in these platforms.

The observed relation between loneliness and computer usage implies that children experiencing loneliness may turn to the internet as a broad coping mechanism. While this study provides important insights into these associations, it is essential to recognize some of the study's limitations. One limitation of the current study is that the analysis is not entirely representative of the entire population of school-aged children in the United States such as those in rural populations. Further longitudinal research is necessary to explore the temporal relation between family structure, loneliness, and computer usage. Moreover, more detailed data on computer usage patterns and content would provide a more comprehensive understanding of the issue.

To improve future research in this area, researchers should consider employing more in- depth measures of computer usage and its content, as well as exploring the potential causal pathways underlying these relations. Moreover, extending the investigation to a larger, more diverse population would enhance the generalizability of the findings. This study's findings have important implications for both research and the real world. In the research realm, future studies should delve deeper into the mediating mechanisms behind the relations uncovered in this research, such as the role of computer access and content in coping with loneliness. Additionally, researchers should explore the impact of targeted interventions aimed at promoting safe and beneficial internet usage among children experiencing loneliness, especially those in grandfamilies.

In the real world, this study suggests that parents, grandparents, and professionals who work with children should be aware of the potential link between loneliness and computer usage. Parents and caregivers should monitor and manage their children's computer usage. Grandparents may benefit from psychoeducation on how to address problematic internet usage in their grandchildren.

In conclusion, this study sheds light on the complex relation between family structure, loneliness, and computer usage among school-aged children. The findings support the importance of understanding the impact of family dynamics on children's emotional well-being and technology usage. As we move forward, future research should build upon these findings and continue to

explore the underlying mechanisms and interventions that can benefit this vulnerable population.

## AUTHOR DISCLOSURES:

The authors have not stated any conflicts of interest.

## LITERATURE CITED


Achterbergh, L., Pitman, A., Birken, M., Pearce, E., Sno, H., & Johnson, S. (2020). The experience of loneliness among young people with depression: A qualitative meta- synthesis of the literature. BMC Psychiatry, 20(1), N.PAG-N.PAG. https://doi.org/10.1186/s12888-020-02818-3

Almeida, I. L. de L., Rego, J. F., Teixeira, A. C. G., & Moreira, M. R. (2022). Social isolation and its impact on child and adolescent development: A systematic review. Revista Paulista de Pediatria, 40, e2020385. https://doi.org/10.1590/1984-0462/2022/40/2020385

Angane, A. Y., Kadam, K. S., Ghorpade, G. S., & Unnithan, V. B. (2020). Unraveling the Net of Self-Esteem, Stress, and Coping Skills in the Era of Internet addiction. Annals of Indian Psychiatry, 4(1), 70. https://doi.org/10.4103/aip.aip_80_19

Cauberghe, V., Van Wesenbeeck, I., De Jans, S., Hudders, L., & Ponnet, K. (2021). How Adolescents Use Social Media to Cope with Feelings of Loneliness and Anxiety During COVID-19 Lockdown. Cyberpsychology, Behavior, and Social Networking, 24(4), 250–257. https://doi.org/10.1089/cyber.2020.0478

Dahlberg, L., McKee, K. J., Frank, A., & Naseer, M. (2022). A systematic review of longitudinal risk factors for loneliness in older adults. Aging & Mental Health, 26(2), 225–249. https://doi.org/10.1080/13607863.2021.1876638

de Heer, C., Bi, S., Finkenauer, C., Alink, L., & Maes, M. (2022). The Association Between Child Maltreatment and Loneliness Across the Lifespan: A Systematic Review and Multilevel Meta-Analysis. Child Maltreatment, 10775595221103420. https://doi.org/10.1177/10775595221103420

Demirtepe-Saygılı, D., & Metin-Orta, I. (2021). An Investigation of Cyberloafing in Relation to Coping Styles and Psychological Symptoms in an Educational Setting. Psychological Reports, 124(4), 1559–1587. https://doi.org/10.1177/0033294120950299

Editorial Team. (2022, January 1). Become more calm and conscious with Ahead—Ness Labs. https://nesslabs.com/ahead-featured-tool

Holt-Lunstad, J., Smith, T. B., Baker, M., Harris, T., & Stephenson, D. (2015). Loneliness and social isolation as risk factors for mortality: A meta-analytic review. Perspectives on Psychological Science: A Journal of the Association for Psychological Science, 10(2), 227–237. https://doi.org/10.1177/1745691614568352

Iannotti, R. J. (2013). Health Behavior in School-Aged Children (HBSC), 2009-2010. Inter-university Consortium for Political and Social Research [distributor]. https://doi.org/10.3886/ICPSR34792.v1

Kelly, S. J. (2019). Grandparent-headed families—A vulnerable population.

Https://Www.Apadivisions.Org. https://www.apadivisions.org/division-37/publications/newsletters/maltreatment/2019/06/best-practice

Lalayants, M., & Prince, J. D. (2015). Loneliness and Depression or Depression-Related Factors Among Child Welfare-Involved Adolescent Females. Child and Adolescent Social Work Journal, 32(2), 167–176. https://doi.org/10.1007/s10560-014-0344-6

Lopez, A. R., Nadorff, D. K., & Peters, D. (2023). The Twelve Ds: An Update to Edwards and Benson's Reasons for Non-Parental Caregiving. International Journal of Environmental Research and Public Health, 20(9), Article 9. https://doi.org/10.3390/ijerph20095618

Maroney, N., Williams, B. J., Thomas, A., Skues, J., & Moulding, R. (2019). A Stress-Coping Model of Problem Online Video Game Use. International Journal of Mental Health and Addiction, 17(4), 845–858. https://doi.org/10.1007/s11469-018-9887-7

Pilkauskas, N., & Dunifon, R. (2016). Understanding Grandfamilies: Characteristics of Grandparents, Nonresident Parents, and Children. Journal of Marriage & Family, 78(3), 623–633. https://doi.org/10.1111/jomf.12291

Prizeman, K., Weinstein, N., & McCabe, C. (2023). Effects of mental health stigma on loneliness, social isolation, and relationships in young people with depression symptoms. BMC Psychiatry, 23(1), 1–15. https://doi.org/10.1186/s12888-023-04991-7

Shillair, R. J., Rikard, R. V., Cotten, S. R., & Tsai, H. Y. (2015). Not So Lonely Surfers: Loneliness, Social Support, Internet Use and Life Satisfaction in Older Adults. iConference 2015 Proceedings. https://hdl.handle.net/2142/73666

Skues, J., Williams, B., Oldmeadow, J., & Wise, L. (2016). The Effects of Boredom, Loneliness, and Distress Tolerance on Problem Internet Use Among University Students.

International Journal of Mental Health and Addiction, 14(2), 167–180. https://doi.org/10.1007/s11469-015-9568-8

United States Census Bureau. (2022). American Community Survey 2021: 5 Year Estimates [dataset]. https://data.census.gov/table?tid=ACSDP5Y2021.DP02&hidePreview=true Xu, Y., Wang, Y., McCarthy, L. P., Harrison, T., & Doherty, H. (2022). Mental/behavioural health and educational outcomes of grandchildren raised by custodial grandparents: A mixed methods systematic review. Health and Social Care in the Community. Scopus. https://doi.org/10.1111/hsc.13876

Yamazi, A. K., Moreira, T. S., Cavicchioli, V. Q., Burin, R. C., & Nero, L. A. 2013. Long cold storage influences the microbiological quality of raw goat milk. Small Ruminant Research, 113(1), 205-210. https://doi.org/10.1016/j.smallrumres.2013.02.004

# Dengue Fever Epidemics and the Prospect of a Vaccine

**Ebele C. Okoye*, Amal K. Mitra, Terica Lomax, Cedric Nunaley**

Department of Epidemiology & Biostatistics, Jackson State University, Jackson, MS, 39213

**Corresponding Author:** Ebele .C. Okoye
Email: ebele.c.okoye@students.jsums.edu
Doi:10.34107/CTJP1687

## ABSTRACT

**Background and Objective:** Dengue fever, a global health concern, poses severe risks and has led to the exploration of vaccines as a preventive measure. This systematic review and meta-analysis evaluated the efficacy, immune response, and safety of dengue vaccines in children through an analysis of clinical trials. **Methods:** The review followed PRISMA guidelines, searching databases for studies focused on dengue fever and vaccine potential. Eligible studies involved children (0-17 years), emphasizing vaccine efficacy, immune response, and safety. Cochrane Collaboration criteria assessed study quality, with thematic data synthesis and meta-analysis. **Results:** Among 38 selected studies, dengue vaccines showed varying efficacy against all four serotypes. CYD-TDV and Takeda vaccines demonstrated strong protection against severe dengue, but their long-term efficacy varied. Vaccines triggered satisfactory immune responses, notably in those previously exposed to dengue. Safety profiles were mostly favorable, noting mild adverse events post-vaccination. The meta-analysis supported vaccine efficacy and immune response but raised safety concerns, warranting further investigation. The results showed risk ratios and confidence intervals for vaccine efficacy, immunogenicity, and safety as 0.62 (0.48-0.81), 0.48 (0.25-0.91), and 0.73 (0.45-1.18) respectively. Statistical significance was observed in vaccine efficacy (p=0.00004) and immunogenicity (p=0.03), favoring the intervention group over the control. However, there wasn't a significant difference in vaccine safety, favoring the control group that received a placebo. A relatively high heterogeneity ($I^2$) was observed across studies indicating the need for further research to address these discrepancies. **Conclusion:** Dengue vaccines demonstrated promising efficacy and immune response, particularly against severe manifestations. While generally safe, mild adverse events were observed, signaling the need for continued safety assessment.

**KEYWORDS:** Dengue Fever, Dengue virus, vaccine

## INTRODUCTION

Dengue fever, caused by the dengue virus (DENV), is a significant global health concern due to its widespread prevalence and impact on public health. It belongs to the Flavivirus genus and is primarily transmitted to humans through the bites of infected female Aedes mosquitoes, notably Aedes *aegypti* and Aedes *albopictus* (Clements, 2012; Joshi et al., 2002; Kyle & Harris, 2008). The World Health Organization (WHO) characterizes dengue fever as an acute mosquito-borne viral infection characterized by fever, severe headache, joint and muscle pain, skin rash, and bleeding tendencies (Bhatt et al., 2013; WHO, 2021). DENV exists in four distinct serotypes (DENV-1 to DENV-4), each capable of causing a range of clinical manifestations, from mild dengue fever to severe forms like dengue hemorrhagic fever (DHF) and dengue shock syndrome (DSS) (Bhatt et al.,2013; Halstead, 2007; Nguyen et al., 2006). Severe cases can lead to complications like plasma leakage, potentially resulting in shock, coagulopathy, or vital organ impairment (Simmons et al., 2012; Wilder-Smith et al., 2019).

Globally, dengue fever has emerged as a significant health challenge, affecting approximately 3.9 billion people across 128 countries, with an estimated 96 million symptomatic cases reported annually (Bhatt et al., 2013; Brady et al., 2012; WHO, 2021). Its prevalence is particularly prominent in tropical and subtropical regions, where favorable climatic conditions sustain mosquito vectors, enabling year-round transmission (Guzman & Harris, 2015). The endemic nature of dengue fever, combined with increased urbanization, population growth, and global travel, has led to its continued geographical range expansion

(Gubler, 2011; Murray et al., 2013). The global incidence of dengue has nearly doubled in the past 30 years and is projected to rise further, especially in Asia, sub-Saharan Africa, and Latin America. Approximately half of the global population resides in regions conducive to dengue transmission (Messina et al., 2019; Yang et al., 2021). The impact of dengue fever on public health is exacerbated by its potential to cause large-scale outbreaks and epidemics, often overwhelming healthcare systems in affected regions (Halstead et al., 2007; Silva et al., 2020). Additionally, the economic burden of dengue fever is substantial, with estimates suggesting an annual cost of billions of dollars in terms of medical care and productivity losses (Shepard et al., 2016). These factors collectively underscore the urgent need for effective preventive measures, with vaccination emerging as a pivotal component in the arsenal against dengue fever.

In the present day, dengue fever remains a pressing global health concern with widespread and increasing geographical distribution. The disease is endemic in over 128 countries, predominantly in tropical and subtropical regions (WHO, 2021). Current trends indicate a steady rise in reported cases, significantly impacting both urban and rural communities. Key regions with high transmission rates include Southeast Asia, the Pacific Islands, parts of the Americas, and Africa (Bhatt et al., 2013). In recent years, there has been a surge in the incidence of dengue fever, partly due to factors such as rapid urbanization, increased travel and trade, and climate change, affecting mosquito habitats and behavior (Guzman & Harris, 2015). These trends highlight the urgent need for comprehensive strategies, including vaccination, to combat the continued spread of dengue fever.

Recently, there has been a dengue outbreak in Bangladesh, between January 1st, 2023, and 7th August 2023, the Ministry of Health, and Family Welfare (MOHFW) reported a total of 69,483 dengue cases, resulting in 327 related deaths (with a case fatality rate of 0.47%), (WHO, 2023). Initially, by 30 June 2023, 7,978 cases and 47 deaths had been recorded. However, a significant surge began in late June, with July alone accounting for 63% of cases (n=43,854) and 62% of deaths (n=204), (WHO, 2023). Comparatively, these figures exceed the numbers reported during similar periods over the past five years in Bangladesh. Dengue cases commenced rising in May 2023 and have persistently risen since then, with a peak yet to be reached. Remarkably, the reported dengue cases for 2023 are the highest compared to the same periods recorded since 2000 (WHO, 2023).

Preventing and controlling dengue fever constitutes a formidable challenge, underscored by a constellation of intricate factors. The complexity of disease dynamics, attributed to the existence of four distinct serotypes of the dengue virus, necessitates the development of a vaccine capable of conferring broad and durable protection against all serotypes (Nguyen et al., 2006). Additionally, vector control measures confront limitations due to the evolving resistance of Aedes mosquitoes, the primary vectors, to conventional insecticides (Dia et al., 2012; Mulderij-Jansen et al., 2022; Weeratunga et al., 2017). Moreover, a substantial proportion of dengue infections manifest as asymptomatic or mild cases, leading to underreporting and consequently impeding timely intervention (WHO,2021).

In regions where dengue is endemic, challenges arise from constrained healthcare infrastructure, potentially resulting in delayed diagnosis and treatment, particularly for severe cases (WHO, 2021). Furthermore, the globalization of dengue facilitated by increased international travel and trade introduces the virus to new regions, sometimes overwhelming unprepared healthcare systems (Gubler, 2011; Kraemer et al., 2015). Addressing these multifaceted challenges mandates a comprehensive and integrated approach, involving not only developing and deploying a dengue vaccine but also concerted efforts in vector control, public health education, and fortifying healthcare infrastructure in endemic regions.

Previous endeavors to develop a dengue vaccine have spanned several decades and involved various approaches, each with its own

set of challenges and achievements. The earliest attempts focused on inactivated or live-attenuated whole-virus vaccines. While these approaches showed promise in providing immunity against all four dengue serotypes, concerns arose regarding safety and the potential for adverse reactions, particularly in individuals with previous exposure to dengue (Guy et al., 2011). Subsequent efforts turned towards recombinant subunit vaccines, which utilize specific portions of the viral proteins to induce an immune response. Notable candidates, such as the CYD-TDV (Dengvaxia) vaccine, progressed to clinical trials. However, challenges emerged, including the need for multiple doses and variation in efficacy based on prior dengue exposure (Sabchareon et al., 2012). Advancements in vaccine technology have spurred the development of novel approaches, including the use of viral vectors and nucleic acid-based vaccines. These innovative strategies hold promise in circumventing the challenges faced by earlier vaccine candidates, with some demonstrating encouraging results in preclinical and early clinical trials (Thomas & Yoon, 2019; Osorio et al., 2014). While progress has been made, the quest for a safe and effective dengue vaccine remains ongoing. The complexities of dengue immunology, including the need for balanced immunity against all serotypes, continue to pose significant hurdles. Nevertheless, the diverse range of approaches and continued research efforts provide optimism for the eventual development of an effective dengue vaccine. This study aims to investigate dengue fever epidemics and the prospect of a vaccine.

## MATERIALS AND METHODS

### Protocol

The Preferred Reporting Items for Systematic Reviews and Meta-Analyses (PRISMA) guideline (Liberati, et al., 2009) was used as a framework to guide the systematic review. The stages followed to perform the systematic review were based on (a) defining the appropriate keywords, (b) searching databases to find and select articles, (c) critical evaluation of the studies, (d) data selection and analysis, and (e) presentation and interpretation of results.

### Eligibility Criteria

This systematic review and meta-analysis concentrated on original, peer-reviewed journal articles that delved into both qualitative and quantitative studies about dengue fever epidemics and the potential for vaccines. The inclusion criteria encompassed studies written in English, specifically journal articles that involved human subjects as the focal population. The primary focus was on original research studies about dengue fever epidemics and vaccine potential. Studies involving individuals from all age groups were considered, and full-text articles were a prerequisite for eligibility. There were no restrictions based on the country in which the study was conducted. On the other hand, exclusion criteria involved non-English articles, literature reviews, systematic reviews, book chapters, and conference papers. Studies that primarily involved animals as the target population were also excluded from consideration.

### Search Strategy

On September 11, 2023, a comprehensive search was conducted across six databases, namely PubMed, CINAHL, Medline, Health Source, Science Direct, and Academic Search Premiere. The search aimed to identify relevant articles written in the English language and focused on peer-reviewed journal publications. We applied the following filters: studies on dengue outbreaks, human studies, children subjects (0-17 years), and full-text articles. Manual searches of reference lists were also performed to ensure comprehensive coverage of the literature. The search strategy utilized adapted and inclusive search terms specific to each database to capture a broad range of literature related to the research of interest (Table 1).

### Study Screening Process

The authors conducted independent searches in the respective databases (Table 1) using identical search keywords. The search yielded 1961 articles from the databases, and 28

additional articles were identified by hand-searching. The PRISMA Flowchart shown in Figure 1 (Liberati et al., 2009), summarized the search process, indicating that a total of 1989 articles were identified. After removing duplicates (n =540), the remaining 1449 articles underwent a two-phase screening process using Excel. In the first phase, titles and abstracts were screened, and in the second phase, full-text articles were screened. Inclusion criteria were applied during this process. Initially, 61 articles were selected for full- text screening based on consensus among the authors and were independently reviewed. Any discrepancies or conflicts in articles were independently reviewed by the authors and resolved through group discussions among the authors. As a result, twenty-three (23) articles were excluded because the full-text articles were restricted and could not be accessed. A total of 38 articles were included in the systematic review, while 27 of these were further analyzed for the meta-analysis.

**Table 1**: Databases searched, the keywords utilized, and the number of articles

| Databases | Search keywords | Number of Articles Found |
|---|---|---|
| PubMed (1) | "Dengue fever" OR "Dengue epidemics" OR "Dengue vaccine" OR "Dengue Vaccine prospects" | 129 |
| PubMed (2) | "Dengue fever" OR "Dengue epidemics" **AND** "Dengue vaccine" OR "Dengue vaccine development" OR "Dengue vaccine prospects" **AND** "Dengue vaccine efficacy" OR "Dengue vaccine safety" OR "Dengue serotypes" | 81 |
| CINAHL | "Dengue fever" OR "Dengue epidemics" **AND** "Dengue vaccine" OR "Dengue vaccine development" OR "Dengue vaccine prospects" **AND** "Dengue vaccine efficacy" OR "Dengue vaccine safety" OR "Dengue serotypes" OR "Clinical trials" OR "Epidemiological studies" | 24 |
| Medline | Dengue fever" OR "Dengue epidemics" **AND** "Dengue vaccine" OR "Dengue vaccine development" OR "Dengue vaccine prospects" **AND** "Dengue vaccine efficacy" OR "Dengue vaccine safety" OR "Dengue serotypes" OR "Clinical trials" OR "Epidemiological studies | 210 |
| Health Source | "Dengue fever" OR "Dengue epidemics" **AND** "Dengue vaccine" OR "Dengue vaccine development" OR "Dengue vaccine prospects" **AND** "Dengue vaccine efficacy" OR "Dengue vaccine safety" OR "Dengue serotypes" OR "Clinical trials" OR "Epidemiological studies" | 2 |
| Science Direct | "Dengue fever" OR "Dengue epidemics" **AND** "Dengue vaccine" OR "Dengue vaccine development" **AND** "Dengue vaccine efficacy" OR "Dengue vaccine safety" OR "Dengue serotypes" | 1,381 |
| Academic Search Premiere | "Dengue fever" OR "Dengue epidemics" AND "Dengue vaccine" OR "Dengue vaccine development" OR "Dengue vaccine prospects" AND "Dengue vaccine efficacy" OR "Dengue vaccine safety" OR "Dengue serotypes" OR "Clinical trials" OR "Epidemiological studies" | 134 |

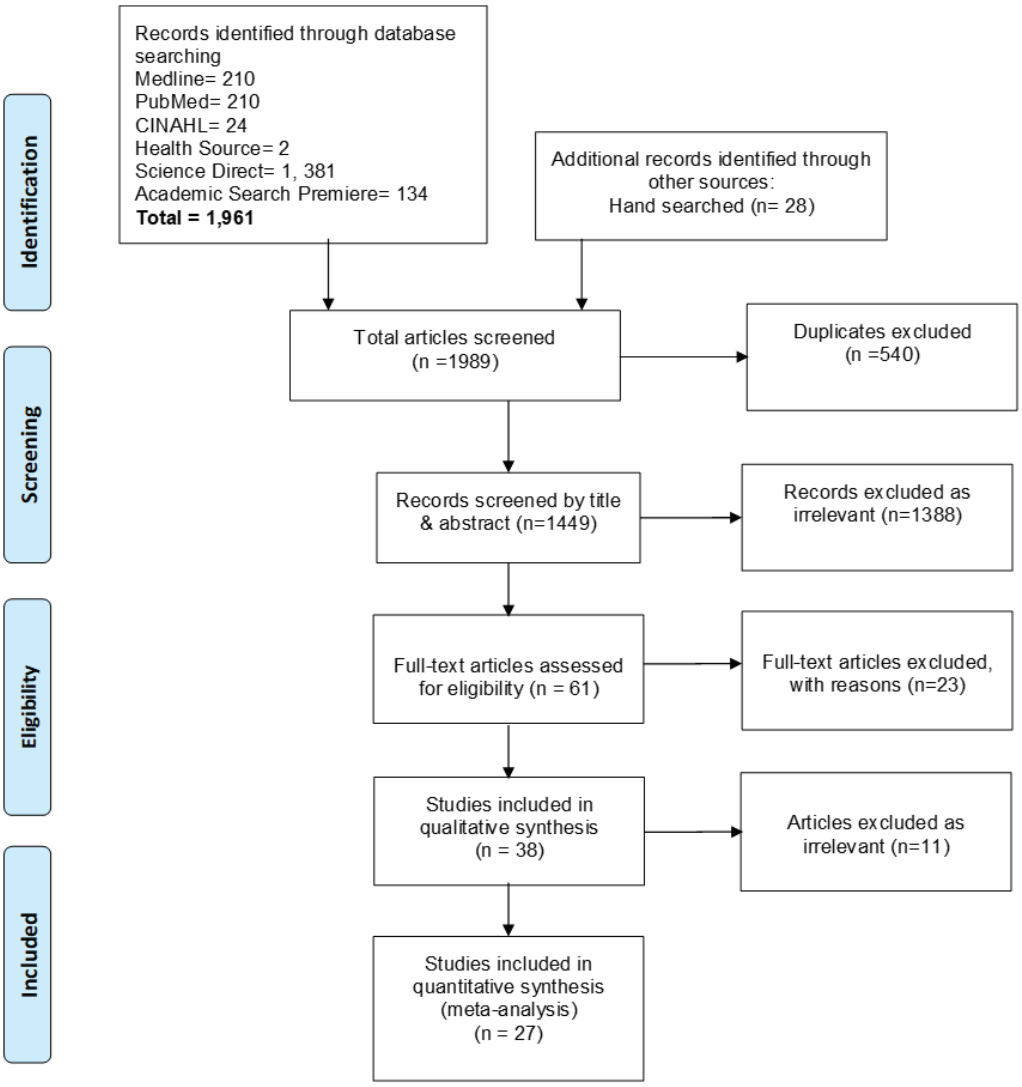


**Fig. 1**: PRISMA Flowchart (Liberati et al., 2009)

## Quality Assessment

The assessment of bias risk was conducted by the authors individually, employing the Cochrane Collaboration tool to evaluate bias in the clinical trials (Higgins et al., 2023). The criteria assessed were confounding/performance bias, selection/allocation bias, attrition bias, information (detection) bias, and reporting bias (Figures 2 & 3).

## Data Extraction

The authors designed a standardized form tailored for data extraction, encompassing fields for study identification details, country of origin, study design, participants' age, main findings, and participant count per intervention (Table 2). Thematic analysis, as outlined by (Thomas & Harden, 2008) will be applied to analyze the data gathered from the included studies. The authors independently identified and developed distinct themes. Subsequently, these themes will be cross-referenced, essential themes will be determined by consensus, and a narrative synthesis will be conducted by the authors.

**Table 2.** Characteristics of included studies

| Author & year of publication | Purpose | Study Design | Sample size | Age of participants | Main findings | Country |
|---|---|---|---|---|---|---|
| Forrat et al, 2021 | This post hoc analysis assessed hospitalized and severe virologically confirmed dengue (VCD) over the complete 6-year follow- up of 3 CYD-TDV efficacy studies (CYD14, CYD15, and CYD23/CYD57). | RCT | 29,229 | 2-16years | CYD-TDV demonstrated robust protection against hospitalized and severe VCD over the entire 6-year follow-up in participants who were seropositive and ≥9 years old. Protection was also observed in seropositive 6–8 year-olds. | Asia and Latin America |
| **Thomas et al., 2022** | Evaluated potential associations of host human leukocyte antigen (HLA) alleles with dengue antibody responses, CYD-TDV vaccine efficacy, and virologically confirmed dengue (VCD) cases. | RCT | 334 | 4-11years | Specific HLA alleles that are significantly associated with dengue NAb titers were identified. | Thailand |
| **España et al., 2019** | Evaluated the vaccine efficacy for susceptibility (VES) as a measure of the protective effects of vaccination against the first symptomatic, virologically confirmed case of dengue caused by any DENV serotype during simulated vaccine trials in Iquitos, Peru. | RCT | 51,253 | 2-16years | Discovered a distinct bias in VE estimates away from the null due to lower detectability of primary DENV infections among seronegative individuals in the vaccinated group. | Peru |
| Yang et al., 2018 | Evaluated the dependence of Tetravalent Dengue Vaccine efficacy on baseline immunity status and age groups (children) | RCT | 31,125 | 5 – 11years | The CYD-TDV vaccine was highly efficacious for all dengue serotypes among children aged >5 years who have acquired baseline immunity from previous exposure. | USA |
| Plennevaux et al., 2016 | Detected dengue cases by serological testing in a dengue vaccine efficacy trial | RCT | 2266 | 4-11years | Reliance on serological assessments would lead to a significant number of false positives during routine clinical practice and surveillance following the introduction of the dengue vaccine | Thailand |
| Sridhar et al., 2018 | The primary objective of the study was to assess the risk of hospitalization for VCD in seronegative vaccine recipients who were 9 years of age or older at enrollment (the primary endpoint). Prespecified secondary objectives included an assessment of this risk in seronegative participants of 2 to 8 & 2 to 16 years. | Case–cohort study | 3578 | 2-16years | CYD-TDV protected against severe VCD and hospitalization for VCD for 5 years in persons who had exposure to dengue before vaccination. | Asia-Pacific region, Latin America, and Thailand |

| | | | | | | |
|---|---|---|---|---|---|---|
| Plennevaux et al., 2018 | Assessed the impact of dengue vaccination on the serological diagnosis of dengue in larger and more diverse epidemiological settings of 2 phase III CYD-TDV efficacy studies. | RCT | 31,000 | 2-16years | Results showed that baseline dengue serostatus (as defined by the PRNT50) had an impact on the IgM and IgG levels observed in VCD and other febrile episodes among CYD-TDV recipients and controls. | 10 Asia and Latin American countries |
| Moodie et al., 2018 | Investigated the association of neutralizing antibody titers with dengue occurrence with the level of vaccine efficacy to prevent dengue | Case-Cohort | 31,144 | 2-16years | Neutralizing antibody titers postdose 3 correlates with CYD-TDV vaccine efficacy to prevent dengue. High titers are associated with high VE for all serotypes, baseline serostatus groups, age groups, and both trials. | USA |
| Olivera-Botello et al., 2016 | Investigated whether vaccination with CYD-TDV protected individuals from asymptomatic infection, using a commonly used surrogate measure, primary, secondary, or other seroconversion | RCT | 31,126 | 2-16 years | Vaccine efficacy was marginally higher in subjects aged 9–16 years (38.6%; 95% CI, 22.1%–51.5%). The annual incidence of asymptomatic dengue virus infection in this age group was 14.8%, which was 4.4 times higher than the incidence of symptomatic dengue (3.4%). | Asia (Indonesia, Malaysia, the Philippines, Thailand, and Vietnam) & Latin America (Colombia, Brazil, Mexico, Puerto Rico, and Honduras) |
| Hadinegoro et al., 2015 | Reported long-term safety phase and integrated analyses of data from the efficacy surveillance phase to provide a global view of the clinical profile of the CYD-TDV dengue vaccine. | RCT | 33,266 | 2-16years | The risk among children 2 to 16 years of age was lower in the vaccine group than in the control group. | 5-Asian–Pacific countries and 5- Latin American countries and Thailand |
| Villar et al., 2015 | Investigated the efficacy of a Tetravalent Dengue Vaccine in Children in Latin America | RCT | 20,869 | 9-16 years | The CYD-TDV dengue vaccine was efficacious against VCD and severe VCD and led to fewer hospitalizations for VCD in five Latin American countries where dengue is endemic. | Colombia, Brazil, Mexico, Puerto Rico, and Honduras |
| Dayan et al., 2015 | Vaccine efficacy against symptomatic virologically confirmed dengue (VCD) was assessed by participant age (any age, _9, <9, 2–5, and 6–8 years at the time of the first injection) and baseline dengue serostatus. | Case cohort | 436 | 3-9years | CYD-TDV provided long-term efficacy against symptomatic VCD in seropositive participants aged _9 years, with evidence of persistent protection up to six years after the first dose in this group. | Asia-Pacific & Latin America |
| Dayan et al., 2020 | Investigated the effectiveness of a single-dose mass dengue vaccination in Cebu, Philippines | Case-control study | 31,126 | 9-14years | A single dose of CYD-TDV given to nine to fourteen-year-old children through a community-based mass vaccination program conferred protection against dengue with warning signs and severe dengue but we were unable to conclude on protection against milder illness. | Philippines |

| | | | | | | |
|---|---|---|---|---|---|---|
| López-Medina et al., 2021 | Investigated the efficacy of a TAK-003 in Healthy Children 2 Years after Vaccination | RCT | 20,099 | 4–16 years | TAK-003 demonstrated continued benefit independent of baseline serostatus in reducing dengue with some decline in efficacy during the second year | Latin America (Brazil, Colombia, Dominican Republic, Panama & Nicaragua), Sri Lanka, Thailand, Philippines |
| Biswal et al., 2020 | Assess the efficacy, safety, and immunogenicity of a live attenuated tetravalent dengue vaccine (TAK-003) in healthy children | RCT | 20,099 | 4-16years | TAK-003 was well tolerated and efficacious against symptomatic dengue in children regardless of serostatus before immunization. Vaccine efficacy varied by serotype, warranting continued follow-up to assess longer-term vaccine performance. | Asia (Philippines, Sri Lanka, and Thailand) and Latin America (Brazil, Colombia, Dominican Republic, Nicaragua, Panama). |
| Rivera et al., 2022 | Investigated a three-year Efficacy and Safety of Takeda's Dengue Vaccine Candidate | RCT | 20,099 | 4-16years | TAK-003 was efficacious against symptomatic dengue over 3 years. There were no safety risks. | Latin America (Panama, Nicaragua) & Asia ( Philippines, Sri Lanka) |
| Biswal et al., 2019 | Investigated the efficacy of a Tetravalent Dengue Vaccine in Healthy Children | RCT | 20,071 | 4-16years | TAK-003 was efficacious against virologically confirmed dengue fever among healthy children, irrespective of previous dengue exposure. | Brazil, Colombia, Dominican Republic, Nicaragua, Panama, Philippines, Sri Lanka, and Thailand |
| Saez-Llorens et al., 2023 | Investigated the effect of the Tetravalent Dengue Vaccine TAK-003 on Sequential Episodes of Symptomatic Dengue | RCT | 13,380 | 4-16years | TAK-003 vaccination resulted in a reduced risk of experiencing sequential episodes of symptomatic dengue in children | Latin America (Columbia) and Asia (Philippines, Sri Lanka, Thailand) |
| Reynales et al., 2020 | Analyzed the efficacy and safety Trial Data of the Tetravalent Dengue Vaccine in children in Colombia. | Case-cohort | 9740 | 9–16 years | CYD-TDV protected against severe VCD and hospitalization for VCD among individuals previously exposed to dengue before vaccination. | Colombia |
| Ylade et al., 2021 | Conducted a case-control study in Cebu province following the dengue mass vaccination. | Case-control | 490 | 9-14years | A single dose of CYD-TDV given to nine to fourteen-year-old children through a community-based mass vaccination program conferred protection against dengue with warning signs and severe dengue but we were unable to conclude on protection against milder illness. | Philippines |
| Sabchareon et al., 2012 | Investigated the efficacy and safety of the recombinant, live-attenuated, CYD tetravalent dengue vaccine in Thai school children | RCT | 4002 | 4–11 years | Efficacious but differed by serotype. The dengue vaccine was well tolerated, with no safety signals after 2 years of follow-up after the first dose. | Thailand |
| Lanata et al., 2012 | Assessed the safety and immunogenicity of a recombinant, live, attenuated, tetravalent dengue vaccine candidate (CYD-TDV) | RCT | 300 | 2-11 years | There were no vaccine-related SAEs, no withdrawals for adverse events after dengue vaccination, and no immediate | Peru |

| | | | | | | |
|---|---|---|---|---|---|---|
| Juraska et al., 2018 | Evaluated the efficacy of a tetravalent dengue vaccine in two phase 3 trials | RCT | 563 | 2-16years | 1. Greater estimated vaccine efficacy of CYD-TDV against serotypes was recorded.<br>2. After accounting for differential VE by serotype, this effect seemed to occur only for younger children, who also had lower baseline seropositivity and potentially a less broadly protective immune response. | Brazil & Thailand |
| Sáez-Llorens et al., 2018 | Assessed the immunogenicity and safety of Takeda's tetravalent dengue vaccine (TDV) candidate over 48 months in children living in dengue-endemic countries. | RCT | 1800 | 2-17years | Takeda vaccine was well tolerated and immunogenic against all four dengue serotypes, irrespective of baseline dengue serostatus. | Dominican Republic, Panama, and the Philippines. |
| Capeding et al., 2011 | Assessed the safety and immunogenicity of the vaccine among children in a flavivirus-endemic region. | RCT | 126 | 2-17years | This phase I study of a live attenuated, tetravalent recombinant dengue vaccine in children as young as 2 years old supports its safety and tolerability in a flavivirus-endemic population. | Philippines |
| Sirivichayakul et al., 2022 | Reported long-term safety and immunogenicity of Takeda's tetravalent dengue vaccine candidate (TAK-003) in healthy children and adults living in dengue-endemic areas | RCT | 212 | 1-11years | The trial demonstrated the persistence of neutralizing antibody titers against TAK-003 over 3 years in children living in dengue-endemic countries, with limited contribution from natural infection. TAK-003 was well tolerated. | Puerto Rico, Columbia, Singapore, and Thailand. |
| Hss et al., 2013 | Evaluated the safety and immunogenicity of Phase III lots of a candidate vaccine (CYD-TDV) in children in Malaysia. | RCT | 250 | 2-11years | This study demonstrated a satisfactory safety profile and a balanced humoral immune response against all four DENV serotypes for CYD-TDV administered via a three-dose regimen to children in Malaysia. | Malaysia |

## RESULTS

The characteristics of the studies including the author and year of publication, the purpose of the study, participants' age, sample size, study design, countries of the studies, and main findings are summarized in Table 2. Out of the 38 studies included most of the studies were conducted in Asian–Pacific countries and Latin American countries where dengue fever is endemic. Also, most studies stratified the ages of the participants to reduce bias. Each of these 38 studies was a clinical trial, focusing on children aged between 0 and 17 years. The sample sizes across the studies ranged from 56 to as large as 51,253 participants. The studies included 32 randomized controlled trials (RCTs) and 6 case-cohort studies.

The risk of bias analysis using the Cochrane Collaboration tool (Higgins et al., 2023) revealed that among the 32 randomized controlled trial (RCT) studies, 25 studies (Arredondo-García et al., 2018; Biswal et al., 2019, 2020; Capeding et al., 2011, 2014; Dayan et al., 2013; Hadinegoro et al., 2015; Hss et al., 2013; Juraska, et al., 2018; Kriengsak et al., 2022; Lanata et al., 2012; López-Medina et al., 2022; Olivera-Botello et al., 2016; Plennevaux et al., 2016, 2018; Rivera et al., 2022; Sabchareon et al., 2004, 2012; Sáez-Llorens et al., 2023; Simasathien et al., 2008; Sirivichayakul et al., 2022; Thomas et al., 2022; Vigne et al., 2017; Villar et al., 2013, 2015) demonstrated a low risk of bias across various domains, including information, confounding, selection, attrition, and reporting biases. Conversely, seven (7) studies (Forrat et al., 2021; España et al., 2019

Yang et al., 2018; Sáez-Llorens et al., 2018; Tricou et al., 2020; Watanaveeradej et al., 2016; Biswal et al., 2021) showed "some concerns" of risk of bias due to insufficient detailed information on the randomization process, such as blinding and concealment (Figures 2a and 2b).

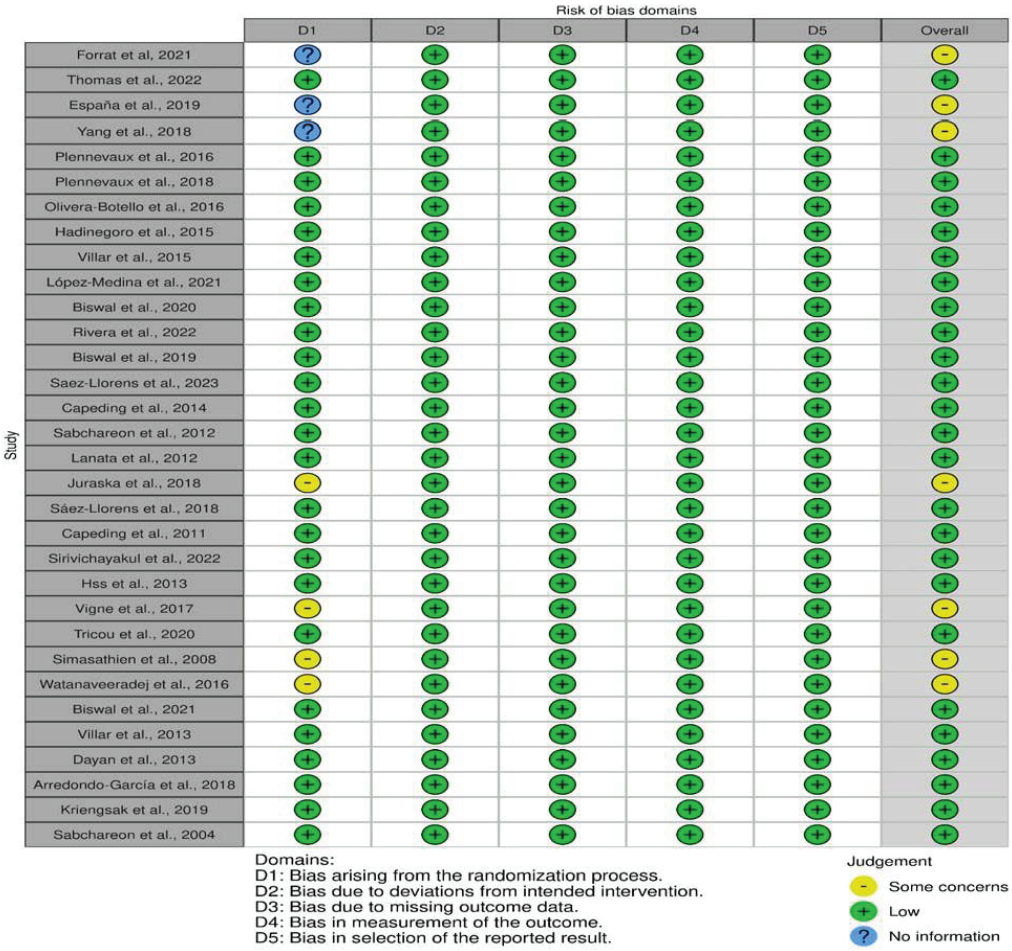


Fig 2a: Risk of Bias for RCTs

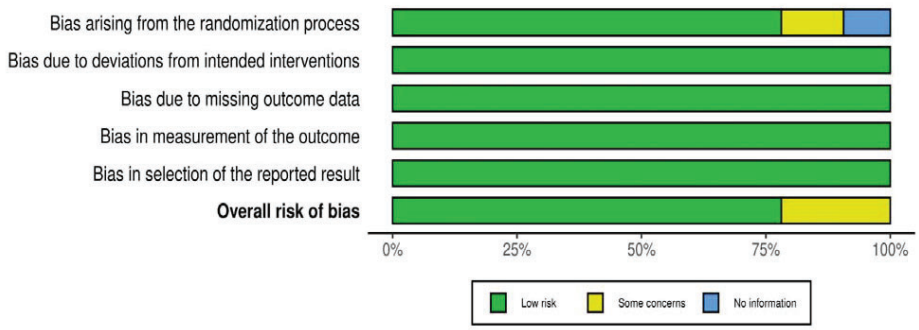


Fig 2b: Risk of Bias for RCTs

Regarding the six cohort studies (Dayan et al., 2015, 2020; Moodie et al., 2018; Reynales et al., 2020; Sridhar et al., 2018; Ylade et al., 2021), three studies [Sridhar et al., 2018; Moodie et al., 2018) exhibited low bias risk across all assessed domains, while the remaining three studies (Dayan et al., 2020; Sridhar et al., 2018; Ylade et al., 2021) displayed a "moderate" risk of bias, notably in reporting bias and missing outcomes (Figures 3a and 3b).

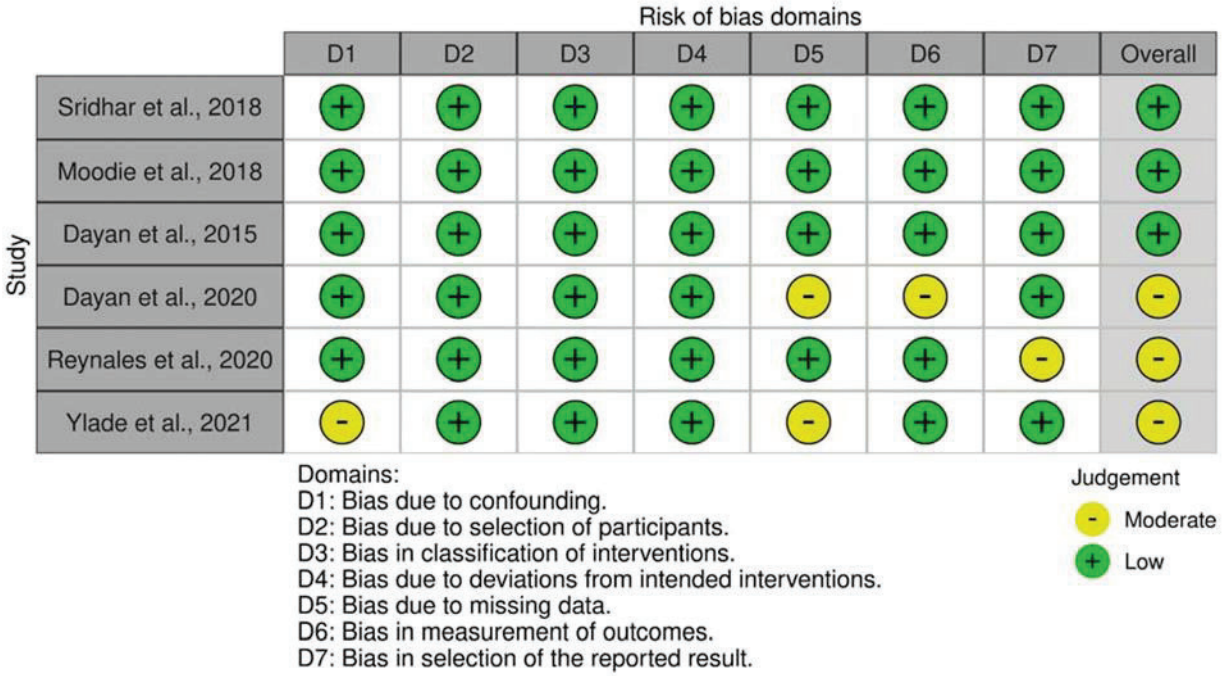


**Fig 3a**: Risk of Bias for Cohort studies

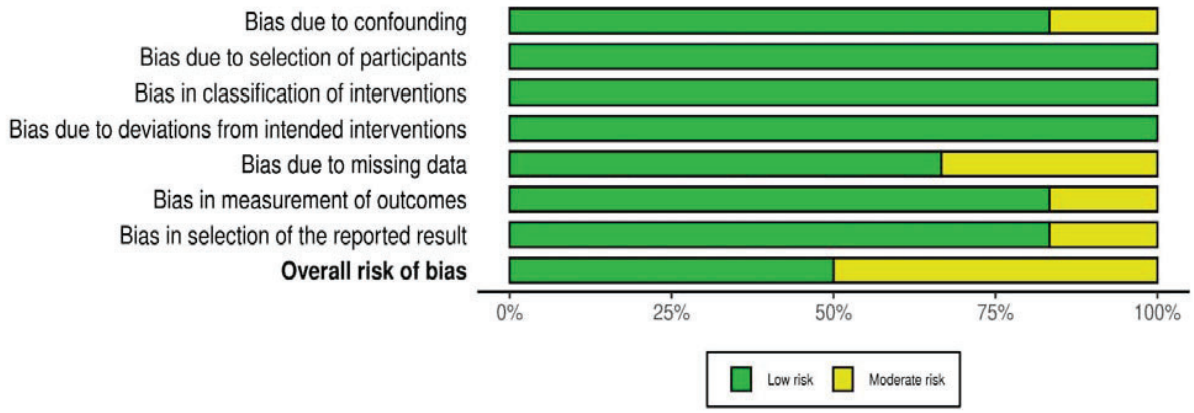


**Fig 3b**: Risk of Bias for Cohort Studies

A comprehensive meta analysis was conducted, pooling data from 27 individual studies, with the primary objective of evaluating the efficacy, immunogenicity, and safety attributes of dengue vaccines. The analysis of these studies revealed invaluable insights summarized in Tables 3, 4, and 5. The results revealed that twelve (12) studies were utilized to assess the efficacy of dengue vaccines, each study contributing unique perspectives and data elucidating the vaccine's performance and effectiveness, as presented in Table 3.

**Table 3. Meta-analysis of vaccine efficacy**

| | Intervention | | Control | | | Risk Ratio | Risk Ratio |
|---|---|---|---|---|---|---|---|
| Study or Subgroup | Events | Total | Events | Total | Weight | IV, Random, 95% CI | IV, Random, 95% CI |
| Capeding et al., 2014 | 402 | 6851 | 245 | 3424 | 9.5% | 0.82 [0.70, 0.96] | |
| Forrat et al., 2021 | 10 | 1460 | 28 | 687 | 5.7% | 0.17 [0.08, 0.34] | |
| Hadinegoro et al., 2015 | 65 | 22177 | 39 | 11089 | 8.1% | 0.83 [0.56, 1.24] | |
| López-Medina et al., 2021 | 97 | 12577 | 106 | 6268 | 8.9% | 0.46 [0.35, 0.60] | |
| Olivera-Bote et al., 2016 | 219 | 2485 | 157 | 1184 | 9.4% | 0.66 [0.55, 0.81] | |
| Plennevaux et al., 2016 | 195 | 1394 | 53 | 733 | 8.8% | 1.93 [1.45, 2.59] | |
| Plennevaux et al., 2018 | 575 | 1284 | 709 | 1284 | 9.8% | 0.81 [0.75, 0.88] | |
| Rivera et al., 2022 | 390 | 13380 | 494 | 6687 | 9.6% | 0.39 [0.35, 0.45] | |
| Sabchareon et al., 2012 | 45 | 2522 | 32 | 1251 | 7.7% | 0.70 [0.45, 1.09] | |
| Saez-Llsoren et al., 2023 | 5 | 13380 | 13 | 6687 | 3.9% | 0.19 [0.07, 0.54] | |
| Thomas et al., 2022 | 106 | 195 | 75 | 139 | 9.3% | 1.01 [0.82, 1.23] | |
| Villar et al., 2015 | 176 | 11793 | 221 | 5809 | 9.3% | 0.39 [0.32, 0.48] | |
| **Total (95% CI)** | | **89498** | | **45242** | **100.0%** | **0.62 [0.48, 0.81]** | |
| Total events | 2285 | | 2172 | | | | |

Heterogeneity: Tau² = 0.18; Chi² = 217.73, df = 11 (P < 0.00001); I² = 95%
Test for overall effect: Z = 3.53 (P = 0.0004)

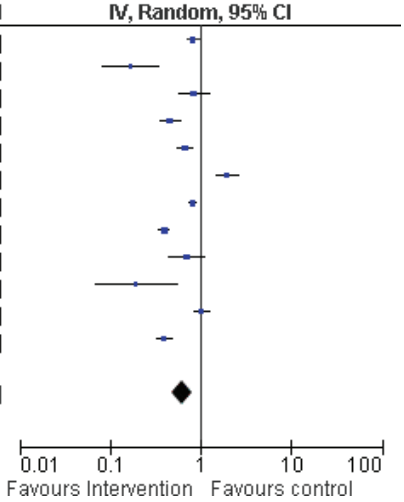


Simultaneously, nine (9) studies assessed the immunogenicity of these vaccines, assessing their ability to stimulate immune responses in the recipients' bodies. A comprehensive overview of vaccine immunogenicity has been presented in Table 4, encapsulating the diverse findings and implications of these individual studies.

**Table 4. Meta-analysis of immunogenicity of vaccine**

| | Intervention | | Control | | | Risk Ratio | Risk Ratio |
|---|---|---|---|---|---|---|---|
| Study or Subgroup | Events | Total | Events | Total | Weight | IV, Random, 95% CI | IV, Random, 95% CI |
| Biswal et al., 2019 | 78 | 13380 | 199 | 6687 | 12.7% | 0.20 [0.15, 0.25] | |
| Biswal et al., 2020 | 114 | 12700 | 206 | 6316 | 12.7% | 0.28 [0.22, 0.35] | |
| Biswal et al., 2021 | 194 | 300 | 50 | 100 | 12.8% | 1.29 [1.05, 1.60] | |
| Dayan et al., 2013 | 5 | 100 | 3 | 50 | 8.1% | 0.83 [0.21, 3.35] | |
| Hss et al., 2013 | 11 | 199 | 6 | 51 | 10.1% | 0.47 [0.18, 1.21] | |
| Sirivichayak et al., 2022 | 23 | 227 | 5 | 97 | 10.2% | 1.97 [0.77, 5.02] | |
| Sáez-Llorens et al., 2017 | 21 | 1596 | 9 | 198 | 11.0% | 0.29 [0.13, 0.62] | |
| Tricou et al., 2020 | 37 | 1596 | 13 | 198 | 11.6% | 0.35 [0.19, 0.65] | |
| Villar et al., 2013 | 10 | 401 | 15 | 199 | 10.9% | 0.33 [0.15, 0.72] | |
| **Total (95% CI)** | | **30499** | | **13896** | **100.0%** | **0.48 [0.25, 0.91]** | |
| Total events | 493 | | 506 | | | | |

Heterogeneity: Tau² = 0.84; Chi² = 164.18, df = 8 (P < 0.00001); I² = 95%
Test for overall effect: Z = 2.23 (P = 0.03)

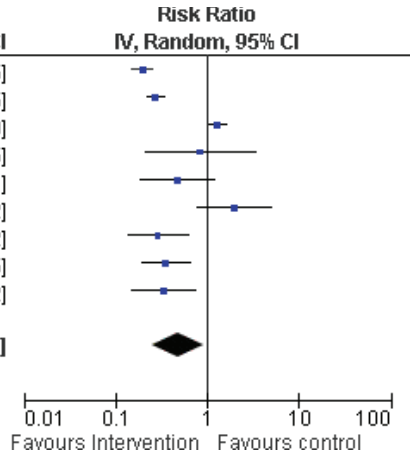

Furthermore, this comprehensive meta-analysis assessed six (6) studies specifically focused on the safety profiles of dengue vaccines. These studies evaluated adverse events, potential side effects, and overall safety measures associated with these vaccines. The findings are shown in Table 5, offering a concise yet comprehensive overview of the safety considerations surrounding dengue vaccine administration.

**Table 5. Meta-analysis vaccine safety**

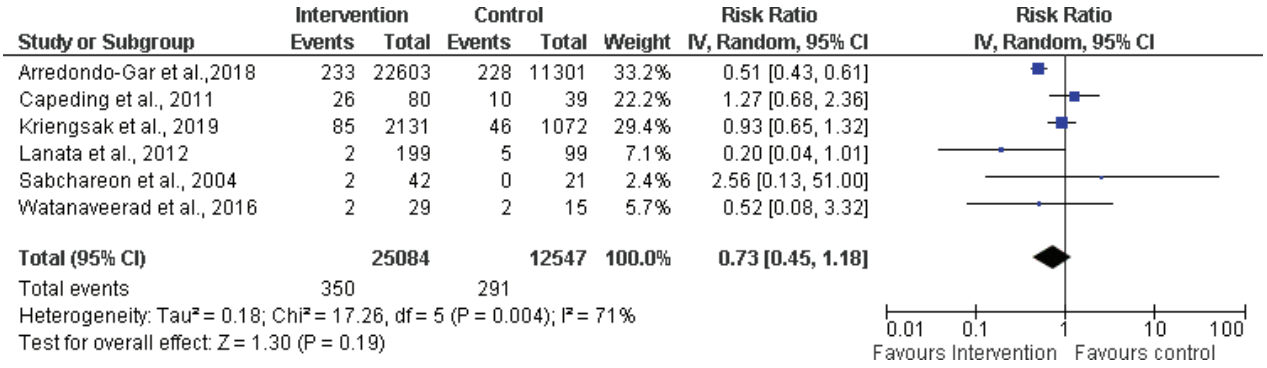


## Systematic Review findings Efficacy of dengue vaccine

Among the 38 studies, 23 demonstrated the effectiveness of dengue vaccines in children involved in clinical trials. The majority of studies consistently demonstrated the efficacy of both CYD-TDV and Takeda vaccines in preventing dengue fever caused by the four serotypes of the dengue virus (Forrat et al., 2021; España et al., 2019; Yang et al., 2018; Sridhar et al., 2018; Dayan et al., 2015, 2020; Reynales et al., 2020; Sabchareon et al., 2012). However, a few studies reported discrepancies in their outcomes, revealing a lack of efficacy (Juraska et al., 2018; Plennevaux et al., 2016; Thomas et al., 2022). The effectiveness of these vaccines varied based on their formulations. While some vaccines displayed differing levels of efficacy against specific serotypes, others showcased broader protection, encompassing multiple serotypes.

## Immunogenicity of dengue vaccine candidates

Out of the 38 studies examined, eleven (11) studies confirmed that children administered with the dengue vaccine during clinical trials successfully triggered an immune response, particularly in the production of antibodies against the dengue virus. Among these studies, seven focused on evaluating the immunogenicity of CYD_TDV in children, while the remaining four investigated the immunogenicity associated with the Tekade vaccine. About seven (7) studies illustrated a robust humoral response against all four DENV serotypes when CYD-TDV was administered to children through a three-dose regimen (Capeding et al., 2011; Dayan et al, 2013; Hss et al., 2013; Simasathien et al., 2008; Vigne et al., 2017; Villar et al., 2013; Watanaveeradej et al., 2016). Conversely, the studies four studies highlighted that the Takeda vaccine exhibited strong immunogenicity against all four dengue serotypes (Biswal et al., 2021; Sáez-Llorens et al., 2018; Sirivichayakul et al., 2022; Tricou et al., 2020).

## Safety concerns about the dengue vaccine

Out of the 38 studies reviewed, 10 studies specifically addressed the safety profile of vaccines administered to children, particularly in regions where dengue is endemic (Hadinegoro et al., 2015; Sridhar et al., 2018; Capeding et al., 2014; Hss et al., 2013; Kriengsak et al., 2022; Sabchareon et al., 2004; Sáez-Llorens et al.,

2018; Simasathien et al., 2008; Tricou et al., 2020; Watanaveeradej et al., 2016; Lanata et al., 2012). These studies reported incidents such as hospitalization due to confirmed dengue cases, occasional deaths, and minor reactions such as rashes and headaches, mainly observed among both vaccinated and control children. These incidents were primarily documented in Asia and Latin America, categorized by the age of study enrollment and the study year.

## DISCUSSION

In this systematic review, the authors investigated the potential prospect of various dengue vaccines by examining the efficacy, immunogenicity, and safety of dengue vaccine candidates in children (ranging from 0-17 years) involved in clinical trials. Based on the findings, children previously exposed to dengue fever (seropositive) before vaccination exhibited superior outcomes in terms of immunogenicity, efficacy, and safety compared to those without prior exposure (seronegative). The clinical studies referenced in this review were registered with ClinicalTrials.gov.

### Efficacy

In terms of efficacy, the results showed that dengue vaccines demonstrated robust protection against hospitalized and severe virologically confirmed dengue (VCD) and were efficacious when administered in children, but the efficacy varied over a long-term follow-up in a clinical trial. According to River et al., 2022, TAK-003 was efficacious against symptomatic dengue over 3 years. However, efficacy declined over time but remained robust against hospitalized dengue. This ongoing phase 3 study demonstrated that TAK-003 was efficacious against symptomatic dengue in children in a varied epidemiological setting across 8 (eight) dengue-endemic countries over 3 years post-vaccination and supports the utility of TAK-003 in dengue control. According to Reynales et al., 2020, participants who had prior exposure to dengue (seropositive) before receiving the Dengvaxia/CYD-TDV vaccination demonstrated protection against severe virologically confirmed dengue (VCD) and subsequent hospitalizations for VCD for up to six (6) years. In contrast, individuals without previous dengue exposure (seronegative) before vaccination might face a potentially higher risk of experiencing these severe outcomes during outbreaks. Although dengue vaccines (CYD-TDV & Tadeka) were reported to be highly efficacious against the four (4) DENV serotypes clinical trials in children (Dayan et al., 2015; Forrat et al., 2021; Olivera-Botello et al., 2018; Rivera et al., 2022; Thomas et al., 2022; Villar et al., 2015; Yang et al., 2018; Capeding et al., 2014; Juraska et al., 2018), some other studies discovered a distinct bias in vaccine efficacy (both CYD-TDV & Tadeka) estimates away from the null due to lower detectability of primary DENV infections among seronegative individuals in the vaccinated group. Also reported variation and decline in vaccine efficacy irrespective of the type of DENV serotype, previous exposure to dengue, as well as symptomatic dengue, warranting continued follow-up to assess longer-term vaccine performance (Biswal et al., 2020; Dayan et al., 2020; España et al., 2019; Hadinegoro et al., 2015; López- Medina et al., 2022; Sabchareon, et al., 2012).

### Immunogenicity

Immunogenicity is the ability of a foreign substance, such as an antigen, to provoke an immune response in the body of a human or other animal (Leroux-Roels et al., 2011). Immunogenicity in the context of dengue vaccines pertains to the capacity of a vaccine to elicit an immune response against the dengue virus. Dengue vaccines aim to stimulate the immune system, triggering responses that protect against infection. This may involve the generation of neutralizing antibodies and the activation of T cells, which are essential for combating the virus (Ghosh & Dar, 2015).

According to the studies, Both CYD-TDV and Takeda vaccines were well tolerated and immunogenic against all four dengue serotypes, irrespective of baseline dengue serostatus (Capeding et al., 2011; Dayan et al., 2013; Hss et al., 2013; Sáez-Llorens et al., 2018; Sirivichayakul et al., 2022; Tricou et al., 2020; Vigne et al., 2017; Villar et al., 2013). Tricou et

al. (2020) who conducted a long-term clinical trial of TAK-003 reported that the vaccine elicited antibody responses against all four serotypes, which persisted to 48 months post-vaccination, regardless of baseline serostatus. On the contrary, Watanaveeradej et al. (2016) reported that the results of two follow-up studies they conducted using the CYD-TDV indicated that the live-attenuated DENV candidate vaccine did not elicit a durable primary humoral immune response. Also, Vigne et al. (2017) reported that CYD-TDV elicits neutralizing antibody responses against all dengue serotypes, with differences by age and endemicity, which persist above baseline levels in endemic countries.

**Safety**

Regarding safety, studies indicated satisfactory safety profiles for the vaccines CYD-TDV and Tekade, with no significant safety concerns identified, particularly among children with prior dengue exposure (Capeding et al., 2011, 2014; Hadinegoro et al., 2015; Hss et al., 2013; Kriengsak et al., 2022; Sridhar et al., 2018; Tricou et al., 2020; Vigne et al., 2017). Arredondo-García et al. (2018) reported the overall Relative Risk in children aged <9 years for Year 1 to Year 4 follow-up, with a higher protective effect in the 6–8-year-olds than in the 2-5-year-olds. CYD-TDV proved effective in shielding children who had encountered dengue before vaccination. Despite its high efficacy, there remained a low risk of some vaccinated individuals contracting dengue. Common side effects experienced by most children included mild to moderate fever, rash, headache, and myalgia occurring within 12 days after the first (1st) dose, typically lasting for three (3) days or less (Sabchareon et al., 2004). Reynales et al. (2020) reported that participants in the CYD-TDV group experienced at least one (1) serious adverse event (SAE), while 16.2% of the control group experienced SAEs, mostly related to infectious diseases. Out of the 29 deaths reported, 20 occurred in the CYD-TDV group, and 9 in the control group. However, none of the deaths and some of the SAEs were related to CYD-TDV (respiratory, thoracic, and mediastinal disorders and asthma); the deaths were due to traffic accidents, violence (i.e., gunshot wounds, stabbing, homicide), intentional self-poisoning and exposure to other unspecified chemicals and noxious substances, etc.

Hadinegoro et al. (2015) conducted a long-term surveillance spanning 3 to 6 years to monitor the safety of children who received the CYD-TDV Dengue vaccine. They recorded a significant increase in hospitalizations, particularly observing an unexplained surge in dengue-related hospital admissions among children under 9 years old during the third year. This trend requires careful monitoring in long-term follow-ups. However, among children aged 2 to 16 years, the risk was lower in the vaccine group compared to the control group. Moreover, there was a reduced risk of hospitalization for dengue overall for up to 2 years after completing the three-dose vaccination schedule among children aged 9 to 16 years.

In the study conducted by Sáez-Llorens et al. (2018), they reported that vaccine-related unsolicited adverse events occurred in 14 (2%) out of 562 participants. However, no vaccine-related serious adverse events were identified. Rivera et al. [45] documented seven deaths during the clinical trials of Takeda's vaccine, TAK-003, where five occurred in TAK-003 recipients and two in placebo recipients. They also reported serious adverse events (SAEs) in 2.9% of those who received TAK-003 and 3.5% of those who received the placebo in the initial phase of part 3. However, none of these deaths or SAEs were related to the study vaccine. Overall, no significant safety risks were identified throughout the study period.

Moreover, Biswal et al. (2021) reported no deaths or adverse effects (AEs) leading to withdrawal in their study. During the study, three participants reported four serious adverse events (SAEs): two in the placebo group (both were moderate, then, appendicitis and ankle fracture occurred after the second vaccination) and two in the TAK-003 group (both were severe, then, abdominal pain and urinary tract issues occurred after the first vaccination). None of these SAEs were attributed to the trial vaccination or procedures, and none resulted in withdrawal from

the trial or discontinuation of the vaccination process. Simasathien et al. (2008) in their study reported that the dengue vaccine was well tolerated with no serious adverse events or alert laboratory values. One volunteer experienced fever (38.2°C, < 2 days) and associated DENV4 vaccine viremia 7 days after Dose 2.

**Meta-analysis findings**

Following article selection and data collection, a meta-analysis was executed as depicted in Tables 3-5. The age range of the participating children spanned from 2 to 17 years. The random-effects model indicated risk ratios (RR) and confidence intervals of 0.62 (0.48-0.81), 0.48 (0.25-0.91), and 0.73 (0.45-1.18) for vaccine efficacy, immunogenicity, and safety respectively. Discrepancies emerged between the outcomes of studies with larger participant numbers and those with smaller cohorts.

**Vaccine Efficacy**

Regarding vaccine efficacy (Table 3), the 95% confidence interval of 10 studies exhibited greater precision (Capeding et al., 2014; Hadinegoro et al., 2015; López-Medina et al., 2022; Olivera-Botello et al., 2016; Plennevaux et al., 2016, 2018; Rivera et al., 2022; Sabchareon et al., 2012; Thomas et al., 2022; Villar et al., 2015), while 2 studies (Forrat et al., 2021; Sáez-Llorens et al., 2023) displayed wider confidence intervals. This discrepancy suggests that the 10 studies provided more precise estimates concerning vaccine efficacy compared to the other 3 studies. When evaluating individual study effects, only 5 studies crossed the line of null effect indicating no significant effect on vaccine efficacy within the intervention group, favoring instead the control group. Eight (8) studies demonstrated statistical significance, indicating the efficacy of dengue vaccines in the intervention group. However, the overall pooled effect yielded a risk ratio of 0.62 (0.48-0.81), highlighting the greater efficacy of dengue vaccines in the intervention (exposed) group compared to the control group. Furthermore, since the confidence interval of the overall effect did not intersect the null effect line, it can be concluded as statistically significant ($p = 0.0004$). Nonetheless, the meta-analysis revealed a high heterogeneity (I2) of 95%, emphasizing the need for additional studies to comprehensively gauge efficacy.

**Vaccine immunogenicity**

Based on the findings from the meta-analysis of vaccine immunogenicity (Table 4), in terms of individual study effects, three (3) studies revealed no significant impact of vaccine immunogenicity within the intervention group, thereby aligning with the null effect (Dayan et al., 2013; Hss et al., 2013; Sirivichayakul et al., 2022). Conversely, six (6) studies exhibited statistical significance, underscoring the immunogenicity of dengue vaccines within the intervention group (Biswal et al., 2019, 2020, 2021; Sáez- Llorens et al., 2018; Tricou et al., 2020; Villar et al., 2013). The overall pooled effect yielded a risk ratio of 0.48 (0.25-0.91), showing notably heightened immunogenicity among those receiving dengue vaccines within the intervention group compared to the control group. Notably, the confidence interval of the overall effect didn't intersect the null effect line, indicating statistical significance ($p = 0.03$), it can be concluded that there's a significant difference. Despite this, the meta-analysis indicated substantial heterogeneity (I2) at 95%, indicating the necessity for further studies to comprehensively evaluate the discrepancy.

**Vaccine Safety**

The findings from the meta-analysis on vaccine safety revealed varying precision in the 95% confidence intervals across the studies. Three studies displayed greater precision (Arredondo-García et al., 2018; Capeding et al., 2011; Kriengsak et al., 2022), while three (3) studies showed wider intervals (Lanata et al., 2012; Sabchareon et al., 2004; Watanaveeradej et al., 2016). This discrepancy indicates that the three studies provided more precise estimates regarding vaccine safety compared to the later. In terms of individual study effects, among the six (6) studies examined, four (4) demonstrated no statistical significance, crossing the null effect line. This suggests that safety concerns were observed within the intervention group compared

to the control group. However, only two (2) studies had statistical significance showing that the dengue vaccine is safe in the intervention group (Arredondo- García et al., 2018; Lanata et al., 2012). The overall pooled effect yielded a risk ratio of 0.73 (0.45-1.18), indicating that safety concerns were indeed recorded in the intervention group compared to the control group. Yet, with the confidence interval of the overall effect intersecting the null effect line ($p = 0.19$), it can be concluded that there's no significant difference, suggesting a preference toward the control group in the analysis. Furthermore, the meta-analysis revealed high heterogeneity (I2) at 71%, emphasizing the imperative need for further studies to address and clarify these observed discrepancies.

## LIMITATIONS

The study has limitations regarding its focus on English-language articles, potentially excluding valuable non-English research. Additionally, the study concentrated on children aged 0-17 years, which may limit its generalizability to adult populations. Most of the studies analyzed were conducted in dengue- endemic regions, which could potentially limit the applicability of the findings to other geographical areas. There's also a reliance on peer-reviewed articles, potentially overlooking unpublished data and ongoing trials. Variability in study methodologies and durations could affect results consistency, while limited extended follow-up periods may impact long-term efficacy and safety assessments. Furthermore, diverse vaccine formulations and dosages make direct comparisons challenging. Lastly, confounding factors like prior dengue exposure and healthcare settings introduce complexities in data interpretation.

## CONCLUSION

This systematic review underscores the promising potential of dengue vaccines in combating the severe impact of dengue fever, particularly in endemic regions. However, the observed variations in efficacy and the influence of prior exposure necessitate further research and long-term follow-ups to ascertain sustained efficacy, safety, and optimal deployment strategies. The meta-analysis underscored the overall efficacy and immunogenicity benefits of dengue vaccines, emphasizing their potential to confer protection against dengue fever. However, safety concerns were evident, albeit without statistically significant differences between the intervention and control groups in the analyzed studies. These findings collectively highlight the positive potential of dengue vaccines for mitigating the disease burden. Yet, it is imperative to address safety concerns, particularly in populations without prior dengue exposure, and optimize vaccine efficacy across diverse epidemiological settings. This study will serve as a valuable resource for guiding future vaccine development, public health policies, and interventions aimed at curbing the global burden of dengue fever.

## REFERENCES


Arredondo-García, J. L., Hadinegoro, S. R., Reynales, H., Chua, M. N., Rivera Medina, D. M., Chotpitayasunondh, T., Tran, N. H., Deseda, C. C., Wirawan, D. N., Cortés Supelano, M., Frago, C., Langevin, E., Coronel, D., Laot, T., Perroud, A. P., Sanchez, L., Bonaparte, M., Limkittikul, K., Chansinghakul, D., Gailhardou, S., Noriega, F., Wartel, T. A., Bouckenooghe, A., & Zambrano, B. (2018). CYD-TDV Dengue vaccine study group. Four-year safety follow-up of the tetravalent dengue vaccine efficacy randomized controlled trials in Asia and Latin America. Clin Microbiol Infect.; 24(7), 755-763. doi: 10.1016/j.cmi.2018.01.018

Bhatt, S., Gething, P. W., Brady, O. J., Messina, J. P., Farlow, A. W., Moyes, C. L., Drake, J. M., Brownstein, J. S., Hoen, A. G., Sankoh, O., Myers, M. F., George, D. B., Jaenisch, T., Wint, G. R., Simmons, C. P., Scott, T. W., Farrar, J. J., & Hay, S. I. (2013). The global distribution and burden of dengue. Nature; 496(7446), 504-7. doi: 10.1038/nature12060

Biswal, S., Mendez Galvan, J. F., Macias Parra, M., Galan-Herrera, J. F., Carrascal Rodriguez, M. B., Rodriguez Bueno, E. P., Brose, M., Rauscher, M., LeFevre, I., Wallace, D., & Borkowski, A. (2021). Immunogenicity, and safety of a tetravalent dengue vaccine in dengue-naïve adolescents in Mexico City. Rev Panam Salud Publica.; 45, e67. doi: 10.26633/RPSP.2021.67

Biswal, S., Borja-Tabora, C., Martinez Vargas, L.,

Velásquez, H., Theresa Alera, M., Sierra, V., Johana Rodriguez-Arenales, E., Yu, D., Wickramasinghe, V. P., Duarte Moreira, E. Jr., Fernando, A. D., Gunasekera, D., Kosalaraksa, P., Espinoza, F., López-Medina, E., Bravo, L., Tuboi, S., Hutagalung, Y., Garbes, P., Escudero, I., Rauscher, M., Bizjajeva, S., LeFevre, I., Borkowski, A., Saez-Llorens, X., & Wallace, D. (2020). TIDES study group. Efficacy of a tetravalent dengue vaccine in healthy children aged 4-16 years: a randomized, placebo-controlled, phase 3 trial. Lancet; 395(10234), 1423-1433. doi: 10.1016/S0140-6736(20)30414-1

Biswal, S., Reynales, H., Saez-Llorens, X., Lopez, P., Borja-Tabora, C., Kosalaraksa, P., Sirivichayakul, C., Watanaveeradej, V., Rivera, L., Espinoza, F., Fernando, L., Dietze, R., Luz, K., Venâncio da Cunha, R., Jimeno, J., López-Medina, E., Borkowski, A., Brose, M., Rauscher, M., LeFevre, I., Bizjajeva, S., Bravo, L., & Wallace, D. (2019). TIDES Study Group. Efficacy of a Tetravalent Dengue Vaccine in Healthy Children and Adolescents. N Engl J Med.; 381(21), 2009-2019. doi: 10.1056/NEJMoa1903869

Brady, O. J., Gething, P. W., Bhatt, S., Messina, J. P., Brownstein, J. S., Hoen, A. G., Moyes, C. L., Farlow, A. W., Scott, T. W., & Hay, S. I. (2012). Refining the global spatial limits of dengue virus transmission by evidence-based consensus. PLoS Negl Trop Dis.; 6(8), e1760. doi: 10.1371/journal.pntd.0001760

Capeding, M. R., Tran, N. H., Hadinegoro, S. R., Ismail, H. I., Chotpitayasunondh, T., Chua, M. N., Luong, C. Q., Rusmil, K., Wirawan, D. N., Nallusamy, R., Pitisuttithum, P., Thisyakorn, U., Yoon, I. K., van der Vliet, D., Langevin, E., Laot, T., Hutagalung, Y., Frago, C., Boaz, M., Wartel, T. A., Tornieporth, N. G., Saville, M., & Bouckenooghe, A. (2014). CYD14 Study Group. Clinical efficacy and safety of a novel tetravalent dengue vaccine in healthy children in Asia: a phase 3, randomized, observer- masked, placebo-controlled trial. Lancet; 384(9951), 1358-65. doi: 10.1016/S0140- 6736(14)61060-6

Capeding, R. Z., Luna, I. A., Bomasang, E., Lupisan, S., Lang, J., Forrat, R., Wartel, A., & Crevat, D. (2011). Live-attenuated, tetravalent dengue vaccine in children, adolescents, and adults in a dengue- endemic country: randomized controlled phase I trial in the Philippines. Vaccine; 29(22), 3863- 72. doi: 10.1016/j.vaccine.2011.03.057

Clements, A. N. (2012). Arboviruses: Characteristics and concepts. In: Clements AN, editor. The biology of mosquitoes: Transmission of viruses and interactions with bacteria. Wallingford: CAB International. p. 125

Dayan, G. H., Langevin, E., Gilbert, P. B., Wu, Y., Moodie, Z., Forrat, R., Price, B., Frago, C., Bouckenooghe, A., Cortes, M., Noriega, F., DiazGranados, C. A. (2020). Assessment of the long- term efficacy of a dengue vaccine against symptomatic, virologically-confirmed dengue disease by baseline dengue serostatus. Vaccine; 38(19), 3531-3536. doi: 10.1016/j.vaccine.2020.03.029

Dayan, G., Arredondo, J. L., Carrasquilla, G., Deseda, C. C., Dietze, R., Luz, K., Costa, M. S. N., Cunha, R. V., Rey, L. C., Morales, J., Reynales, H., Miranda, M., Zambrano, B., Rivas, E., Garbes, P., & Noriega, F. (2015). Prospective cohort study with active surveillance for fever in four dengue-endemic countries in Latin America. American Journal of Tropical Medicine and Hygiene; 93(1), 18– 23. doi:10.4269/ajtmh.13-0663

Dayan, G. H., Thakur, M., Boaz, M., & Johnson, C. (2013). Safety, and immunogenicity of three tetravalent dengue vaccine formulations in healthy adults in the USA. Vaccine; 31(44), 5047-54. doi: 10.1016/j.vaccine.2013.08.088

Dia, I., Diagne, C. T., Ba, Y., Diallo, D., Konate, L., & Diallo, M. (2012). Insecticide susceptibility of Aedes aegypti populations from Senegal and Cape Verde Archipelago. Parasites & Vectors; 5, 238. http://www.parasitesandvectors.com/content/5/1/238

España, G., Hogea, C., Guignard, A., ten Bosch, Q. A., Morrison, A. C., Smith, D. L., Scott, T. W., Schmidt, A., & Perkins, T. A. (2019). Biased efficacy estimates in phase-III dengue vaccine trials due to heterogeneous exposure and differential detectability of primary infections across trial arms. PLoS ONE;14(1), e0210041. https://doi.org/10.1371/journal.pone.0210041

Forrat, R., Dayan, G. H., DiazGranados, C. A, Bonaparte, M., Laot, T., Capeding, M. R., Sanchez, L., Coronel, D. L., Reynales, H., Chansinghakul, D., Hadinegoro, S. R. S., Perroud, A. P., Frago, C., Zambrano, B., Machabert, T., Wu, Y., Luedtke, A., Price, B., Vigne, C., Haney, O., Savarino, S. J., Bouckenooghe, A., & Noriega, F. (2021). Analysis of hospitalized and severe dengue cases over the 6 years of follow-up of the tetravalent dengue vaccine (CYD-TDV) efficacy trials in Asia and

Latin America. Clin Infect Dis.; 73(6), 1003-1012. doi: 10.1093/cid/ciab288

Ghosh, A., & Dar, L. (2015). Dengue vaccines: challenges, development, current status, and prospects. Indian J Med Microbiol.; 33(1), 3-15. doi: 10.4103/0255-0857.148369

Gubler, D. J. (2011). Dengue, urbanization, and globalization: The Unholy trinity of the 21st century. Trop Med Health; 39(4 Suppl), 3-11. doi: 10.2149/tmh.2011-S05

Guy, B., Barrere, B., Malinowski, C., Saville, M., Teyssou, R., & Lang, J. (2011). From research to phase III: preclinical, industrial, and clinical development of the Sanofi Pasteur tetravalent dengue vaccine. Vaccine; 29(42), 7229-7241. doi: 10.1016/j.vaccine.2011.06.094

Guzman, M. G., & Harris, E. (2015). Dengue. Lancet; 385(9966), 453-65. doi: 10.1016/S0140-6736(14)60572-9

Hadinegoro, S. R., Arredondo-García, J. L., Capeding, M. R., Deseda, C., Chotpitayasunondh, T., Dietze, R., Muhammad, Ismail, H. I., Reynales, H., Limkittikul, K., Rivera-Medina, D. M., Tran, H. N., Bouckenooghe, A., Chansinghakul, D., Cortés, M., Fanouillere, K., Forrat, R., Frago, C., Gailhardou, S., Jackson, N., Noriega, F., Plennevaux, E., Wartel, T. A., Zambrano, B., & Saville, M. (2015). CYD-TDV dengue vaccine working group. Efficacy and long-term safety of a dengue vaccine in regions of endemic disease. N Engl J Med.; 373(13), 1195-1206. doi: 10.1056/NEJMoa1506223

Halstead, S. B. (2007). Dengue. Lancet; 370(9599), 1644-1652. doi: 10.1016 /S0140-673 6(07)61687-0

Higgins, J. P. T., Thomas, J., Chandler, J., Cumpston, M., Li, T., Page, M. J., & Welch, V. A. (2023). Cochrane Handbook for Systematic Reviews of Interventions version 6.4 (updated August 2023). Cochrane, 2023. Available from www.training.cochrane.org/handbook

Hss, A. S., Koh, M. T., Tan, K. K., Chan, L. G., Zhou, L., Bouckenooghe, A., Crevat, D., & Hutagalung, Y. (2013). Safety and immunogenicity of a tetravalent dengue vaccine in healthy children aged 2-11 years in Malaysia: a randomized, placebo-controlled, Phase III study. Vaccine; 31(49), 5814-21. doi: 10.1016/j.vaccine.2013.10.013

Joshi, V., Mourya, D. T., & Sharma, R. C. (2002). Persistence of dengue-3 virus through transovarial transmission passage in successive generations of Aedes aegypti mosquitoes. Am J Trop Med Hyg.; 67, 158–161. doi: 10.4269/ajtmh.2002.67.158

Juraska, M., Magaret, C. A., Shao, J., Carpp, L. N., Fiore-Gartland, A. J., Benkeser, D., Girerd-Chambaz, Y., Langevin, E., Frago, C., Guy, B., Jackson, N., Duong Thi Hue, K., Simmons, C. P., Edlefsen, P. T., & Gilbert, P. B. (2018). Viral genetic diversity and protective efficacy of a tetravalent dengue vaccine in two phase 3 trials. Proc Natl Acad Sci U.S.A.; 115(36), E8378-E8387. doi: 10.1073/pnas.1714250115

Kraemer, M. U. G., Sinka, M. E., Duda, K. A., Mylne, A. .Q. N., Shearer, F. M., Barker, C. M., Moore, C. G., Carvalho, R. G., Coelho, G. E., Bortel, W. V., Hendrickx, G., Schaffner, F., Elyazar, I. R. F., Teng, H- J., Brady, O. J., Messina, J. P., Pigott, D. M., Scott, T. W., Smith, D. L., Wint, G. R. W., Golding, N., & Hay, S. I. (2015). The global distribution of the arbovirus vectors Aedes aegypti and Ae. albopictus. eLife; 4, e08347

Kriengsak. L., Chanthavanich, P., Lee, K. S., Lee, J-S., Chatchen, S., Lim, S-K, Arunsodsai1, W., Yoon, I-K., & Lim, J. K. (2022). Dengue virus seroprevalence study in Bangphae district, Ratchaburi, Thailand: A cohort study in 2012-2015. PLoS Negl Trop Dis.; 16(1), e0010021. https://doi. org/10.1371/journal.pntd.0010021

Kyle, J. L., & Harris, E. (2008). Global spread and persistence of dengue. Annu Rev Microbiol.; 62, 71-92. doi: 10.1146/annurev.micro.62.081307.163005

Lanata, C. F., Andrade, T., Gil, A. I., Terrones, C., Valladolid, O., Zambrano, B., Saville, M., & Crevat, D. (2012). Immunogenicity and safety of tetravalent dengue vaccine in 2-11 year-olds previously vaccinated against yellow fever: randomized, controlled, phase II study in Piura, Peru. Vaccine; 30(41), 5935-41. doi: 10.1016/j.vaccine.2012.07.043

Leroux-Roels, G., Bonanni, P., Tantawichien, T., & Zepp, F (2011). Vaccine development. Perspectives in Vaccinology; 1 (1), 115–150. doi:10.1016/j.pervac.2011.05.005

Liberati, A., Altman, D. G., Tetzlaff, J., Mulrow, C., Gøtzsche, P. C., Ioannidis, J. P., Clarke, M., Devereaux, P. J., Kleijnen, J., & Moher, D. (2009). The PRISMA statement for reporting systematic reviews and meta-analyses of studies that evaluate health care interventions: Explanation and elaboration. PLoS Medicine; 6(7), e1000100. doi:

10.1371/journal.pmed.1000100

López-Medina. E., Biswal, S., Saez-Llorens, X., Borja-Tabora, C., Bravo, L., Sirivichayakul, C., Vargas, L. M., Alera, M. T., Velásquez, H., Reynales, H., Rivera, L., Watanaveeradej, V., Rodriguez-Arenales, E. J., Yu, D., Espinoza, F., Dietze, R., Fernando, L. K., Wickramasinghe, P., Duarte Moreira, E., Fernando, A. D., Gunasekera, D., Luz, K., da Cunha, R. V., Tricou, V., Rauscher, M., Liu, M., LeFevre, I., Wallace, D., Kosalaraksa, P., & Borkowski, A. (2022). Efficacy of a Dengue Vaccine Candidate (TAK-003) in Healthy Children and Adolescents 2 Years after Vaccination. J Infect Dis.; 225(9), 1521-1532. doi: 10.1093/infdis/jiaa761

Messina, J. P., Brady, O. J., Golding, N., Kraemer, M. U. G., Wint, G. R. W., Ray, S. E., Pigott, D. M., Shearer, F. M., Johnson, K., Earl, L., Marczak, L. B., Shirude, S., Davis, W. N., Gilbert, M., Velayudhan, R., Jones, P., Jaenisch, T., Scott, T. W., Reiner, R. C Jr, & Hay, S. I. (2019). The current and future global distribution and population at risk of dengue. Nat Microbiol.; 4(9), 1508-1515. doi: 10.1038/s41564-019-0476-8

Moodie, Z., Juraska, M., Huang, Y., Zhuang, Y., Fong, Y., Carpp, L. N., Self, S. G., Chambonneau, L., Small, R., Jackson, N., Noriega, F., & Gilbert, P. B. (2018). Neutralizing antibody correlates analysis of tetravalent dengue vaccine efficacy trials in Asia and Latin America. J Infect Dis.; 217(5), 742- 753. doi: 10.1093/infdis/jix609

Mulderij-Jansen, V., Pundir, P., Grillet, M. E., Lakiang, T., Gerstenbluth, I., Duits, A., Tami, A., & Bailey, A. (2022). Effectiveness of Aedes-borne infectious disease control in Latin America and the Caribbean region: A scoping review. PLoS ONE 17(11), e0277038. https://doi.org/10.1371/journal.pone.0277038

Murray, N. E., Quam, M. B., & Wilder-Smith, A. (2013). Epidemiology of dengue: past, present, and future prospects. Clin Epidemiol.; 5, 299-309. doi: 10.2147/CLEP.S34440

Nguyen, T. H., Nguyen, T. L., Lei, H. Y., Lin, Y. S., Le, B. L., Huang, K. J., Lin, C. F., Do, Q. H., Vu, T. Q., Lam, T. M., Yeh, T. M., Huang, J. H., Liu, C. C., & Halstead, S. B. (2006). Volume replacement in infants with dengue hemorrhagic fever/dengue shock syndrome. Am J Trop Med Hyg.;74(4), 684-91

Olivera-Botello, G., Coudeville, L., Fanouillere, K., Guy, B., Chambonneau, L., Noriega, F., & Jackson, N. (2016). CYD-TDV Vaccine Trial Group. Tetravalent dengue vaccine reduces symptomatic and asymptomatic dengue virus infections in healthy children and adolescents Aged 2-16 years in Asia and Latin America. J Infect Dis.; 214(7), 994-1000. doi: 10.1093/infdis/jiw297

Osorio, J. E., Velez, I. D., Thomson, C., Lopez, L., Jimenez, A., Haller, A. A., Silengo, S., Scott, J., Boroughs, K. L., Stovall, J. L., Luy, B. E., Arguello, J., Beatty, M. E., Santangelo, J., Gordon, G. S., Huang, C. Y., & Stinchcomb, D. T. (2014). Safety and immunogenicity of a recombinant live attenuated tetravalent dengue vaccine (DENVax) in flavivirus-naive healthy adults in Colombia: a randomized, placebo-controlled, phase 1 study. Lancet Infect Dis.;14(9), 830-838. doi: 10.1016/S1473-3099(14)70811-4

Plennevaux, E., Moureau, A., Arredondo-García, J. L., Villar, L., Pitisuttithum, P., Tran, N. H., Bonaparte, M., Chansinghakul, D., Coronel, D. L., L'Azou, M., Ochiai, R. L., Toh, M. L., Noriega, F., & Bouckenooghe, A. (2018). Impact of dengue vaccination on serological diagnosis: Insights from phase III dengue vaccine efficacy trials. Clin Infect Dis.; 66(8), 1164-1172. doi: 10.1093/cid/cix966

Plennevaux, E., Sabchareon, A., Limkittikul, K., Chanthavanich, P., Sirivichayakul, C., Moureau, A., Boaz, M., Wartel, T. A., Saville, M., & Bouckenooghe, A. (2016). Detection of dengue cases by serological testing in a dengue vaccine efficacy trial: Utility for efficacy evaluation and impact of future vaccine introduction. Vaccine; 34(24), 2707-12. doi: 10.1016/j.vaccine.2016.04.028

Reynales, H., Carrasquilla, G., Zambrano, B., Cortes, S. M.; Machabert, Tifany; Jing, Jin; Pallardy, Sophie; Haney, Owen; Faccini, Martha; Quintero, Juliana; Noriega, Fernando (2020). Secondary analysis of the efficacy and safety trial data of the tetravalent dengue vaccine in children and adolescents in Colombia. The Pediatric Infectious Disease Journal, 39(4), e30–e36. doi:10.1097/inf.0000000000002580

Rivera, L., Biswal, S., Sáez-Llorens, X., Reynales, H., López-Medina, E., Borja-Tabora, C., Bravo, L., Sirivichayakul, C., Kosalaraksa, P., Martinez Vargas, L., Yu, D., Watanaveeradej, V., Espinoza, F., Dietze, R., Fernando, L., Wickramasinghe, P., Duarte Moreira, Jr. E., Fernando, A. D., Gunasekera, D., Luz, K., Venâncioda Cunha, R., Rauscher, M., Zent, O., Liu, M., Hoffman, E.,

LeFevre, I., Tricou, V., Wallace, D., Alera, M., & Borkowski, A. (2022). Three-year Efficacy and Safety of Takeda's Dengue Vaccine Candidate (TAK-003). Clin Infect Dis.; 75(1), 107-117. doi: 10.1093/cid/ciab864

Sabchareon, A., Lang, J., Chanthavanich, P., Yoksan, S., Forrat, R., Attanath, P., Sirivichayakul, C., Pengsaa, K., Pojjaroen-Anant, C., Chambonneau, L., Saluzzo, J. F., & Bhamarapravati, N. (2004). Safety and immunogenicity of a three-dose regimen of two tetravalent live-attenuated dengue vaccines in five- to twelve-year-old Thai children. Pediatr Infect Dis J.; 23(2), 99-109. doi: 10.1097/01.inf.0000109289.558three-doseD: 14872173

Sabchareon, A., Wallace, D., Sirivichayakul, C., Limkittikul, K., Chanthavanich, P., Suvannadabba, S., Jiwariyavej, V., Dulyachai, W., Pengsaa, K., Wartel, T. A., Moureau, A., Saville, M., Bouckenooghe, A., Viviani, S., Tornieporth, N. G., & Lang, J. (2012). Protective efficacy of the recombinant, live-attenuated, CYD tetravalent dengue vaccine in Thai schoolchildren: a randomized, controlled phase 2b trial. Lancet;380(9853), 1559-1567. doi: 10.1016/S0140- 6736(12)61428-7

Sabchareon, A., Wallace, D., Sirivichayakul, C., Limkittikul, K., Chanthavanich, P., Suvannadabba, S., Jiwariyavej, V., Dulyachai, W., Pengsaa, K., Wartel, T. A., Moureau, A., Saville, M., Bouckenooghe, A., Viviani, S., Tornieporth, N. G., & Lang, J. (2012). Protective efficacy of the recombinant, live-attenuated, CYD tetravalent dengue vaccine in Thai schoolchildren: a randomized, controlled phase 2b trial. Lancet; 380(9853), 1559-67. doi: 10.1016/S0140-6736(12)61428-7

Sáez-Llorens, X., Biswal, S., Borja-Tabora, C., Fernando, L., Liu, M., Wallace, D., Folschweiller, N., Reynales, H., & LeFevre, I. (2023). TIDES Study Group. Effect of the tetravalent dengue vaccine TAK-003 on sequential episodes of symptomatic dengue. Am J Trop Med Hyg.; 108(4), 722-726. doi: 10.4269/ajtmh.22-0673

Sáez-Llorens, X., Tricou, V., Yu, D., Rivera, L., Jimeno, J., Villarreal, A. C., Dato, E., Mazara, S., Vargas, M., Brose, M., Rauscher, M., Tuboi, S., Borkowski, A., & Wallace, D. (2018). Immunogenicity and safety of one versus two doses of tetravalent dengue vaccine in healthy children aged 2-17 years in Asia and Latin America: 18-month interim data from a phase 2, randomized, placebo- controlled study. Lancet Infect Dis.; 18(2), 162-170. doi: 10.1016/S1473-3099(17)30632-1

Shepard, D. S., Undurraga, E. A., Halasa, Y. A., & Stanaway, J. D. (2016). The global economic burden of dengue: a systematic analysis. Lancet Infect Dis.;16(8), 935-41. doi: 10.1016/S1473-3099(16)00146-8

Silva, N. M., Santos, N. C., & Martins, I. C. (2020). Dengue and Zika Viruses: Epidemiological History, Potential Therapies, and Promising Vaccines. Trop Med Infect Dis.; 5(4), 150. doi: 10.3390/tropicalmed5040150

Simasathien, S., Thomas, S. J., Watanaveeradej, V., Nisalak, A., Barberousse, C., Innis, B. L., Sun, W., Putnak, J. R., Eckels, K. H., Hutagalung, Y., Gibbons, R. V., Zhang, C., De La Barrera, R., Jarman, R. G., Chawachalasai, W., & Mammen, M. P. Jr. (2008). Safety and immunogenicity of a tetravalent live-attenuated dengue vaccine in flavivirus naive children. Am J Trop Med Hyg.; 78(3), 426-33

Simmons, C. P., Farrar, J. J., Nguyen, V., & Wills, B. (2012). Dengue. N Engl J Med.; 366(15), 1423–1432 Sirivichayakul, C., Barranco-Santana, E. A., Rivera, I. E., Kilbury, J., Raanan, M., Borkowski, A., Papadimitriou, A., & Wallace, D. (2022). Long-term safety and immunogenicity of a tetravalent dengue vaccine candidate in children and adults: A randomized, placebo-controlled, phase 2 study. J Infect Dis.; 225(9), 1513-1520. doi: 10.1093/infdis/jiaa406

Sridhar, S., Luedtke, A., Langevin, E., Zhu, M., Bonaparte, M., Machabert, T., Savarino, S., Zambrano, B., Moureau, A., Khromava, A., Moodie, Z., Westling, T., Mascareñas, C., Frago, C., Cortés, M., Chansinghakul, D., Noriega, F., Bouckenooghe, A., Chen, J., Ng, Su-P., Gilbert, P. B., Gurunathan, S., & DiazGranados, C. A. (2018). Effect of Dengue Serostatus on Dengue Vaccine Safety and Efficacy. New England Journal of Medicine; 379(4), 327-340. doi: 10.1056/NEJMoa1800820

Thomas, J., & Harden, A. (2008). Methods for the thematic synthesis of qualitative research in systematic reviews. BMC Medical Research Methodology; 8(1), 45. doi: 10.1186/1471-2288-8-45.

Thomas, R., Chansinghakul, D., Limkittikul, K., Gilbert, P. B., Hattasingh, W., Moodie, Z., Shangguan, S., Frago, C., Dulyachai, W., Li, S. S.,

Jarman, R. G., Geretz, A., Bouckenooghe, A., Sabchareon, A., Juraska, M., Ehrenberg, P., Michael, N. L., Bailleux, F., Bryant, C., & Gurunathan, S. (2022). Associations of human leukocyte antigen with neutralizing antibody titers in a tetravalent dengue vaccine phase 2 efficacy trial in Thailand. Hum Immunol.; 83(1), 53-60. doi: 10.1016/j.humimm.2021.09.006

Thomas, S. J., & Yoon, I. K. (2019). A review of Dengvaxia: development to deployment. Hum Vaccin Immunother.; 15(10), 2295-2314. doi: 10.1080/216 45515.2019.1658503

Tricou, V., Sáez-Llorens, X., Yu, D., Rivera, L., Jimeno, J., Villarreal, A. C., Dato, E., Saldaña de Suman, O., Montenegro, N., DeAntonio, R., Mazara, S., Vargas, M., Mendoza, D., Rauscher, M., Brose, M., Lefevre, I., Tuboi, S., Borkowski, A., & Wallace, D. (2020). Safety and immunogenicity of a tetravalent dengue vaccine in children aged 2-17 years: a randomized, placebo-controlled, phase 2 trial. Lancet.; 395(10234), 1434-1443. doi: 10.1016/S0140-6736(20)30556-0

Vigne, C., Dupuy, M., Richetin, A., Guy, B., Jackson, N., Bonaparte, M., Hu, B., Saville, M., Chansinghakul, D., Noriega, F., & Plennevaux, E. (2017). Integrated immunogenicity analysis of a tetravalent dengue vaccine up to 4 y after vaccination. Hum Vaccin Immunother.; 13(9), 2004-2016. doi: 10.1080/21645515.2017.1333211

Villar, L. Á., Rivera-Medina, D. M., Arredondo-García, J. L., Boaz, M., Starr-Spires, L., Thakur, M., Zambrano, B., Miranda, M. C., & Rivas, E. (2013). Dayan, G. H. Safety and immunogenicity of a recombinant tetravalent dengue vaccine in 9-16 year olds: a randomized, controlled, phase II trial in Latin America. Pediatr Infect Dis J.; 32(10), 1102-9. doi: 10.1097/INF.0b013e31829b8022

Villar, L., Dayan, G. H., Arredondo-García, J. L., Rivera, D. M., Cunha, R., Deseda, C., Reynales, H., Costa, M. S., Morales-Ramírez, J. O., Carrasquilla, G., Rey, L. C., Dietze, R., Luz, K., Rivas, E., Miranda Montoya, M. C., Cortés Supelano, M., Zambrano, B., Langevin, E., Boaz, M., Tornieporth, N., Saville, M., & Noriega, F. (2015). CYD15 study group. Efficacy of a tetravalent dengue vaccine in children in Latin America. N Engl J Med.; 372(2), 113-123. doi: 10.1056/NEJMoa1411037

Watanaveeradej, V., Simasathien, S., Mammen, M. P., Nisalak, A., Tournay, E., Kerdpanich, P., Samakoses, R., Putnak, R. J., Gibbons, R. V., Yoon, I. K., Jarman, R. G., De La Barrera, R., Moris, P., Eckels, K. H., Thomas, S. J., & Innis, B. L. (2016). Long-Term safety and immunogenicity of a tetravalent live-attenuated dengue vaccine and evaluation of a booster dose administered to healthy Thai children. Am J Trop Med Hyg.; 94(6), 1348-1358. doi: 10.4269/ajtmh.15-0659

Weeratunga, P., Rodrigo, C., Fernando, S. D., & Rajapakse, S. (2017). Control methods for Aedes albopictus and Aedes aegypti. Cochrane Database Syst Rev.;(8), CD012759. doi: 10.1002/14651858.CD012759

Wilder-Smith, A., Ooi, E-E., Horstick, O., & Wills, B. (2019). Dengue. Lancet; 393 (10169), 350–363

World Health Organization (WHO). (2021). Dengue and severe dengue. Retrieved from https://www.who.int/en/news-room/fact-sheets/detail/ dengue -and - severe-dengue. Accessed September 13, 2023

World Health Organization (WHO). (2023). Disease Outbreak News; Dengue in Bangladesh. Available at: https://www.who.int/emergencies /disease-outbreak-news /item/2023-DON481

Yang, X., Quam, M. B. M., Zhang, T., & Sang, S. (2021). Global burden for dengue and the evolving pattern in the past 30 years. J Travel Med.; 28(8), 146

Yang, Y., Meng, Y., Halloran, M. E., & Longini, I. M. Jr. (2018). Dependency of vaccine efficacy on preexposure and age: A closer look at a tetravalent dengue vaccine. Clin Infect Dis.; 66(2), 178- 184. doi: 10.1093/cid/cix766

Ylade, M., Agrupis, K. A., Daag, J. V., Crisostomo, M. V., Tabuco, M. O., Sy, A. K., Nealon, J., Macina, D., Sarol, J., Deen, J., & Lopez, A. L. (2021). Effectiveness of a single-dose mass dengue vaccination in Cebu, Philippines: A case-control study. Vaccine; 39(37), 5318-5325. doi: 10.1016/j.vaccine.2021.07.042

# Effects of Pre-and Post-Anthesis Drought Stress on Corn Physiology and Yield

Ranadheer Reddy Vennam[1], Xinyan Jian[1], Jagman Dhillon[1], K. Raja Reddy[1], Krishna N. Reddy[2], Raju Bheemanahalli[1*]

[1]*Department of Plant and Soil Sciences, Mississippi State University, Mississippi State, MS, USA*

[2]*Crop Production Systems Research Unit, USDA-ARS, Stoneville, MS, USA*

***Corresponding Author:** Raju Bheemanahalli

**Email:** rajubr@pss.msstate.edu

Doi:10.34107/CTJP1687

## ABSTRACT

The developmental transition from vegetative to reproductive growth stage is highly sensitive to drought stress in corn (*Zea mays* L.). Understanding the physiological responses of corn to withstand and recover from drought during early reproductive development is crucial for ensuring stable yields. Therefore, the present study assessed the effects of short-term (7 days) drought stress on the physiology of corn and its ability to recover during the pre-anthesis, mid-silking, and blistering stages. Furthermore, the study examined the effect of drought stress on kernel yield and quality. On average, drought stress during the tasseling, mid-silking, and blistering stages significantly reduced stomatal conductance (82%) and transpiration (81%). These changes under drought led to an average increase in leaf temperature by 3 °C compared to the control. Leaf chlorophyll content declined by 46% and did not recover after rewatering. Unlike pigments, canopy temperature and quantum efficiency of photosystem II showed substantial recovery after rewatering across growth stages. Drought stress during mid-silking and blistering led to a significant decline of kernel weight by 33% and 34% compared to the control. Average kernel starch was 65%, and protein was 11% across treatments, reflecting kernel quality. Compared with control, drought stress during tasseling led to significant yield losses followed by mid-silking and blistering. The study highlights the importance of managing drought stress by maintaining optimum irrigation around pre- and post-anthesis plant health and efficient kernel set in corn.

Keywords: Blistering, Corn, Drought, Physiology, Quality, Tasseling, Mid-silking, Yield.

## INTRODUCTION

Corn, a major annual monoecious crop, requires a substantial amount of water, with a footprint of 1,222 L, to produce one kg of kernels (Mekonnen and Gerbens-Leenes, 2020; Erenstein et al., 2022). In recent times, extreme weather events have become more intense, posing a significant threat to sustaining food security (Campos et al., 2004; Avramova et al., 2015; Mbow et al., 2019). In addition, declining groundwater levels in corn-growing regions across the United States, including Mississippi, are affecting the yields (Kebede et al., 2014; Li et al., 2019). Persistent drought events during corn growing seasons are becoming more frequent and severe due to climate change (Zhao et al., 2017; Ebi et al., 2021; NASA, 2023). More than 80% of the corn production in the United States depends on rainfed conditions, necessitating proper irrigation scheduling to meet crop water demands during dry periods (Jin et al., 2017; USDA-ERS, 2019). Drought stress, characterized by limited water availability during crop growing season, can disrupt processes associated with growth and development (Avramova et al., 2015; Song et al., 2018).

The water requirements of corn vary across different growth stages, with a 30% increase in water demand during the transition from vegetative growth to reproductive development (Kranz et al., 2008). Drought stress around reproductive and grain filling accelerates leaf senescence and limits assimilate transfer from leaves to kernels (Yang and Zhang, 2006; Seleiman et al., 2021; Luo et al., 2021). These impaired activities hinder plant growth and development, leading to lower yields (Yang and Zhang, 2006; Oury et al., 2016; Bheemanahalli et al., 2022a; b; Tang et al., 2023). Numerous studies have examined the mechanisms underlying drought effects on kernel development (Bheemanahalli et al., 2022a; b; Tang et al., 2023). Oury et al. (2016).

It was found that reduced assimilate production and transfer negatively affected kernel development. Among various indicators proposed to assess drought stress impact on crops, reductions in gas exchange, such as stomatal conductance and transpiration rates, are commonly used to evaluate the physiological responses of plants (Xu and Zhou, 2008; Seleiman et al., 2021; Poudel et al., 2023). In addition, changes in photosynthetic pigments, such as chlorophyll content and chlorophyll fluorescence, were employed as indicators of drought-induced alterations in photosynthetic activity (Zhuang et al., 2020). Moreover, antioxidant pigments, including carotenoids and anthocyanins were also utilized as potential markers for oxidative stress (Seleiman et al., 2021; Ding et al., 2022).

Studies show that yield losses due to stress around the flowering stage can be more severe than the vegetative stage (Cakir, 2004; Lauer, 2018). Corn has a unique inflorescence, containing separate male and female flowers, each with distinct characteristics and roles during fertilization (Vollbrecht and Schmidt, 2009; Shao et al., 2021). Drought around flowering in induces significant damage to reproductive structures, such as tassel, silk, ears, and embryo, which are essential for yield determination (Oury et al., 2016; Trachsel et al., 2016; Dietz et al., 2021; Bheemanahalli et al., 2022b; Tang et al., 2023). Drought stress decreases the synchronous emergence of both male and female inflorescence during pollination in corn, causing overall yield losses of up to 90% (Cakir, 2004; Fuad-Hassan et al., 2008; Bheemanahalli et al., 2022a). Efforts to address the impact of drought at different growth stages have been made, primarily focusing on reducing soil moisture levels to sub-optimal levels and quantifying morphophysiological and yield responses to drought (Vennam et al. 2023). However, the recovery response to drought regarding physiology and yield during different reproductive growth stages (tasseling, mid-silking, and blistering) have been overlooked. Understanding the effects of drought stress is essential for developing strategies to mitigate its adverse impacts on corn production. Therefore, the main objectives of this study were to (i) assess the effects of pre- and post-flowering drought stress on physiology and pigments and (ii) evaluate the recovery responses of corn at different growth stages in terms of yield and quality.

## MATERIALS AND METHODS

### Crop husbandry

An experiment was conducted in the greenhouse facility at the R.R. Foil Plant Science Research Center, Mississippi State University (33°28'21.8"N 88°46'51.9"W). Each pot, with a capacity of 25 L, was filled with farm soil. Four seeds of Dekalb corn hybrid (DKC 68-69, a robust canopy cover with high yield) recommended for the Southern United States were planted in each pot and thinned to one seedling per pot at the two-leaf (V2) stage. To ensure that the soil moisture in each pot was sufficient, an automated drip system was installed as a source of irrigation. The plants received optimal irrigation conditions around 0.15 $m^3$ $m^{-3}$ until they reached the vegetative tasseling stage (VT). The fertilizer needs were met by applying a controlled release of Osmocote (14-14-14 of N-P-K; ICL Specialty Fertilizers, Dublin, Ohio, USA) at a rate of 4g per pot every two weeks until they reached the VT stage translating to 240 kg $ha^{-1}$ with a planting density of 60,000 plants $ha^{-1}$.

### Stress treatments

To study the impact of short-term (7 days) drought stress on pre- and post-flowering, corn plants grown under optimal irrigation conditions for 56 days were divided into four groups. One set was used as the control (CNT), while the other three groups were exposed to drought stress treatment at different growth stages: tasseling (VT - T1), mid-silking (R1 - T2), and blistering (R2 - T3) stages (Figure 1). The experiment was performed following a completely randomized design and each treatment had at least 12 replications. At the VT stage, the first drought treatment was initiated by withholding irrigation for seven days.

Likewise, independent set of plants was exposed to drought stress during the mid-silking (R1) and blistering (R2) stages. After the drought treatment, plants were rewatered and maintained under optimal irrigation conditions until they reached physiological maturity. Soil moisture of control plants was increased from ~0.15 $m^3$ $m^{-3}$ to ~ 0.25 $m^3$ $m^{-3}$ after the plants reached the VT stage by providing 1000 mL irrigation per day during treatment.

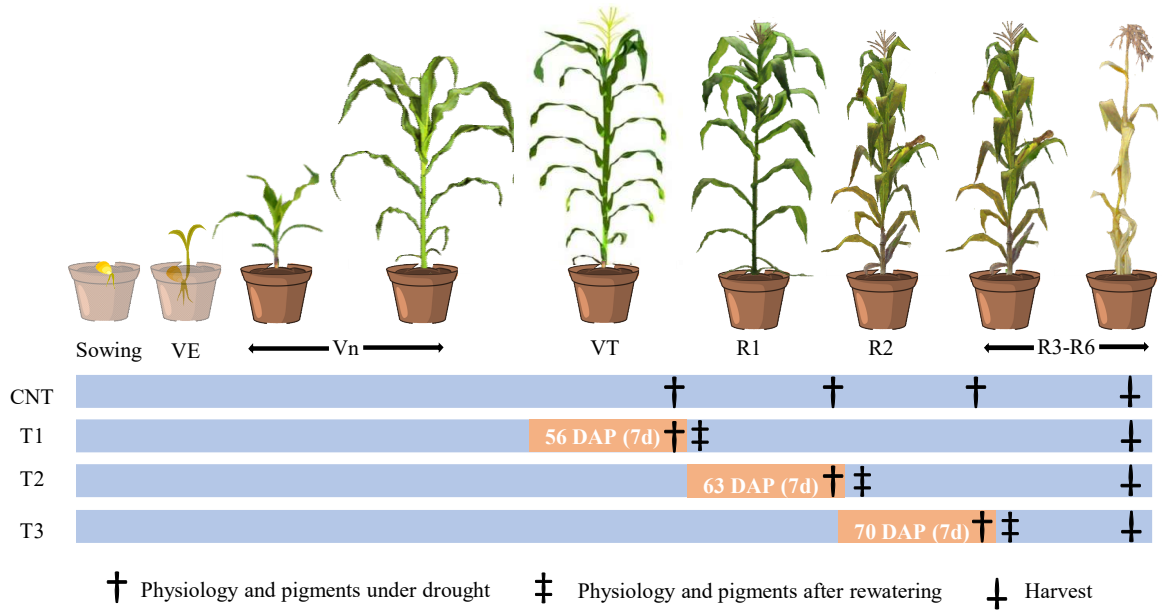


Figure 1. An illustrative summary of material and methods showing treatments and data collection during the tasseling stage (VT, T1), mid-silking (R1, T2), and blistering (R2, T3). Horizontal blue bars indicate control (optimum irrigation), and horizontal orange bars indicate drought stress (no irrigation for seven days) at the growth stage. *VE – emergence, Vn – $n^{th}$ leaf stage, VT – tasseling stage, R1 – silking stage, R2 – blistering stage, R3 – milking stage, R6 – physiological maturity, DAP – days after planting.*

**Data collection**

Stomatal conductance, transpiration, canopy temperature difference (CTD), and quantum efficiency of photosystem II (PhiPS2) data were collected using a handheld LI-600 porometer integrated with a fluorometer system (LI-COR Biosciences, Lincoln, USA). Leaf pigments (chlorophyll content, anthocyanin index, and nitrogen balance index) data were collected using a Dualex optical leaf clip meter (Force A DX16641, Paris, France). Data were collected from the ear leaf at the end of each stress period, i.e., seven days after initiation of stress and 24 hours after rewatering between 10:00 h and 12:00 h across growth stages.

At physiological maturity, ear length was measured using a meter scale, and ear diameter was measured using vernier calipers. Ears were hand threshed to assess treatment impact on yield and quality components. The kernel number was recorded using a seed counter (NP5056-Model 850–2, LI-COR, Lincoln, NE, USA), along with data on kernel weight per cob. Kernel quality, such as starch, protein, and oil were determined using a near-infrared spectrometer (Perten DA7250, Perten Instruments, Springfield, IL, USA). Each sample was scanned three times using a small moving cup (Bheemanahalli et al., 2022b). Quality data for tasseling (T1 treatment) was omitted due to insufficient kernels for scanning.

**Statistical analysis**

The statistical analyses were conducted using R programming version 4.4.2 (R Core Team, 2022) and library "doebioresearch" to estimate the significant variations among the measured traits across treatments. The mean separation between treatments was done within the treatment using the Fischer's least significant difference (LSD) multiple comparison test at 5% ($\alpha$ = 0.05). Graphs were generated using Sigmaplot 14.5 (Systat Software Inc., San Jose, California, USA).

## RESULTS

### Physiological responses of corn to drought stress and recovery

Drought stress applied at different growth stages (tasseling, mid-silking, and blistering) significantly reduced stomatal conductance compared to control (Figure 2A). After seven days of stress, the average decline in stomatal conductance was found to be 90%, 63%, and 93% for tasseling, mid-silking, and blistering stages, respectively. A decrease in stomatal conductance and transpiration during periods of stress is a common adaptive response in plants to minimize water loss. However, reduced stomatal conductance and transpiration increased leaf temperature by 2 - 4 ºC under stress compared to the control (Figure 2C). This temperature increase was pronounced during stress periods at the tasseling and blistering stages, compared to the mid-silking stage. Under drought stress, PhiPS2 (a parameter used to measure the efficiency of photosystem II) experienced a decline, ranging between 79% at the blistering stage and 85% at the mid-silking stage (Figure 2D). The study found that rewatering did not significantly affect the recovery of stomatal conductance and transpiration across growth stages, except for the blistering stage (Figures 2A and 2B). In contrast to stomatal conductance and transpiration, the CTD was significantly reduced after rewatering (Figure 2C). On average, PhiPS2 increased from 0.1 to 0.4 after rewatering following a week of drought stress (Figure 2D). Among the various traits measured, stomatal conductance and transpiration displayed a greater sensitivity to drought during mid-silking, as they failed to show any significant recovery even after rewatering.

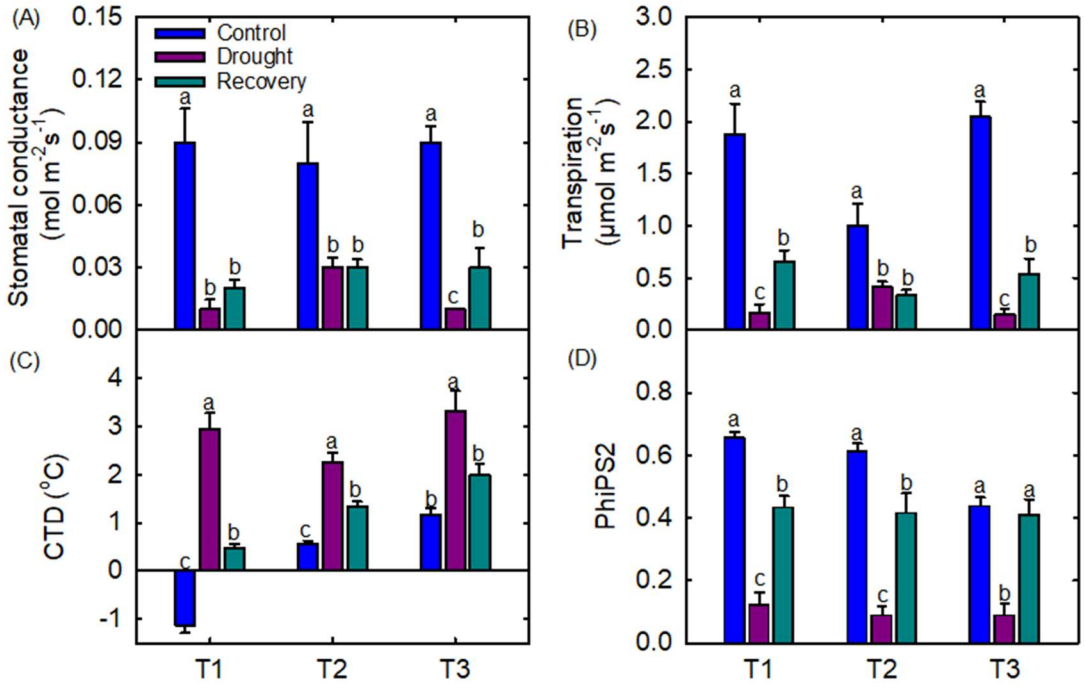


**Figure 2**. Impact of drought stress and rewatering during tasseling (T1), mid-silking (T2), and blistering (T3) on stomatal conductance (A), transpiration (B), canopy temperature difference (CTD, ºC), and quantum efficiency of photosystem 2 (PhiPS2, D). Vertical bars represent mean values ± SE. Different letters indicate significant differences between control, drought, and recovery within the growth stage by Fisher's LSD test ($p < 0.05$).

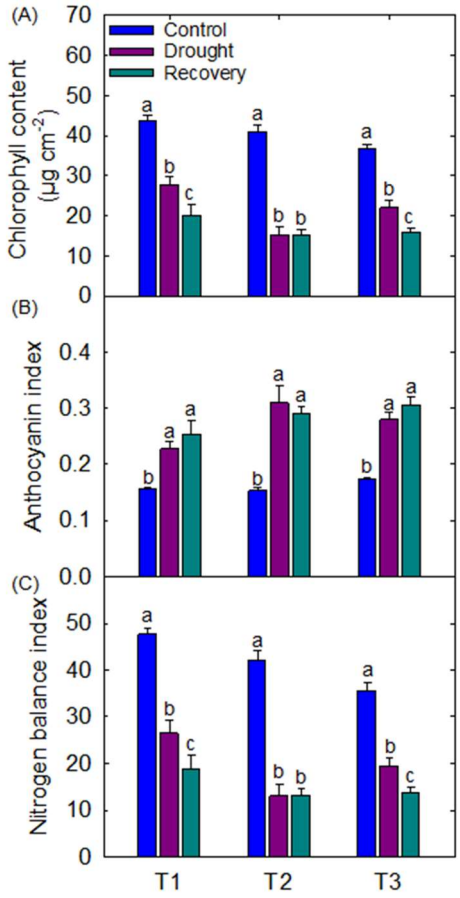


Figure 3. Impact of drought stress and rewatering during tasseling (T1), mid-silking (T2), and blistering (T3) on chlorophyll content (A), anthocyanin index (B), and nitrogen balance index (C. Vertical bars represent mean values ± SE. Different letters indicate significant differences between control, drought, and recovery within the growth stage by Fisher's LSD test ($p < 0.05$).

**Response of photosynthetic and antioxidant pigments to drought stress and recovery**

Drought stress significantly impacted the chlorophyll content at all growth stages. The decline in chlorophyll content was most pronounced during the mid-silking stage, with a reduction of 63%. The chlorophyll content consistently declined after rewatering during the tasseling and blistering stages, while no significant change was observed under the mid-silking stage stress (Figure 3A). A decline of 40% was observed at the blistering stage and 36% during the tasseling stage (Figure 3A). Chlorophyll pigment didn't recover after rewatering, indicating a continuous decline due to degradation. On the other hand, an increase in the anthocyanin index was linked to the proportional decline in chlorophyll content. Under stress conditions at the mid-silking stage, the anthocyanin index values exhibited a twofold increase compared to the control. During the blistering stage, there was a significant rise (61%) in the anthocyanin index. During the tasseling stage, a notable 47% increase in the anthocyanin index values was observed. However, after rewatering, no significant change was observed in the anthocyanin index (Figure 3B). Compared to the control, the ear leaf's nitrogen balance index (NBI) decreased by 52% under drought stress. In agreement with chlorophyll content, the NBI continued to decline even after rewatering, which aligns with the findings regarding chlorophyll content (Figures 3A, C).

**Yield and quality parameters**

Short-term drought stress during the initial stages of reproductive development (tasseling) significantly impacted yield traits, including ear length, ear diameter, kernel weight, and kernel number (Figure 4). At the same time, ear length and diameter did not significantly change between the control and stress during blistering stage. A notable reduction was observed in both ear length (23%) and diameter (41%) due to drought stress at the tasseling stage (Figures 4A, B). Drought stress at tasseling significantly reduced kernel number and weight compared to the control. Compared to the control, kernel number was reduced under drought conditions during mid-silking (11%) and blistering stages (18%) (Figure 4C). However, significant reductions in kernel weight were found between the control and mid-silking or blistering stages (Figure 4D). Kernel weight varied across different stages in response to treatments, with the highest average weight observed under the control condition (133 g plant$^{-1}$) followed by the mid-silking and blistering stage, which exhibited a slight decline of 33% and 34% in kernel weight (Figure 4D). Kernels produced under the control had the highest starch content of 64% (Table 1). On the other hand, the protein

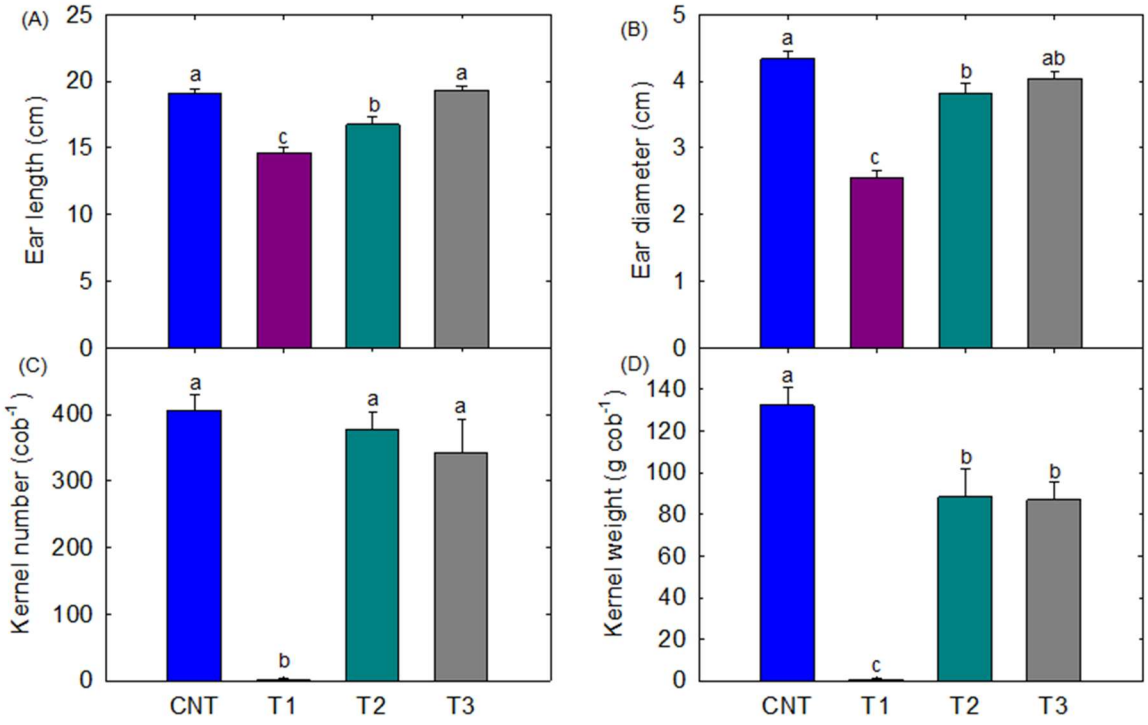


**Figure 4.** Impact of drought stress and rewatering during tasseling (T1), mid-silking (T2), and blistering (T3) on ear length (A), ear diameter (B), kernel number (C), and kernel weight (D). Vertical bars represent mean values ± SE. Different letters indicate significant differences between treatments by Fisher's LSD test ($p < 0.05$).

content in kernels had an opposite response to starch composition (Table 1). Kernels produced under blistering stage stress had a higher protein content of about 11%, whereas those produced under optimal irrigation conditions had a protein content of around 10% (Table 1). The oil content of the kernels did not show any significant variation, with an average oil content consistently maintained at approximately 3.5% across all treatments (Table 1).

**Yield and quality parameters**

Short-term drought stress during the initial stages of reproductive development (tasseling) significantly impacted yield traits, including ear length, ear diameter, kernel weight, and kernel number (Figure 4). At the same time, ear length and diameter did not significantly change between the control and stress during blistering stage. A notable reduction was observed in both ear length (23%) and diameter (41%) due to drought stress at the tasseling stage (Figures 4A, B). Drought stress at tasseling significantly reduced kernel number and weight compared to the control. Compared to the control, kernel number was reduced under drought conditions during mid-silking (11%) and blistering stages 18%) (Figure 4C). However, significant reductions in kernel weight were found between the control and mid-silking or blistering stages (Figure 4D). Kernel weight varied across different stages in response to treatments, with the highest average weight observed under the control condition (133 g plant$^{-1}$) followed by the mid-silking and blistering stage, which exhibited a slight decline of 33% and 34% in kernel weight (Figure 4D). Kernels produced under the control had the highest starch content of 64% (Table 1). On the other hand, the protein content in kernels had an opposite response to starch composition (Table 1). Kernels produced under blistering stage stress had a higher protein content of about 11%, whereas those produced under optimal irrigation conditions had a protein content of around 10% (Table 1). The oil content of the kernels did not show any significant variation, with an average oil content consistently maintained at approximately 3.5% across all treatments (Table 1).

**Table 1**. Impact of drought stress during mid-silking (T2), and blistering (T3) stages on kernel composition of starch, protein, and oil in corn.

| Treatment | Starch, % | Protein, % | Oil, % |
|---|---|---|---|
| CNT | 64.9 ± 0.3 a | 10.0 ± 0.3 b | 3.3 ± 0.1 a |
| T2 | 64.4 ± 0.4 b | 10.6 ± 0.4 ab | 3. 5 ± 0.1 a |
| T3 | 63.9 ± 0.3 c | 11.2 ± 0.4 a | 3.5 ± 0.1 a |

Values indicate mean values averaged across twenty replications ± SE (n = 12). Different letters indicate significant variation across treatments by Fisher's LSD test ($p < 0.05$).

## DISCUSSION

Climate change is expected to cause more extreme weather events, including drought, which can negatively impact corn production systems (Clarke et al., 2022). Drought stress during the reproductive stage can disrupt the yield components, and quality of corn, due to decreased pigment production and physiological performance (Aslam et al., 2015; Bheemanahalli et al., 2022a; Tang et al., 2023). However, the data presented in this study demonstrate that drought impact and recovery responses vary with growth stages in corn. Stressors often reduce the ability of plants to tolerate stress and maintain normal physiological functions. However, they can recover from stress, a fundamental aspect of resilience to changing environmental conditions. The concept of resilience plays a key role in improving stress tolerance from individual plants to entire ecosystems. It refers to plants ability to withstand and recover from stress. During the recovery process, plants restore their physiological functions and repair the damage caused by stress (Efeoğlu et al., 2009; Kränzlein et al., 2022). However, the ability to recover may depend on the growth stage of the crop as well as the intensity and duration of the stress (Efeoğlu et al., 2009; Kränzlein et al., 2022).

### Effects of drought stress at different growth stages on physiological and pigment traits

Drought stress at different growth stages has a varied impact on corn physiological traits. Various plant traits respond differently to drought, with some aiding survival and minimizing water loss. For instance, plants close their stomata during drought to reduce water loss, decreasing $CO_2$ uptake and biomass production ( al., 2015; Bartlett et al., 2016). Drought causes dehydration of mesophyll cells, which hinders gas exchange processes and impairs the metabolic functions of cells (Xu et al., 2010; Cai et al., 2020). Previous research has identified different mechanisms involved in the plant's response to drought, such as active signaling mediated by abscisic acid and passive hydraulic mediated signaling from the roots to regulate stomatal closure and prevent dehydration (Tombesi et al., 2015; Bartlett et al., 2016). This ultimately affects assimilate production and reduces yield. Exposure of corn to short-term drought stress resulted in a decline in chlorophyll levels across growth stages, which might indicate the production of a high amount of reactive oxygen species (ROS), as well as increased membrane permeability and oxidative stress (Qu et al., 2012; Anjum et al., 2017). However, subsequent rewatering led to rapid restoration of PhiPS2 responses in corn, indicating the ability of PSII to convert light energy into chemical energy upon recovery. (Efeoğlu et al., 2009; Chen et al., 2016; Zhang et al., 2018). At the same time, the decline in chlorophyll content and stomatal conductance did not recover upon rewatering. This phenomenon associated with reduced yield has been reported in previous studies involving cereals and legumes (Ghassemi-Golezani and Hosseinzadeh- Mahootchy, 2009; Ghanbari et al., 2013; Sehgal et al., 2018; Luo et al., 2021).

### Effects of drought stress at different growth stages on yield and quality traits

Corn showed varying responses to drought stress during pre- and post-flowering (Figure 4). Among the three growth stages studied, the most sensitive stage was tasseling, which caused a significant reduction in productive ears, which might be due to delayed inflorescence emergence (Oury et al., 2016; Tang et al., 2023; Vennam et al., 2023). In addition, there was a significant reduction in ear size (length and diameter) compared to the mid-silking and blistering stages (Figures 4A, B). These findings align with results showing that variations in soil moisture levels during tasseling or pollination can result in significant yield losses ranging from 30% to 90% in corn (Cakir, 2004; Bheemanahalli et al., 2022b; Tang et al., 2023; Vennam et al., 2023). This reduction could be due to slower cell differentiation and lower cell number (Long et al., 2006; Shao et al., 2021; Naidu et al., 2023). Even after rewatering, the plants stressed at tasseling did not set seeds. This response indicates that corn plants adjust their growth at the

individual organ level in response to stress (Verbraeken et al., 2021). However, poor organ coordination results in delayed flowering, lower seed sets, and reduced plant health (Verbraeken et al., 2021). Therefore, understanding the response of individual organs to drought at target growth stages can aid in better crop management.

Unlike tasseling, short-term drought stress occurring during the mid-silking and blistering stages had no significant impact on the number of kernels. This suggests that the plants had successful pollination before the onset of drought. However, post-flowering stress affected the kernels' size and weight (Figure 4), possibly due to impaired carbon partitioning or assimilates translocation. Notably, drought stress significantly impacted the starch and protein content during the mid-silking and blistering stages (Li et al., 2018; Ning et al., 2018). The reduction in kernel starch could be due to reduced activities of enzymes associated with starch biosynthesis, which are essential for grain development (Verbraeken et al., 2021). Additionally, increased protein might be due to reduced starch. The reallocation of resources, such as amino acids, from source to sink may have enhanced nitrogen accumulation and consequently increased the kernel protein (Seebauer et al., 2010; Singh et al., 2012; Ben Mariem et al., 2021; Ledvinka et al., 2022). These findings align with earlier research on corn inbred and demonstrate the significant impact of varying soil moisture levels during tasseling on crop yield (Bheemanahalli et al., 2022b). Further investigations are required to understand the association between stress recovery and kernel yield or quality, emphasizing the carbon-to-nitrogen ratio and source-to-sink relationships.

## CONCLUSION

This study examined the impact of drought stress during crucial growth periods of corn. The findings revealed that drought stress affects corn yield depending differently at different growth stage. Drought stress at tasseling can result in pollination failure, preventing the typical yield even after rehydration. Furthermore, even if successful pollination occurs, drought stress during grain filling can lead to apical ovary abortion, resulting in yield reductions. Recovery response indicated a close link between PhiPS2 levels and canopy temperature under drought. This study emphasizes the need for further research to develop improved drought tolerance and resilience during tasseling to sustain corn yield in rainfed environments.

### Data availability statement

The original contributions presented in the study are included in the article. Further inquiries can be directed to the corresponding author.

### Conflict of Interest

The authors declare no potential conflict of interest.

### Author Contributions

RB conceptualized the research and acquired the funding. RRV, XJ performed data collection. RRV performed data analysis and visualization and composed the first draft. RRV, JD, KNR, KRR, RB edited and reviewed the document. All authors contributed to the article and approved the submitted version.

## FUNDING

This work was funded by the Mississippi Agricultural and Forestry Experiment Station, Special Research Initiative, Undergraduate Research Scholars Program, the USDA- Agricultural Research Service (327429), and the National Institute of Food and Agriculture (MIS 043050).

## ACKNOWLEDGMENTS

We thank the Plant Stress Physiology Laboratory members for their support during the experiment setup and data collection.

## REFERENCES

Anjum, S. A., Ashraf, U., Tanveer, M., Khan, I., Hussain, S., Shahzad, B., et al. (2017). Drought Induced Changes in Growth, Osmolyte Accumulation and Antioxidant Metabolism of Three Maize Hybrids. *Front Plant Sci* 8, 69. https://doi.org/10.3389/fpls.2017.00069

Aslam, M., Maqbool, M. A., and Cengiz, R. (2015). "Biological practices for improvement of maize performance," in *Drought stress in maize (Zea mays* L.*): Effects, resistance mechanisms, global achievements, and biological strategies for improvement.* SpringerBriefs in Agriculture., eds. M. Aslam,

M. A. Maqbool, and R. Cengiz (Cham: Springer International Publishing), 45–55. https://doi.org/10.1007/978-3-319-25442-5_5

Avramova, V., AbdElgawad, H., Zhang, Z., Fotschki, B., Casadevall, R., Vergauwen, L., et

al. (2015). Drought induces distinct growth response, protection, and recovery mechanisms in the maize leaf growth zone. *Plant Physiology* 169, 1382–1396. https://doi.org/10.1104/pp.15.00276

Bartlett, M. K., Klein, T., Jansen, S., Choat, B., and Sack, L. (2016). The correlations and sequence of plant stomatal, hydraulic, and wilting responses to drought. *Proceedings of the National Academy of Sciences* 113, 13098–13103. https://doi.org/10.1073/pnas.1604088113

Ben Mariem, S., Soba, D., Zhou, B., Loladze, I., Morales, F., and Aranjuelo, I. (2021). Climate change, crop yields, and grain quality of C3 cereals: a meta-analysis of $CO_2$, temperature, and drought effects. *Plants* 10, 1052. https://doi.org/10.3390/plants10061052

Bheemanahalli, R., Ramamoorthy, P., Poudel, S., Samiappan, S., Wijewardane, N., and Reddy,

K. R. (2022a). Effects of drought and heat stresses during reproductive stage on pollen germination, yield, and leaf reflectance properties in maize (Zea mays L.). *Plant Direct* 6, e434. https://doi.org/10.1002/pld3.434

Bheemanahalli, R., Vennam, R. R., Ramamoorthy, P., and Reddy, K. R. (2022b). Effects of post-flowering heat and drought stresses on physiology, yield, and quality in maize (*Zea mays* L.). *Plant Stress* 6, 100106. https://doi.org/10.1016/j.stress.2022.100106

Cai, F., Zhang, Y., Mi, N., Ming, H., Zhang, S., Zhang, H., et al. (2020). Maize (*Zea mays* L.) physiological responses to drought and rewatering, and the associations with water stress degree. *Agricultural Water Management* 241, 106379.

https://doi.org/10.1016/j.agwat.2020.106379

Cakir, R. (2004). Effect of water stress at different development stages on vegetative and reproductive growth of corn. *Field Crops Research* 89, 1–16. https://doi.org/10.1016/j.fcr.2004.01.005

Campos, H., Cooper, M., Habben, J. E., Edmeades, G. O., and Schussler, J. R. (2004). Improving drought tolerance in maize: A view from industry. *Field Crops Research* 90, 19–34. https://doi.org/10.1016/j.fcr.2004.07.003

Chen, D., Wang, S., Cao, B., Cao, D., Leng, G., Li, H., et al. (2016). Genotypic variation in growth and physiological response to drought stress and re-watering reveals the critical role of recovery in drought adaptation in maize seedlings. *Frontiers in Plant Science* 6, 172337.

https://doi.org/10.3389/fpls.2015.01241 Clarke, B., Otto, F., Stuart-Smith, R., and Harrington, L. (2022). Extreme weather impacts of climate change: an attribution perspective. *Environ. Res.: Climate* 1, 012001. https://doi.org/10.1088/2752-5295/ac6e7d

Dietz, K.-J., Zörb, C., and Geilfus, C.-M. (2021). Drought and crop yield. *Plant Biology* 23, 881–893. https://doi.org/10.1111/plb.13304

Ebi, K. L., Vanos, J., Baldwin, J. W., Bell, J. E., Hondula, D. M., Errett, N. A., et al. (2021). Extreme weather and climate change: Population health and health system implications. *Annu Rev Public Health* 42, 293–315. https://doi.org/10.1146/annurev- publhealth-012420-105026

Efeoğlu, B., Ekmekçi, Y., and Çiçek, N. (2009). Physiological responses of three maize cultivars to drought stress and recovery. *South African Journal of Botany* 75, 34–42. https://doi.org/10.1016/j.sajb.2008.06.005

Erenstein, O., Jaleta, M., Sonder, K., Mottaleb, K., and Prasanna, B. M. (2022). Global maize production, consumption and trade: trends and R&D implications. *Food Sec.* 14, 1295–1319. https://doi.org/10.1007/s12571-022-01288-7

Fuad-Hassan, A., Tardieu, F., & Turc, O. (2008). Drought-induced changes in anthesis-silking interval are related to silk expansion: A spatio-temporal growth analysis in maize plants subjected to soil water deficit. *Plant, Cell & Environment*, 31(9), 1349–1360. https://doi.org/10.1111/j.1365-3040.2008.01839.x

Ghanbari, A. A., Shakiba, M. R., Toorchi, M., and Choukan, R. (2013). Nitrogen changes in the leaves and accumulation of some minerals in the seeds of red, white and chitti beans ('Phaseolus vulgaris') under water deficit conditions. Australian Journal of Crop Science 7, 706–712. https://doi.org/10.3316/informit.364966564049239

Ghassemi-Golezani, K., and Hosseinzadeh-Mahootchy, A. (2009). Changes in seed vigour of faba bean (Vicia faba L.) cultivars during development and maturity. *Seed Science and Technology* 37, 713–720.

https://doi.org/10.15258/sst.2009.37.3.18

Jin, Z., Zhuang, Q., Wang, J., Archontoulis, S. V., Zobel, Z., and Kotamarthi, V. R. (2017). The combined and separate impacts of climate extremes on the current and future US rainfed maize and soybean production under elevated CO2. *Global Change Biology* 23, 2687–2704. https://doi.org/10.1111/gcb.13617

Kebede, H., Sui, R., Fisher, D. K., Reddy, K. N., Bellaloui, N., and Molin, W. T. (2014). Corn yield response to reduced water use at different growth stages. *Agricultural Sciences* 05, 1305.

https://doi.org/10.4236/as.2014.513139 Kranz, W. L., Irmak, S., Donk, S. J. van, Yonts,

C. D., and Martin, D. L. (2008). Irrigation management for corn. https://extensionpublications.unl.edu/assets/html/g1850/build/g1850.htm [Accessed January 21, 2023].

Kränzlein, M., Geilfus, C.-M., Franzisky, B. L., Zhang, X., Wimmer, M. A., and Zörb, C. (2022). Physiological Responses of Contrasting Maize (*Zea mays* L.) Hybrids to Repeated Drought. *J Plant Growth Regul* 41, 2708–2718. https://doi.org/10.1007/s00344-021-10468-2

Lauer, J. (2007). How do you manage a corn crop after stress. *Corn Agronomy*. http://corn.agronomy.wisc.edu/AA/A046.asp x [Accessed June 18, 2023]

Ledvinka, H. D., Toghyani, M., Tan, D. K. Y., Khoddami, A., Godwin, I. D., and Liu, S. Y. (2022). The impact of drought, heat and elevated carbon dioxide levels on feed grain quality for poultry production. *Agriculture* 12, 1913.

https://doi.org/10.3390/agriculture12111913 Li, Y., Guan, K., Schnitkey, G. D., DeLucia, E., and Peng, B. (2019). Excessive rainfall leads to maize yield loss of a comparable magnitude to extreme drought in the United States. *Global Change Biology* 25, 2325–2337. https://doi.org/10.1111/gcb.14628

Li, Y., Tao, H., Zhang, B., Huang, S., and Wang, P. (2018). Timing of water deficit limits maize kernel setting in association with changes in the source-flow-sink relationship. *Front Plant Sci* 9, 1326. ttps://doi.org/10.3389/fpls.2018.01326

Long, S. P., Zhu, X.-G., Naidu, S. L., and Ort, D. R. (2006). Can improvement in photosynthesis increase crop yields? *Plant, Cell & Environment* 29, 315–330. https://doi.org/10.1111/j.1365- 3040.2005.01493.x

Luo, Y., Li, W., Huang, C., Yang, J., Jin, M., Chen, J., et al. (2021). Exogenous abscisic acid coordinating leaf senescence and transport of assimilates into wheat grains under drought stress by regulating hormones homeostasis. *The Crop Journal* 9, 901–914. https://doi.org/10.1016/j.cj.2020.08.012

Mekonnen, M. M., and Gerbens-Leenes, W. (2020). The Water Footprint of Global Food Production. *Water* 12, 2696.

https://doi.org/10.3390/w12102696

Mbow, C., Rosenzweig, C., Barioni, L. G., Benton, T. G., Herrero, M., Krishnapillai, M., et al. (2019). "Chapter 5: Food security — Special report on climate change and land," in *Climate Change and Land: an IPCC special report on climate change, desertification, land degradation, sustainable land management, food security, and greenhouse gas fluxes in terrestrial ecosystems*.

https://doi.org/10.1017/9781009157988.007

Naidu, G. K., Hugar, R., M, K. R., S, B. J., Talekar, S. C., and P, C. V. (2023). Simulated drought stress unravels differential response and different mechanisms of drought tolerance in newly developed tropical field corn inbreds. *PLOS ONE* 18, e0283528.

https://doi.org/10.1371/journal.pone.0283528

NASA (2023). The effects of climate change. *Climate Change: Vital signs of the planet*. Available at: https://climate.nasa.gov/effects [Accessed June 18, 2023].

Ning, P., Yang, L., Li, C., and Fritschi, F. B. (2018). Post-silking carbon partitioning under nitrogen deficiency revealed sink limitation of grain yield in maize. *J Exp Bot* 69, 1707–1719. https://doi.org/10.1093/jxb/erx496

Oury, V., Caldeira, C. F., Prodhomme, D., Pichon, J.-P., Gibon, Y., Tardieu, F., et al. (2016). Is change in ovary carbon status a cause or a consequence of maize ovary abortion in water deficit during flowering? *Plant Physiology* 171, 997–1008. https://doi.org/10.1104/pp.15.01130

Poudel, S., Vennam, R. R., Shrestha, A., Reddy, K. R., Wijewardane, N. K., Reddy, K. N., et al. (2023). Resilience of soybean cultivars to drought stress during flowering and early-seed setting stages. *Sci Rep* 13, 1277. https://doi.org/10.1038/s41598-023-28354-0

Qu, L., Gu, X., Li, J., Guo, J., & Lu, D. (2023). Leaf photosynthetic characteristics of waxy maize in response to different degrees of heat stress during grain filling. *BMC Plant Biology*, *23*(1), 469. https://doi.org/10.1186/s12870-023-04482-7

R Core Team (2022). R: A language and environment for statistical computing. R Foundation for Statistical Computing, Vienna, Austria. Available at: https://www.R-project.org/

Seebauer, J. R., Singletary, G. W., Krumpelman, P. M., Ruffo, M. L., and Below, F. E. (2010). Relationship of source and sink in determining kernel composition of maize. *Journal of Experimental Botany* 61, 511–519. https://doi.org/10.1093/jxb/erp324

Sehgal, A., Sita, K., Siddique, K. H. M., Kumar, R., Bhogireddy, S., Varshney, R. K., et al. (2018). Drought or/and heat-stress effects on seed filling in food crops: impacts on functional biochemistry, seed yields, and nutritional quality. *Frontiers in Plant Science* 9. https://doi.org/10.3389/fpls.2018.01705

Seleiman, M. F., Al-Suhaibani, N., Ali, N., Akmal, M., Alotaibi, M., Refay, Y., et al. (2021). Drought stress impacts on plants and different approaches to alleviate its adverse effects. *Plants (Basel)* 10, 259. https://doi.org/10.3390/plants10020259

Shao, R., Jia, S., Tang, Y., Zhang, J., Li, H., Li, L., et al. (2021). Soil water deficit suppresses development of maize ear by altering metabolism and photosynthesis. Environmental and Experimental Botany 192, 104651. https://doi.org/10.1016/j.envexpbot.2021.104651

Singh, S., Gupta, A. K., and Kaur, N. (2012). Influence of drought and sowing time on protein composition, antinutrients, and mineral contents of wheat. *The Scientific World Journal* 2012, e485751. https://doi.org/10.1100/2012/485751

Song, H., Li, Y., Zhou, L., Xu, Z., and Zhou, G. (2018). Maize leaf functional responses to drought episode and rewatering. *Agricultural and Forest Meteorology* 249, 57–70. https://doi.org/10.1016/j.agrformet.2017.11.023

Tang, Y., Guo, J., Jagadish, S. V. K., Yang, S., Qiao, J., Wang, Y., et al. (2023). Ovary abortion in field-grown maize under water- deficit conditions is determined by photo- assimilation supply. *Field Crops Research* 293, 108830. https://doi.org/10.1016/j.fcr.2023.108830

Tombesi, S., Nardini, A., Frioni, T., Soccolini, M., Zadra, C., Farinelli, D., et al. (2015). Stomatal closure is induced by hydraulic signals and maintained by ABA in drought- stressed grapevine. *Scientific Reports* 5, 12449. https://doi.org/10.1038/srep12449

Trachsel, S., Sun, D., SanVicente, F. M., Zheng, H., Atlin, G. N., Suarez, E. A., et al. (2016). Identification of QTL for early vigor and stay-green conferring tolerance to drought in two connected advanced backcross populations in tropical maize (*Zea mays* L.). *PLoS One* 11, e0149636. https://doi.org/10.1371/journal.pone.0149636

USDA-ERS (2019). Most corn production in U.S. and Mexico is geographically concentrated. http://www.ers.usda.gov/data-products/chart-gallery/gallery/chart-detail/?chartId=95199 [Accessed June 18, 2023].

Vennam, R. R., Poudel, S., Ramamoorthy, P., Samiappan, S., Reddy, K. R., and Bheemanahalli, R. (2023). Impact of soil moisture stress during the silk emergence and grain-filling in maize. *Physiologia Plantarum* 175, e14029. https://doi.org/10.1111/ppl.14029

Verbraeken, L., Wuyts, N., Mertens, S., Cannoot, B., Maleux, K., Demuynck, K., De Block, J., Merchie, J., Dhondt, S., Bonaventure, G. and Crafts-Brandner, S., 2021. Drought affects the rate and duration of organ growth but not inter-organ growth coordination. *Plant Physiology*, *186*(2), pp.1336-1353. https://doi.org/10.1093/plphys/kiab155

Vollbrecht, E., & Schmidt, R. J. (2009). Development of the inflorescences. In J. L. Bennetzen & S. C. Hake (Eds.), Handbook of Maize: Its biology (pp. 13–40). *Springer*. https://doi.org/10.1093/plphys/kiab155

Xu, Z., and Zhou, G. (2008). Responses of leaf stomatal density to water status and its relationship with photosynthesis in a grass. *J Exp Bot* 59, 3317–3325. https://doi.org/10.1093/jxb/ern185

Xu, Z., Zhou, G., and Shimizu, H. (2010). Plant responses to drought and rewatering. *Plant Signaling & Behavior,* 5:6, 649-654,

https://doi.org/10.4161/psb.5.6.11398

Yang, J., & Zhang, J. (2006). Grain filling of cereals under soil drying. *New Phytologist*, 169(2), 223–236.

https://doi.org/10.1111/j.1469- 8137.2005.01597.x

Zhang, X., Lei, L., Lai, J., Zhao, H., and Song, W. (2018). Effects of drought stress and water recovery on physiological responses and gene expression in maize seedlings. *BMC Plant Biology* 18, 68.

https://doi.org/10.1186/s12870-018-1281-x

Zhao, C., Liu, B., Piao, S., Wang, X., Lobell, D. B., Huang, Y., et al. (2017). Temperature increase reduces global yields of major crops in four independent estimates. *PNAS* 114, 9326–9331. https://doi.org/10.1073/pnas.1701762114

Zhuang, J., Wang, Y., Chi, Y., Zhou, L., Chen, J., Zhou, W., et al. (2020). Drought stress strengthens the link between chlorophyll fluorescence parameters and photosynthetic traits. *PeerJ* 8, e10046. https://doi.org/10.7717/peerj.10046

# Survival, Persistence, Regrowth, And Isolation of Colony Variants of *Listeria Monocytogens* Strains After Exposure to First Generation Quaternary Ammonium Compound (Benzalkonium Chloride) in Water

**Stephen Schade[1], Emily Tucker[1], Ramakrishna Nannapaneni[1*], Divya Kode[1], Mohit Bansal[2], Li Zhang[2], Shecoya White[1], Sam Chang[1]**

[1]Department of Food Science, Nutrition and Health Promotion, Mississippi State University, Mississippi State, MS 39762, USA and [2]Poultry Science Department, Mississippi State University, Mississippi State, MS 39762, USA.

**Corresponding Author:** Ramakrishna Nannapaneni
**E-mail:** nannapaneni@fsnhp.msstate.edu
**Phone**: 662-325-7697, Fax: 662-325-8728
**Doi:**10.34107/CTJP1687

## ABSTRACT

*Listeria monocytogenes* occurrence in food products has changed over the past twenty years. This dangerous foodborne pathogen has been historically associated with the consumption of soft cheeses (queso fresco, etc.) and ready-to-eat processed meats, but over the past two decades, there has been a notable increase in *L. monocytogenes* outbreaks in other food products. With the increasing frequency of recalls due to *L. monocytogenes*, and its frequent association with foods that are not normally considered a high risk for this pathogen, there is a need for understanding the factors that contribute to its survival and persistence in the food processing environments. Quaternary ammonium compounds (QACs) are the most common sanitizing agents used in the food processing environment and are essential in controlling the spread of *L. monocytogenes*. Of the seven generations of QACs have been developed over nearly 100 years, the first generation QAC, benzalkonium chloride (BAC) has been most widely used in various QAC formulations to kill bacteria, fungi, and viruses. Though QACs are used at very high concentrations of 150-200 ppm which is 50-100 times greater than the minimum inhibitory concentration (MIC), residual concentrations of 14 µg/ml were found in the food processing environments. Therefore, the objective of this study is to investigate the survival of two strains of *L. monocytogenes*, Bug600 (serotype 1/2a) and ScottA (serotype 4b) in bactericidal concentrations of BAC in water, and their subsequent persistence in high or low nutrient conditions. Using a concentration range of BAC in 96 well plates, we first observed the real-time growth rate of *L. monocytogenes* strains possibly mimicking the sublethal BAC conditions that it may encounter in some environments. The MIC of BAC of *L. monocytogenes* varied for two strains which was 2 µg/ml for Bug600 and 4 µg/ml for ScottA. In a concentration-to-kill test, when 7 log CFU/ml of *L. monocytogenes* cells were exposed to the bactericidal concentrations of BAC at 10-14 µg/ml, it resulted in the survivors of 1-3 log CFU/ml of Bug600 and 2-4 log CFU/ml of ScottA after 1 h, and none were detectable for both strains after 24 h. However, when such bactericidal concentrations were diluted to ½ or ¼ with high or nutrient conditions which may possibly occur in the natural environments that resulted in exposure to sublethal BAC of 3.5-7 µg/ml for 24 h, these aliquots yielded 1-2 log CFU/ml of *L. monocytogenes*. Under such sublethal BAC conditions, two distinct colony variants of *L. monocytogenes* (small and large colonies) were also observed on agar plates which were not published before. These colony variants were reconfirmed as *L. monocytogenes* and awaiting further characterization for BAC tolerance. These findings are useful in understanding the potential link between extensive QAC usage and occurrence of colony variants of *L. monocytogenes* cells which may create potential food safety risk.

**Keywords:** *Listeria monocytogenes*, quaternary ammonium compounds, QAC, disinfectant tolerance

## INTRODUCTION

*Listeria monocytogenes* is a Gram-positive, rod-shaped bacterium that is the causative agent of the disease listeriosis, which is almost always acquired through the consumption of food contaminated with the pathogen. In healthy adults, noninvasive listeriosis is the most common presentation which will cause typical gastroenteritis symptoms including stomach pain,

nausea, vomiting and diarrhea but without serious complications. In children, the elderly, pregnant women, and other immunocompromised patients however the risk for invasive listeriosis is much higher. This disease occurs when *L. monocytogenes* spreads beyond the digestive tract and causes life threatening sepsis and meningitis. This results in a fatality rate of close to 20-30%, much higher than most other foodborne pathogens (Mazaheri et al., 2021). *L. monocytogenes* is a major challenge to the food industry due to its severity, but also due to the difficulty in controlling the pathogen. *L. monocytogenes* is a ubiquitous organism that can be found in soil, water, and various animals (Linke et al., 2014). This widespread dispersal makes it very difficult to keep the pathogen out of processing plants (Lepe, 2020). Furthermore, *L. monocytogenes* is one of the most cold-tolerant foodborne pathogens as refrigeration alone is not enough to stop the growth of *L. monocytogenes* (Hingston et al., 2019).

Due to this cold tolerance, *L. monocytogenes* has historically been associated with ready to eat foods of animal origin such as dairy products and deli meat. As these products are not designed to be cooked and their only method of preservation once they leave the plant is refrigeration, these foods are at high risk for *L. monocytogenes*. More recently however, many new types of food not traditionally considered high risk have served as vectors for listeriosis. This includes fresh and frozen fruit and vegetables, mushrooms, ice cream, and seafood among many others (Desai et al., 2019).

To prevent outbreaks like this, thorough sanitization of plant equipment and proper hygiene of employees is required. Both processes rely heavily on the use of quaternary ammonium compounds (QACs). This most common disinfectant in the world, QACs consist of a central nitrogen cation, with attached groups varying widely from there. The N+ ion is bound to up to four other functional groups, typically with one or more alkyl chains measuring 8-18 carbons in length (Buffet-Battalion et al., 2012). When a cell is exposed to QACs, the positively charged quaternary nitrogen associates with the head groups on the phospholipid membrane. After this association, the hydrophobic R groups can insert themselves into the cell membrane, destabilizing them and killing the cell (Gilbert and Moore, 2005).

QACs are effective against bacteria, fungi, and enveloped viruses due to this mechanism (Bures, 2019). The broad spectrum, low toxicity, and corrosiveness of QACs have made them indispensable to the medical and food industry. The effectiveness of a QAC treatment however can be influenced by several factors. QACs are biodegradable when exposed to light or oxygen, and they can lose potency as they become diluted on wet surfaces. (Zhang et al., 2015). These conditions can result in less effective treatment. Both these factors have resulted in wide ranges of QAC concentrations being found in processing facilities ranging from the initial concentration, down to 14 µg/ml (Møretrø et al., 2017).

As most outbreaks of listeriosis are traced back to food processing plants despite sanitization with QACs, the possibility of *L. monocytogenes* persistence after QACs exposure must be evaluated as a potential risk factor.

Therefore, the purpose of the present study was to determine the survival of *L. monocytogenes* strains Bug600 (serotype 1/2a) and ScottA (serotype 4b) in varying increasing concentrations of BAC in water (that may normally be found in effluents) to observe for pathogen persistence in high or low nutrient conditions. Another objective of this study was to isolate the subpopulations of *L. monocytogenes* when exposed to BAC that may give rise to different colony variants.

## MATERIALS AND METHODS

**Bacterial strains and media.** Two *L. monocytogenes* strains Bug600 (serotype 1/2a) and ScottA (serotype 4b) were tested in all experiments. The source of these strains and their lineages are described in Table 1. These strains were stored at -80°C in tryptic soy broth containing 0.6% yeast extract supplemented with 25% glycerol (TSBYE) (BD Bio sciences, San Jose, CA). The frozen stocks were revived by streak plating on PALCAM agar (BD Bio

Sciences, San Jose, CA) which was then stored at 4°C for 1 month. A single colony was taken from these plates and used to inoculate a 10 ml of TSBYE to create an overnight culture (ONC) that was incubated at 37°C for 24 h.

**Table 1. List of *L. monocytogenes* strains used in this study.**

| Species | Designation | Lineage | Serotype | Source | Isolation Source |
|---|---|---|---|---|---|
| *L. monocytogenes* | EGD (Bug600) | II | 1/2a | Institute Pasteur | Guinea Pigs |
| *L. monocytogenes* | ScottA | I | 4b | FDA | Human epidemic |

**QAC preparation.** *L. monocytogenes* strains were exposed to the first generation QAC, benzalkonium chloride (BAC, Acros Organics, Fisher Scientific). A 99.9% stock solution of the compound was diluted in distilled water at a 1:4 ratio, resulting in a 250,000-ppm working stock which was stored in a dark cabinet at room temperature. Samples from the 250,000-ppm working stock were used to prepare various 1:10 dilutions in distilled water depending on the need of the experiments.

**Determination of minimum inhibitory concentration (MIC) of BAC against *L. monocytogenes* strains.** The MIC of BAC for *L. monocytogenes* strains was measured by microdilution method in round bottom 96-well microtiter plates (Midsci, Fenton MO). The 250,000 ppm working stock was diluted to yield a solution of 250 µg/ml in sterile distilled water. Using this solution, an 8 µg/ml solution of BAC was prepared in TSB, of which 200 µl was then transferred to each well in the first and seventh columns of a microtiter plate. Every other column then received 100 µl of TSB before the plate was serially diluted by transferring 100 µl of the BAC solution from columns 1 and 7 down each row, resulting in concentrations of 8, 4, 2, 1, 0.5, and 0 µg/ml of BAC with a final volume of 100 µl. Next a 20 µl sample of *L. monocytogenes* ONCs was diluted at a 1:10 ratio in distilled water before being transferred to every well using an eight-channel pipette, resulting in final volumes of 120 µl in each well of the 96-well microtiter plate. The plate was then incubated at 37°C for 24 h. The MIC was determined to be the lowest concentration of BAC in which no turbidity could be visually detected after observing the top and bottom of each well.

**Growth curves of *L. monocytogenes* strains in different concentrations of BAC.** Two sets of six BAC concentrations of 8, 4, 2, 1, 0.5, and 0 µg/ml were prepared in six columns of the 96 well microtiter plate at 100 µl/well in the same manner as before, except all dilutions were performed in distilled water rather than TSBYE. Then, *L. monocytogenes* cell suspensions of $10^8$ CFU/ml were added at 20 µl/well (which yielded a final cell number of approximately $10^7$ CFU/ml) to every well by using four rows per strain. Following inoculation, the strains were left to sit for 1 h without a source of nutrition to experience both QAC and starvation stress. After the1 h kill time in a 96-well microtiter plate, the surviving cells of *L. monocytogenes* strains at different BAC concentrations were treated with a higher nutrient condition (80 µl/well of 100 % TSB in the first set of 6 columns) or a lower nutrient condition (80 µl/well of 20% TSB in the second

set of 6 columns) and were incubated overnight in an optical density reader at 22°C. *L. monocytogenes* growth curves were determined based on the changes in optical density at $600_{nm}$ at 15 min intervals by incubating the 96-well microtiter plate in a temperature controlled microtiter plate reader without shaking (800 TS Microplate Reader, Biotek Instruments). All experiments were performed at room temperature close to 22°C for 24 h. In growth curve experiments, two *L. monocytogenes* strains were tested at six BAC concentrations at two nutrient conditions in four replications per 96-well microtiter plate and all experiments were repeated four times.

**Determination of survival of *L. monocytogenes* strains in bactericidal concentrations of BAC and regrowth in high and low nutrient condition based on colony forming units (CFU).** Three selected bactericidal concentrations of 14, 12 and 10 µg/ml of BAC prepared in Eppendorf tubes (Thomas Scientific, Swedesboro NJ) were exposed to *L. monocytogenes* cell suspensions of $10^7$ CFU/ml for a 1 h kill time in sterile distilled water at 22°C. After the 1 h kill step, *L. monocytogenes* cells surviving at each BAC concentration were determined by spread plating 100 µl aliquots on TSA before incubating the plates at 37°C for 24 h. The remaining cells of *L. monocytogenes* in BAC concentrations in Eppendorf tubes were diluted with a higher nutrient condition (to give 1:2 or 1:4 dilution of BAC in 100 % TSB) or a lower nutrient condition (to give 1:2 or 1:4 dilution of BAC in 20% TSB) and were incubated for 24 h at 22°C. After 24 h incubation, *L. monocytogenes* CFUs growing in sublethal BAC concentrations were enumerated by spread plating 100 µl aliquots on TSA. For these 24 h CFU experiments, two *L. monocytogenes* strains were tested at six BAC concentrations at two nutrient conditions and all experiments were repeated four times.

**Isolation of colony variants of *L. monocytogenes* after exposure to bactericidal and sublethal BAC.** Figure 1 shows the sequence of steps for the isolation of colony morphotypes of *L. monocytogenes*. Briefly, after the 1 h exposure of *L. monocytogenes* strains to bactericidal concentrations of BAC as described above, such cells suspensions were diluted ½ or ¼ with high or low nutrition and incubated for 24 h. The CFUs of *L. monocytogenes* strains obtained after 24 h growth in high or low nutrition were plated on TSA to examine for variation between the colonies.

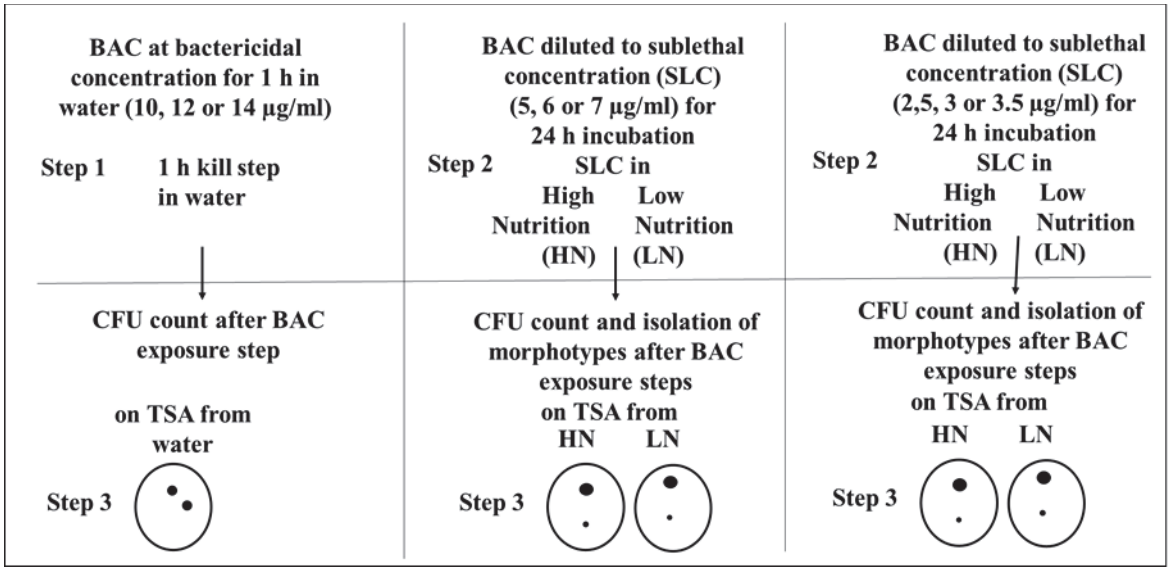


Figure 1. Three-step sequence for survival, persistence and isolation of colony variants of *L. monocytogenes* Bug600 or ScottA after exposure to first generation QAC (BAC) at bactericidal and sublethal concentrations.

**Statistical Analysis.** A completely randomized design (2 strains x 6 BAC concentrations x two nutrient levels) with factorial structure in a randomized complete block design with replication considered as blocks. The statistical significance of the difference in MIC of BAC and lag phase duration at OD600nm between BAC concentrations versus control was tested using the unpaired two-tailed t-test at three significance levels ($P < 0.05$; $P < 0.01$; and $P < 0.001$) in Microsoft Excel (Microsoft Excel, Version 2008). Statistical analysis was performed using one-way ANOVA at a significance level of $P < 0.05$. Logs transformed counts for survivals were analyzed using One-way ANOVA in a completely randomized block design and means were separated by Fisher's protected LSD when $P < 0.05$ (SAS 9.4 TS Level 1M5: SAS Institute Inc., Cary, NC, USA).

## RESULTS

**MIC of BAC for *L. monocytogenes* strains.** The MIC of BAC for *L. monocytogenes* Bug600 was 2 µg/ml, while *L. monocytogenes* ScottA had an MIC of 4 µg/ml as these were the lowest concentrations of BAC that prevented the wells from becoming turbid.

**Growth curves of *L. monocytogenes* strains in different concentrations of BAC.** Figure 2 shows the growth curves ($OD_{600nm}$) for *L. monocytogenes* Bug600 and ScottA in high and low nutrition at 22°C for 24 h after the initial exposure to different concentrations of BAC for 1 h in water. The length of the lag phase for this strain was determined to be the time at which the $OD_{600nm}$ reading exceeded 0.1. In the absence of BAC, the lag phase of *L. monocytogenes* Bug600 was about 2 h in high nutrition (100% TSB, Fig, 2A) or extended to 4 h in low nutrition (20% TSB, Fig. 2B). The highest $OD_{600nm}$ *L. monocytogenes* Bug600 reached in high nutrition was about 0.4 compared to about 0.15 in low nutrition at 22°C in 24 h in the absence of BAC. In the presence of a low concentration of BAC at 0.5 µg/ml, both the lag phase and growth rate of *L. monocytogenes* Bug600 was unaffected relative to that of the control in both high and low nutrition. Increasing the concentration of BAC to 1 µg/ml resulted in the lag phase of *L. monocytogenes* Bug600 increasing to 5 h in high nutrition (Fig. 2A). After such a slower lag phase at 1 µg/ml, *L. monocytogenes* Bug600 growth reached almost the same high optical density as that of control at 600 nm within 24 h at 22°C in high nutrition conditions. By contrast, *L. monocytogenes* Bug600 lag phase was extended for up to 12 h at 1 µg/ml BAC when grown in low nutrition and grew extremely slowly afterwards (Fig. 2B). With higher concentrations of BAC at 2 to 8 µg/ml, there was no growth of *L. monocytogenes* Bug600 in either high nutrition or low nutrition at 24 h at 22°C.

In the absence of BAC, like Bug600, the lag phase of *L. monocytogenes* ScottA was about 2 h in high nutrition (100% TSB, Fig, 2C) as well as in low nutrition (20% TSB, Fig. 2D). In high nutrition, the growth rate of *L. monocytogenes* ScottA was very fast with a sharp exponential phase continuing up to 12 h, but its growth rate was much slower in low nutrition. The highest $OD_{600nm}$ of *L. monocytogenes* ScottA in high nutrition was about 0.45 compared to about 0.175 in low nutrition at 22°C for 24 h in the absence of BAC. In the presence of a low concentration of BAC at 0.5 µg/ml, both the lag phase and growth rate of *L. monocytogenes* ScottA was unaffected relative to the control in both high and low nutrition. With an increase in the concentration of BAC to 1 µg/ml, the lag phase of *L. monocytogenes* ScottA was increased to 5 h in high nutrition (Fig. 2C). After a slower lag phase at 1 µg/ml, *L. monocytogenes* ScottA growth reached almost the same high optical density as that of control at 600 nm within 24 h at 22°C in high nutrition conditions. Unlike Bug600, *L. monocytogenes* ScottA reached the same level as that of control at 1 µg/ml BAC in low nutrition (Fig. 2D). With further higher concentrations of BAC at 2 µg/ml, ScottA's lag phase was extended for 10 h in high nutrition though it could still reach a similar $OD_{600}$. In low nutrition, ScottA just barely crossed the 0.1 $OD_{600}$ threshold at 24 h. For all higher concentrations, there was no growth of *L. monocytogenes* ScottA detectable in either high nutrition or low nutrition at 24 h at 22°C.

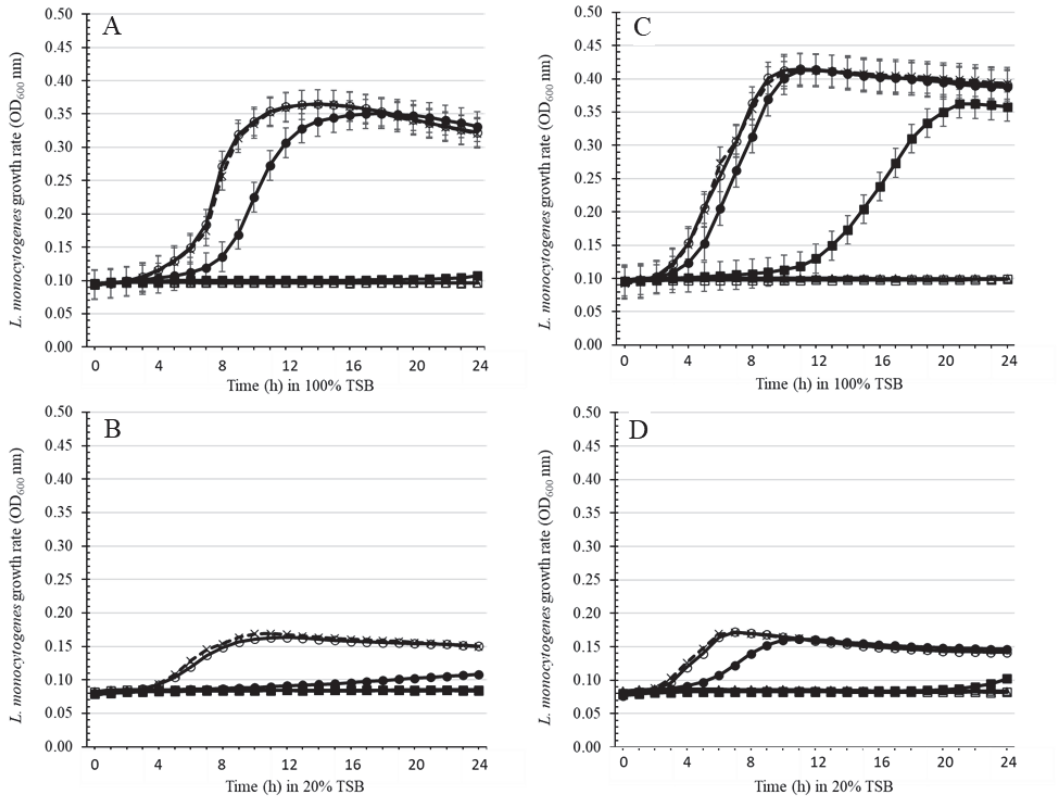


Figure 2. Growth curves of *L. monocytogenes* Bug600 (A, B) and ScottA (C, D) in gradually increasing concentration (x 0 µg/ml, ○ 0.5 µg/ml, ● 1 µg/ml, ■ 2 µg/ml, □ 4 µg/ml, and Δ 8 µg/ml) ) of first generation QAC (BAC) in high (A, C, 100% TSB, HN) or low (B, D, 20% TSB, LN) nutrient conditions at 22°C for 24 h measured by optical density at 600 nm.

**Survival of *L. monocytogenes* strains in bactericidal concentrations of BAC in water followed by regrowth or persistence after BAC dilution.** Figure 3 shows the survival of *L. monocytogenes* Bug600 and ScottA after exposure to bactericidal concentrations of BAC at 22°C for 1 h in water followed by the recovery of persistent cells when BAC concentrations were diluted with high or low nutrition for 24 h. In this concentration-to-kill assay, *L monocytogenes* Bug600 cell count was immediately decreased by 5 logs from the initial 7 logs after exposure to BAC at 10 µg/ml for 1 h in water. When BAC concentrations were increased to 12-14 µg/ml for 1 h in water, the survivors obtained decreased to about 0.5-1 logs of *L. monocytogenes* Bug600. No detectable *L. monocytogenes* Bug600 cells were found at these higher concentrations of BAC after 24 h in water. After BAC concentration was diluted by one half from the initial 10 µg/ml down to 5 µg/ml with high or low nutrition, about 0.5 log of survivors were found in high nutrition after 24 h, and none detected in low nutrition. When BAC was further diluted by a one fourth dilution from the initial 10 µg/ml down to 2.5 µg/ml about 2 logs of survivors were recoverable in high nutrition, or about 1 log in low nutrition after 24 h. Also, some survivors of *L. monocytogenes* Bug600 were recoverable when the BAC concentration of 14 or 12 µg/ml were diluted by one fourth down to 3.5 or 3 µg/ml in high and low nutrient conditions after 24 h at 22°C (Fig. 3A).

The survival and regrowth pattern for *L. monocytogenes* ScottA was quite like that of *L. monocytogenes* Bug600 (Fig. 3B). From the initial 7 logs, about 4-5 logs survived after exposure to 10 µg/ml BAC for 1 h, 3.5 log

survived after exposure to 12 µg/ml, and 2 log survived after exposure to 14 µg/ml BAC in water for 1 h (Fig. 3B). About 1.5 logs in high nutrition and 0.5 logs in low nutrition of persistent CFUs of *L. monocytogenes* ScottA were observed after one half dilution from the initial 10 µg/ml down to 5 µg/ml for 24 h.

When 12 or 14 µg/ml were diluted to 6 or 7 µg/ml, less than 0.5 logs were recoverable in high nutrition, and no survivors were present in low nutrition. When BAC was further diluted by one fourth from the initial 10 µg/ml down to 2.5 µg/ml with high or low nutrition, about 3.5 logs of ScottA survivors were found in high nutrition, and about 3 logs in low nutrition after 24 h. Also, 0.5-3 log cells of *L. monocytogenes* ScottA were recoverable when the higher initial BAC concentrations of 14 or 12 µg/ml were diluted down to 3.5 or 3 µg/ml in high and low nutrient conditions after 24 h at 22°C (Fig. 3B).

Overall, the BAC concentration was found to significantly impact the number of survivors of both *L. monocytogenes* strains ($p<0.05$). The level of nutrition however did not significantly impact the amount of CFU's recovered ($p>0.05$) for either strain, suggesting that at low concentrations of BAC, both levels of nutrition will be sufficient to allow the survival of *L. monocytogenes*.

**Colony variants of *L. monocytogenes* strains after exposure to BAC.** Figure 4 shows the small and large colony variants of *L. monocytogenes* Bug600 and ScottA CFUs obtained after exposure to high or low concentration of BAC at 22°C. These small and large variants of *L. monocytogenes* Bug600 and ScottA were observed on TSA plates from any sublethal BAC concentrations for 24 h after the 1 h initial exposure to bactericidal concentration. However, no size variation was observed when *L. monocytogenes* Bug600 and ScottA cells were immediately plated out after the 1 h kill step. These small and large colony variants were isolated and reconfirmed as *L. monocytogenes* on both PALCAM and *Listeria* chromogenic agar which are waiting for further characterization.

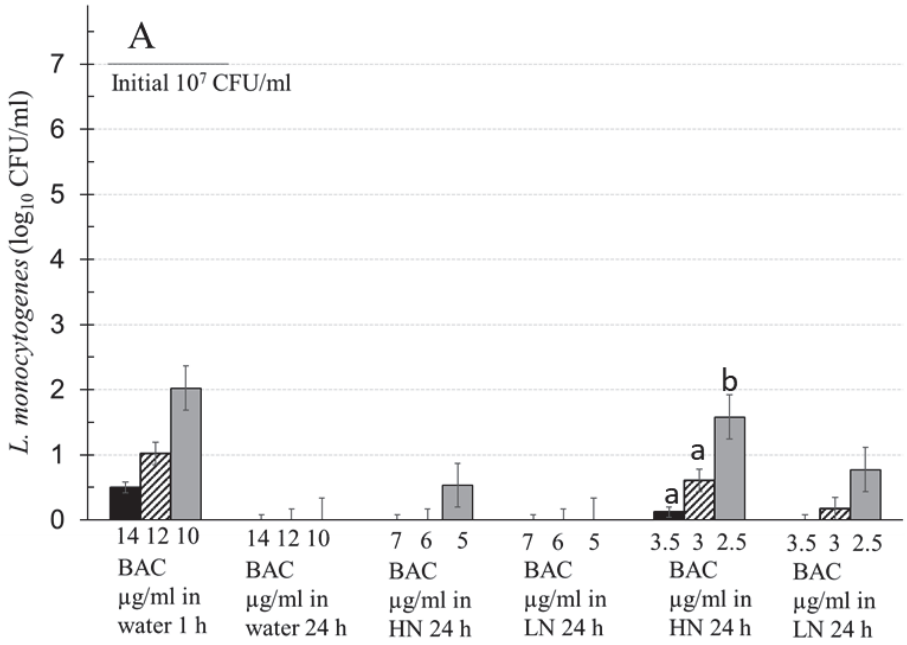


Figure 3 (A). Concentration-to-kill assay in water for survival of *L. monocytogenes* Bug600 in first generation QAC (BAC) at 14, 12 and 10 µg/ml for 1 h followed by persistence in high (100% TSB, HN) or low (20% TSB, LN) nutrient conditions containing ½ or ¼ diluted (sublethal) concentrations of BAC for 24 h.

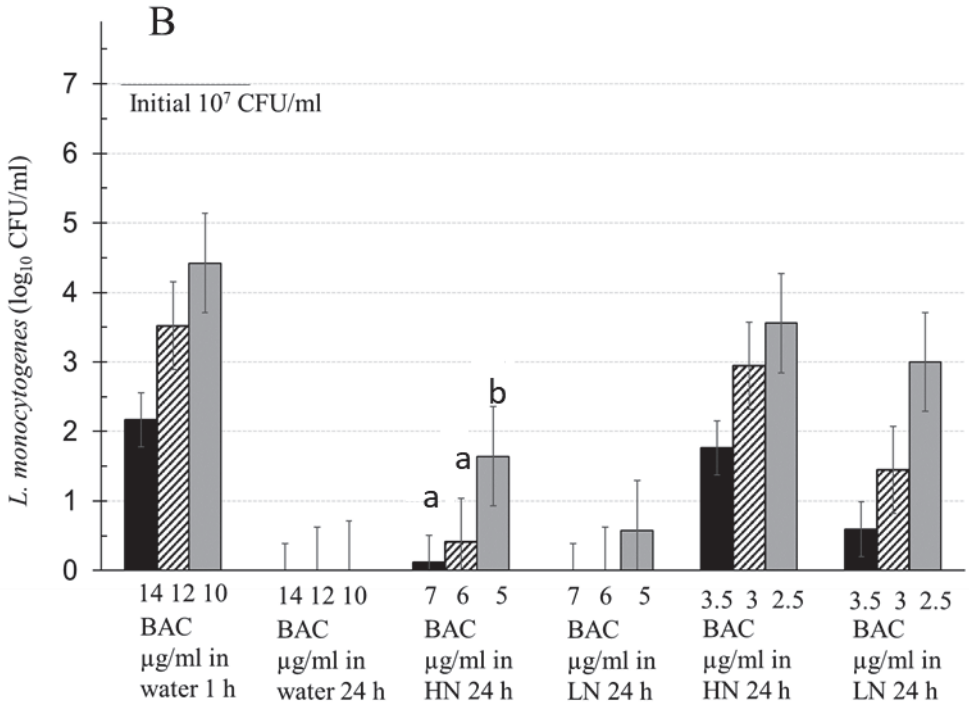


Figure 3 (B). Concentration-to-kill assay in water for survival of *L. monocytogenes* Bug600 ScottA in first generation QAC (BAC) at 14, 12 and 10 µg/ml for 1 h followed by persistence in high (100% TSB, HN) or low (20% TSB, LN) nutrient conditions containing ½ or ¼ diluted (sublethal) concentrations of BAC for 24 h.

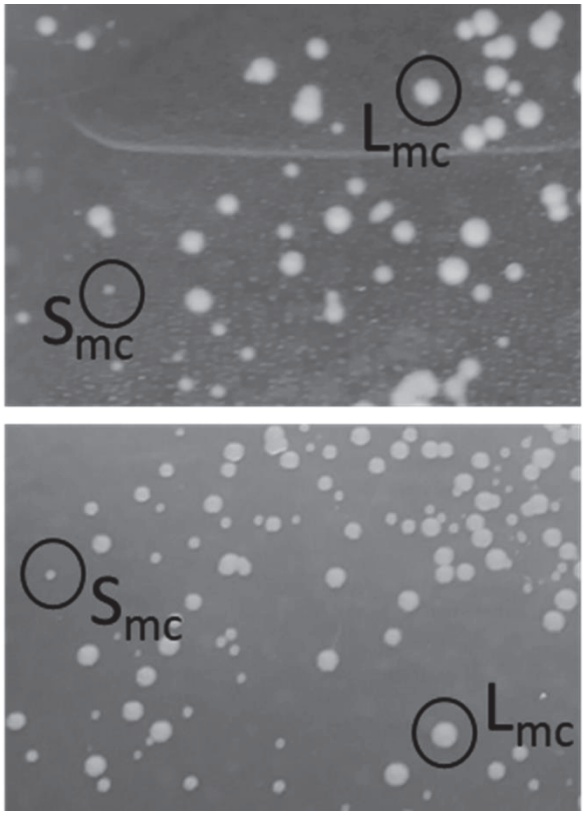


Figure 4. Isolation of small colony variant ($S_{mc}$) and large colony variant ($L_{mc}$) of *L. monocytogenes* Bug600 and ScottA on non-selective TSA after exposure to first generation QAC (BAC) at 10 µg/ml for 1 h in water and then followed by 2.5 µg/ml overnight in low nutrition (*L. monocytogenes* colonies were reconfirmed on selective PALCAM).

## DISCUSSION

Despite the use of highly effective sanitizers, previous studies have demonstrated that the persistence of *L. monocytogenes* in the food processing environments has been rising (Ferreira et al., 2014; Matereke and Okoh, 2020). What causes *L. monocytogenes* to persist in processing plants is still debated. Some studies have suggested that genetic characteristics of the strain itself are not that important in the persistence of *L. monocytogenes*, but rather the presence of difficult-to-clean niches (Carpentier and Cerf, 2011). More recent surveys of processing plants however have revealed that among the strains isolated on at least four separate occasions, 42.8% harbored either the bcrABC or EmrC QAC efflux pumps while only 4.5% of these persistent isolates lacked both pumps (Cherifi et al., 2020).

To understand the predisposing conditions that play a role in the survival and persistence of *L. monocytogenes* in the food processing environment, we tested varying concentrations of BAC in water for survival differences in *L. monocytogenes* strains. Normally *L. monocytogenes* cells are killed within a few minutes of exposure to high concentrations of BAC. Even though QAC is applied at very high recommended doses at 150 to 200 ppm which is about 50-100 times greater than the MIC, low but persistent level of QAC (up to 14 µg/ml) may remain in the food processing environment (Møretrø et al., 2017). Therefore, in this study, we tested such bactericidal concentrations of BAC to examine *L. monocytogenes* survival and persistence. Our findings showed significant differences between *L. monocytogenes* Bug600 and ScottA survival in concentration-to-kill assay with BAC in water. Compared to Bug600, about 1.5 to 3.0 more logs of ScottA CFU/ml survived from the initial 7.0 log CFU/ml when exposed to bactericidal concentration of BAC 10-14 µg/ml in water for 1 h.

Another objective of our study is to investigate *L. monocytogenes* subpopulations that do not get killed in the initial kill step and if they may grow back when the bactericidal concentrations get diluted by the availability of a nutrition source. In this study, the two nutrient levels comprising of high or low nutrition conditions revealed slight differences in regrowth patterns of *L. monocytogenes* strains surviving 1 h kill time with BAC in water. Our results show that both *L. monocytogenes* strains exhibited about 1-3 logs of survivors in both high and low nutrient conditions after the BAC concentrations were diluted. Under both high and low nutrient conditions, the persistence patterns of both Bug600 and ScottA strains were quite similar. These findings indicate that some cells of *L. monocytogenes* strains can persist in certain concentrations of BAC where nutrients are available, which may lead to recontamination.

To our knowledge, the size variation observed in these studies of *L. monocytogenes* Bug600 or ScottA in diluted BAC concentrations after 24 h have not been previously observed in *L. monocytogenes*. Such colony variants were obtained from any sublethal BAC concentration and nutrient level, provided they had been allowed to incubate for 24 h after 1 h initial exposure to bacterial concentrations of BAC. In other studies, the characteristics of such colonies were not described, but the exposure to similar levels of BAC induced in a dramatic shift in the fatty acid composition of *L. monocytogenes* structural lipids. A reduction in branched fatty acids and overall phosphorous was observed which would reduce membrane fluidity to help survive BAC, while also altering the adhesive properties of the membrane (Bisbiroulas et al., 2011). Such lipid alterations if selected by BAC could therefore be a possible mechanism to explain the unique morphotypes observed in our experiments. Other research has noted that prior exposure to BAC stress can induce the formation of longer, slimmer *L. monocytogenes* cells relative to a parent strain, which was also explained by shifts in the fatty acid profile of the membrane (To et al., 2002). The altered membrane composition of BAC adapted strains resulting in different adhesive properties as well as the structure of the cell itself is a possible explanation for the morphotype variants observed in our experiments, though more research is needed to further confirm.

In conclusion, while BAC is still an effective sanitizer, its efficacy can be influenced by the time of exposure and by the presence or absence of contaminating food residues. These conditions can dictate whether *L. monocytogenes* will survive a lethal exposure of BAC. Our findings also show that 24 h exposure to sublethal or low levels of BAC following a 1 h shock against bactericidal concentrations of BAC will result in the formation of unique colony morphotypes. Currently, we are evaluating such *L. monocytogenes* colony variants for significant changes in MIC, growth rate and survival in relation to their parent strains in the presence of lethal and sublethal concentrations of BAC. Further research will also explore their genetics to determine definitively the cause of such size variation in *L. monocytogenes* and connection to QAC tolerance.

## ACKNOWLEDGEMENTS

This material is based upon the work that is supported by the Food Safety Initiative award to Nannapaneni from the Mississippi Agricultural and Forestry Experiment Station under project MIS-81710.

## CONFLICT OF INTEREST

There is no conflict of interest to declare.

## LITERATURE CITED

Bisbiroulas, P., Psylou, M., Iliopoulou, I., Diakogiannis, I., Berberi, A., & Mastronicolis, S. K. (2011). Adaptational changes in cellular phospholipids and fatty acid composition of the food pathogen *Listeria monocytogenes* as a stress response to disinfectant sanitizer benzalkonium chloride. *Letters in Applied Microbiology 52*(3), 275-280.

Buffet-Bataillon, S., Tattevin, P., Bonnaure-Mallet, M., & Jolivet-Gougeon, A. (2012). Emergence of resistance to antibacterial agents: the role of quaternary ammonium compounds—a critical review. *International Journal of Antimicrobial Agents 39*(5), 381-389.

Bureš, F. (2019). Quaternary ammonium compounds: simple in structure, complex in application. *Topics in Current Chemistry 377*(3), 14.

Carpentier, B., & Cerf, O. (2011). Persistence of *Listeria monocytogenes* in food industry equipment and premises. *International Journal of Food Microbiology*, *145*(1), 1-8.

Cherifi, T., Arsenault, J., Pagotto, F., Quessy, S., Côté, J.C., Neira, K., Fournaise, S., Bekal, S. and Fravalo, P. (2020). Distribution, diversity and persistence of *Listeria monocytogenes* in swine slaughterhouses and their association with food and human listeriosis strains. *PLoS One 15*(8), p.e0236807.

Desai, A. N., Anyoha, A., Madoff, L. C., & Lassmann, B. (2019). Changing epidemiology of *Listeria monocytogenes* outbreaks, sporadic cases, and recalls globally: A review of ProMED reports from 1996 to 2018. *International Journal of Infectious Diseases 84*, 48-53.

Ferreira, V., Wiedmann, M., Teixeira, P., & Stasiewicz, M. J. (2014). *Listeria monocytogenes* persistence in food-associated environments: epidemiology, strain characteristics, and implications for public health. *Journal of Food Protection 77*(1), 150-170.

Gilbert, P., & Moore, L. E. (2005). Cationic antiseptics: diversity of action under a common epithet. *Journal of Applied Microbiology 99*(4), 703-715.

Hingston, P. A., Hansen, L. T., Pombert, J. F., & Wang, S. (2019). Characterization of *Listeria monocytogenes* enhanced cold-tolerance variants isolated during prolonged cold storage. *International Journal of Food Microbiology 306*, 108262.

Ibusquiza, P. S., Herrera, J. J., Vázquez-Sánchez, D., Parada, A., & Cabo, M. L. (2012). A new and efficient method to obtain benzalkonium chloride adapted cells of *Listeria monocytogenes*. *Journal of Microbiological Methods 91*(1), 57-61.

Kode, D., Nannapaneni, R., Bansal, M., Chang, S., Cheng, W. H., Sharma, C. S., & Kiess, A. (2021). Low-level tolerance to fluoroquinolone antibiotic ciprofloxacin in QAC-adapted subpopulations of *Listeria monocytogenes*. *Microorganisms 9*(5), 1052.

Kovacevic, J., Ziegler, J., Wałecka-Zacharska, E., Reimer, A., Kitts, D. D., & Gilmour, M. W. (2016). Tolerance of *Listeria monocytogenes* to quaternary ammonium sanitizers is mediated by a novel efflux pump encoded by emrE. *Applied and Environmental Microbiology 82*(3), 939-953.

Lepe, J. A. (2020). Current aspects of listeriosis. *Medicina Clínica (English*

*Edition) 154*(11), 453-458.

Linke, K., Rückerl, I., Brugger, K., Karpiskova, R., Walland, J., Muri-Klinger, S., Tichy, A., Wagner, M. and Stessl, B. (2014). Reservoirs of *Listeria* species in three environmental ecosystems. *Applied and Environmental Microbiology 80*(18), pp.5583-5592.

Matereke, L. T., & Okoh, A. I. (2020). *Listeria monocytogenes* virulence, antimicrobial resistance and environmental persistence: A review. *Pathogens 9*(7), 528.

Mazaheri, T., Cervantes-Huamán, B. R., Bermúdez-Capdevila, M., Ripolles-Avila, C., & Rodríguez-Jerez, J. J. (2021). *Listeria monocytogenes* biofilms in the food industry: is the current hygiene program sufficient to combat the persistence of the pathogen? *Microorganisms 9*(1), 181.

Møretrø, T., Schirmer, B. C., Heir, E., Fagerlund, A., Hjemli, P., & Langsrud, S. (2017). Tolerance to quaternary ammonium compound disinfectants may enhance growth of *Listeria monocytogenes* in the food industry. *International Journal of Food Microbiology 241*, 215-224.

To, M. S., Favrin, S., Romanova, N., & Griffiths, M. W. (2002). Postadaptational resistance to benzalkonium chloride and subsequent physicochemical modifications of *Listeria monocytogenes*. *Applied and Environmental Microbiology 68*(11), 5258-5264.

# A Plant Anatomical Investigation of *Hydrocotyle bonariensis* (Araliaceae)

**Geona Miles, Nina Baghai-Riding, JuEun Yun, and William Katembe**
**Delta State University, Cleveland, MS**

**Corresponding Author:** Nina Baghai-Riding
**Email:** nbaghai@deltastate.edu
**Doi:** 10.34107/CTJP1687

## ABSTRACT

The anatomy of *Hydrocotyle bonariensis* Comm. ex Lam. (largeleaf pennywort, Araliaceae) was investigated. Anatomical observations of the petioles, peduncles, rhizomes, roots, and other parts of this plant species have not been described previously. Using fresh samples, anatomical observations and cell measurements on stems, roots, leaves, and inflorescence components were compiled and analyzed. Single-edged razor blades and hand-held microtomes were used in preparing thin-sections, and prepared slides were stained with methylene blue, neutral red, safranin, or toluidine blue. A JEOL scanning electron microscope was used to analyze transverse sections of petioles and surface features of leaf epidermal regions. Thirty-five measurements were taken on major cell components: parenchyma in petiole, internodes between verticils, rhizome and peduncle; collenchyma in petiole and peduncle; guard cells on the abaxial and adaxial leaf surfaces; and more. Several cell types had a significant size range: cortex parenchyma (length 29 - 70 μm and width 20 - 81 μm), pedicel epidermal cells (length 8 - 20 μm and width 8 - 22 μm), and subsidiary cells on the leaf adaxial surface (length 8 - 45 μm, width 16 - 46 μm). Significant anatomical features include: amphistomatic stomata on leaf blades; anisocytic stomata on the leaf blades; paracytic stomata on sepals, petals, and the petiole; secretory ducts in rhizomes, petioles, and leaves; an abnormal eustele configuration of vascular bundles in the petiole; roots with an actinostele; and subprolate, tricolporate pollen.

**KEYWORDS:** Hydrocotyle bonariensis, plant anatomy, Mississippi Delta, wetland plant

## INTRODUCTION

Araliaceae (Ginseng family, order Apiales) is a relatively large family of angiosperms (Simpson, 2019) consisting of 43 genera and 1,450 species. The family consists of trees, shrubs, lianas, and herbs (Simpson, 2019). Most species have a tropical distribution, but some species are endemic to temperate climates. Leaves are pinnately compound, palmately compound, or simple, usually stipulate, and are arranged spirally, rarely opposite or whorled (Simpson, 2019). Flowers are mostly complete, actinomorphic, possess five petals, and have simple terminal umbels or head inflorescences. Fruits are berries, rarely drupes (Elpel, 2013). Several species are economically important, including: *Tetraoabaz papyriferum* (rice-paper plant) which is the source of rice paper: *Panax ginseng* (ginseng root) is used to treat physical or psychomotor performance, diabetes, herpes, and cognitive functions (Ernst, 2010): and species of *Hedera* are grown as ornamental plants.

*Hydrocotyle* L. (water pennyworts) is a widely distributed and extensive genus of herbs in the Araliaceae (Jurica, 1922; Mathias and Constance, 1962; Hamdy et al., 2018); it occurs on all continents except Antarctica (Mathias and Constance, 1962). This genus was formerly placed in the Apiaceae subfamily Hydrocotyloideae (Anderson et al., 2006), but was transferred to Araliaceae, a sister family, based on comparative DNA sequences and phylogenetic studies (Plunkett and Lowry, 2001; Plunkett and Nicolas, 2017). The genus

*Hydrocotyle* contains about 130 herbaceous species (Karuppusamy et al., 2014; Hamdy et al., 2018; Perkins, 2019). Thirty-five are annual species, and 95 are perennial species (Perkins, 2019). The genus is regarded as a basal group in the Araliaceae (Yi et al., 2004). Species of *Hydrocotyle* exist in mesic, semi-aquatic to aquatic environments (Mendoza and Fuentes, 2010), or in seasonally arid environments (Perkins, 2017). Australia and the Neotropics possess the highest diversity of *Hydrocotyle* species (Nery et al., 2020). Traditional taxonomy has separated species of *Hydrocotyle* (Nery et al., 2020) based on their leaf morphology, but the wide variation of leaf characters created confusion in delimiting species (Nery et al., 2020). As a result, some species of *Hydrocotyle* are problematic; although molecular studies for several species are well established (Karuppusamy et al., 2014) more genetic analysis would be useful (Nery et al., 2020). Other diagnostic morphological characters for delineating species of *Hydrocotyle* include the stem, trichomes, petiole length, number of flowers per inflorescence, peduncle width, flower width, fruit shape, and number and distinctiveness of ribs on the fruit (Karuppusamy et al., 2014). Most species of *Hydrocotyle* have circular, elliptical or kidney-shaped leaf blades with scalloped margins and palmate venation; hispid hairs on aerial surfaces; and small, complete actinomorphic flowers on pedunculated terminal or axillary umbels (Pimenov and Leonov, 1993; Karuppusamy et al., 2014).

This study focuses on anatomical features of *Hydrocotyle bonariensis* Comm. ex Lam. (largeleaf pennywort), which is a $C_3$, clonal, low-growing perennial herb (Evans, 1988, Mendoza et al., 2015). Synonyms for this species include *Hydrocotyle umbellata var. bonariensis*, *Hydrocotyle bonariensis var. multiflora*, *Hydrocotyle multiflora*, *Hydrocotyle umbellata var. texana*, and *Hydrocotyle yucatanensis* (Atlas of Florida Plants). The geographical range for *H. bonariensis* extends from Virginia, USA to Chile (Joesting et al., 2012, 2016). It also occurs in Asian countries including China, India, Indonesia, Malaysia, Sir Lanka, (Goh, 2007), sub-Saharan Africa, Central America, and the Caribbean (Mazurndar et al., 2022). It is a semi-aquatic, wetland plant (Iverson, 1949; Justin and Armstrong, 1987; Evans and Whitney, 1992). Extensive populations exist on barrier islands, swales, secondary dunes, and dune meadows along the coastline of the southeastern United States and Gulf Coastal States (Evans, 1992; Carr et al., 1995). It is indigenous on salt flats (Lanning and Eleuterius, 1983); moist sandy areas that possess sediment movement, salt spray, and high solar irradiance within shrub lines that border forests (Joesting et al., 2012, 2016); in wet trenches (Mazumdar, 2022); and along edges of ponds (Mazumdar et al., 2022).

Individual populations of *H. bonariensis* are often clonal. The seed survival rate is less than 1% (Evans, 1992). Seeds of *H. bonariensis* lack a distinct dispersal mechanism, and they are moved passively by wind which may impact their survival (Evans 1992). Horizontal branching rhizomes are a principal method of reproduction (Evans, 1988, 1991, 1992; Joesting et al., 2016). A branching rhizome system may consist of 1,500 interconnected ramets that can spread over one hundred square meters (Evans, 1992). Rhizome connections between ramets may persist for three years; ramets can be severed by trampling, grazing, exposure to heat and cold, erosion, and more (Evans, 1992). Each ramet consists of one to five glossy, round to peltate-shaped leaf/leaves (1.2 - 3 cm diameter) and has an independent nodal root system (Joesting et al., 2012, 2016; Mazumdar et al., 2022). Each leaf has a slender, green petiole that can vary in length

from 2 – 20.5 cm. New leaves occur throughout the growing season (Evans, 1992). Leaf life spans from two to eight weeks (Evans,1992; Joesting et al., 2012); mature leaves last two weeks if exposed to full sun and four to eight weeks in the shade (Evans, 1992). Inflorescences develop directly opposite of a leaf on a ramet. Each inflorescence possesses a long peduncle that supports terminal umbels consisting of numerous small white fragrant flowers that bloom throughout the growing season (Mathias, 1936). Umbels may be simple to profusely branched and compound (Mathias, 1936; Evans, 1992; Nesom and Levin, in prep.). Primary umbels may produce two to six branches with each one bearing none to four verticils and a terminal umbel (Fig. 1). Each flower consists of five distinct sepals, five green to white distinct petals, five stamens with longitudinal anther dehiscence, and a two-carpellate inferior ovary (Mazumdar et al., 2022; Nesom and Levin, in prep.). The fruit is a schizocarp that splits into two mericarps that detach easily at maturity (Tseng, 1965; Nesom and Levin, in prep.). Mericarps are orbicular to triangular in transverse section (Mathias, 1936) and are prominently ribbed (Nesom and Levin, in prep.).

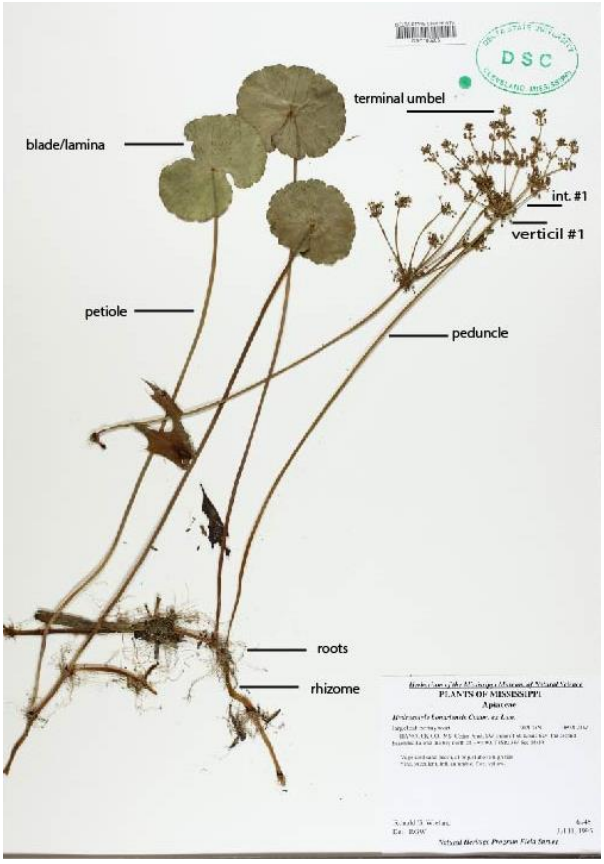


Figure 1. A sample specimen of *Hydrocotyle bonariensis* from Hancock County, MS. Labels indicate specific plant features: int. designates internode.

## Previous Work and Purpose of Study

Approximately 50% of the species in *Hydrocotyle* have published anatomical studies (**Appendix 1)**. All these studies are incomplete, however. Information is often only provided for one or two vegetative or reproductive components: blade, petiole, rhizomes, roots, fruits, seeds, and/or pollen. Tseng (1965), for example, described both pollen and fruits for seventeen *Hydrocotyle* species, but only pollen or fruit for an additional thirty-three species (Appendix 1). Recent anatomical studies have focused on species from Australia (Lemesle, 1925; Henwood, 2014), Brazil (Rios and Dalvi, 2020), Egypt (Hamdy et al., 2018), India (Mittal, 1961), North Carolina (Joesting et al., 2012), Thailand (Klapfer, 2018; Umroong, 2018), and South Africa (Lemesle, 1925). Measurements of assorted cell types occur in only a few publications: Joesting et al., 2012; Hamdy et al., 2018; Klapfer, 2018; Umroong, 2018. Our study on *H. bonariensis* provides a description of assorted anatomical features and will fill gaps about the petiole, rhizome, adventitious roots, leaf lamina, internodes between verticils, and more.

Recent reports on *Hydrocotyle* emphasize how it has environmental and medicinal uses. Using phytoremediation, *H. umbellata* effectively hyperaccumulates metals such as chromium, copper, and zinc through rhizofilitration, therefore, helping to remove harmful elements from polluted aquatic environments and soils (Khilji and Firdaus-e-Bareen, 2008). In southern Brazil, in situ, populations of *H. ranunculoides* successfully phytoextracted phosphorous, sodium, and arsenic from water and translocated these elements into their shoots (Demarco et al., 2018). Additionally, Yoon et al. (2006) found that *H. americana* can concentrate copper, lead, and zinc from soils that grew on a contaminated Florida site. Other recent reports on *Hydrocotyle* emphasize its use in plasticity regarding nutrient availability. Evans (1988) reported how *H. bonariensis* exhibits plasticity depending on soil nitrogen levels. For example, individuals growing in coastal areas of North Carolina that contain low nitrogen levels (less than 2 ppm of $NO_3$ and $NH_4$) possess rhizomes with few branches; rhizomes with secondary and tertiary branches occur when nitrogen levels are high (Evans, 1988). Additional research studies highlight how species of *Hydrocotyle* are important for medicinal purposes as well as for food and beverages. For example, *Hydrocotyle umbellata* is known for its anxiolytic effects and for potential memory stimulation in Brazilian, Taiwanese folk, and Ayurvedic cultures (Hamdy et al., 2018). In Nigeria, *H. bonariensis* is used to treat tuberculosis, pain associated with arthritis, enhance memory stimulation, and more (Masoumian et al., 2011; Mazumdar et al., 2022). In India, stalks and leaves of *H. bonariensis* are consumed in fresh salads and fermented vegetable products, served as a condiment, and added to herbal teas (Reihani and Azhar, 2012; Mazumdar et al., 2022).

## MATERIALS and METHODS

Fresh living specimens of *H. bonariensis* were collected from July 2022 – August 2023 from the southern part of Bear Pen Park and by the bayou that intersects Terrace Road in Cleveland, Mississippi. The population at Bear Pen Park consists of several hundred individual ramets. A few specimens had one to four verticils (Table 3). Vouchers were collected and deposited in the Delta State University Herbarium (DSC). Voucher specimens, DSC116028 and DSC116029, were collected during that time and used for this study. Anatomical features studied include mature roots, rhizomes, leaf lamina, petioles, peduncles, internodes connected to verticils, sepals, petals, and pollen. Distal, medial, and proximal views, middle of petioles, and peduncles were examined and

compared to discern cell size and morphological variations of dermal, ground, and vascular tissues. Peridermal cuts of leaves were prepared to observe details of leaf mesophyll, veins, and stomata.

Transverse and longitudinal anatomical sections were made manually using commercial single-edged razor blades, hand-held microtomes, or with an American Optical rotary microtome. Plant sections requiring the use of a microtome were embedded in FAA and then fixed in 70–100% alcohol solutions for three days because longitudinal sections of the leaves and roots are difficult to prepare with fresh specimens when cut using single-edge razor blades. Fixed specimens were transferred to a 1:1 ratio of xylene and embedding paraffin wax and were put overnight in a THELCO: Model 19 oven at 60° C. Specimens were immersed in ice water and left for 10 minutes to harden the wax prior to being sectioned with a microtome. Transverse cuts made with the American Optical rotary microtome were set at 15 µm. Methylene blue, neutral red, safranin, and toluidine blue dyes were applied to stain the transverse and longitudinal sections of leaves, rhizomes, roots, and peduncles. Clear nail polish was applied to adaxial and abaxial epidermal surfaces of leaves and petioles to make peels that show the guard cells, subsidiary cells, trichomes, regular epidermal cells, and more.

Digital photographs were taken at 40×, 100×, and 400× magnifications with an Olympus Q-Color 3 camera attached to an Olympus BX43 compound light microscope at Delta State University (Plates 1-3). A phase-contrast condenser aided in observing unstained transparent features, such as, guard cells on leaf epidermal peels (Plate 1, Figs. 1-2). Some images of root, rhizome, and leaf sections were taken in Dr. Mac Alford's lab at the University of Southern Mississippi using a Zeiss Axiolmager compound microscope (Plate 1, Figs. 3-4, Plate 2, Figs, 3-4, 6-7; Plate 4, Figs. 1,4-5). A few digital images were taken with the JSM-6010LASEM Scanning Electron Microscope at Delta State University (Plate 2, Fig. 2).

Measurements preformed include the length and width of cell types in leaf blades, petioles, peduncles, internodes #1 and #2 associated with verticils, rhizomes, total inflorescence height, pollen, and more (Tables 1-3). Figure 1 shows verticil #1 is closest to the peduncle and internode #2 is attached to verticil #2 on a branched inflorescence.

Thirty-five measurements for each specified anatomical feature were acquired for statistical purposes; twelve measurements only were acquired for internode #2 because of lack of specimens. To reduce bias, two to six microscope slides, from different individual plant specimens, were analyzed. Recorded data were entered into an Excel spreadsheet for acquiring statistical values: mean, standard deviation, median, and range.

Chromosome counts were conducted on fresh roots harvested from nodes of actively growing ramets. Root tips were fixed in alcohol/acetic acid 3:1 v/v, hydrolyzed in 1N HCL at 60 ºC for 10 min, incubated in Schiff's Reagent for 40 min., then rinsed three times in a beaching solution (5 mL 1N HCL, 5 mL 10% potassium metabisulfite ($K_2S_2O_5$), and 90 mL $dH_2O$) to remove background dye. Stained root tips were cut and placed on a clean microscope slide with one drop of 45% acetic acid. Root tips were broken into tiny fragments before placement of a cover slip (tapping with the rubber end of a standard pencil aided in breaking apart the root cells). Chromosomes were seen using Primo Zeiss and Olympus BX32 compound light microscopes (Plate 3, Figs. 3 - 4).

## RESULTS

### Leaves

#### Lamina/ Blade

Blades are bifacial and amphistomatic and have two lateral wings. Nail-polish epidermal leaf peels and transverse cuts portray that thin cuticular layers occur on both the adaxial and abaxial surfaces (Plate 1, Figs. 1-4). The epidermis surfaces contain a single layer of rectangular to polygonal epidermal cells that possess four to six straight anticlinal walls. The length of epidermal cells on the abaxial surface (Table 1) is greater (20 – 65 µm, median 37 µm) compared to the length of epidermal cells on the adaxial surface (length 19-63 µm, median 33 µm). The width of the epidermal cells is greater on the adaxial surface (21 – 70 µm, median 34 µm) compared to the width of epidermal cells on the abaxial surface (20 – 44 µm, median 25 µm). Chloroplasts are apparent in regular epidermal cells. The adaxial and abaxial epidermis enclose a dorsiventral mesophyll. Widely scattered papillae are attached randomly along the outer edge of some adaxial epidermal cells. The abaxial epidermis is somewhat undulating, uneven, and smaller compared to the adaxial epidermis (Plate 1, Figs. 3-4).

Stomata are anisocytic and irregularly spaced throughout the epidermis. There is a higher density of stomata on the abaxial surface compared to the adaxial surface (Plate 1, Figs.1-2). Guard cells on the abaxial surface are 13 – 36 µm (median 23 µm) in length and 10 – 20 µm (median 13 µm) in width compared to guard cells on the adaxial surface that ranged from 11 – 24 µm (median 18 µm) in length and 13 - 36 µm in width (median 23 µm) (Table 1). Chloroplasts are present in some guard cells. Subsidiary cells are wider (11 – 46 µm, median 22 µm) on the abaxial surface compared to the adaxial surface (5 – 37 µm, median 12 µm).

There are three distinct layers of radially, elongated, columnar palisade parenchyma cells with straight anticlinal walls situated below the adaxial epidermis. The palisade parenchyma comprises about 33% of the total leaf thickness (Plate 1, Fig. 3). Spongy mesophyll comprises approximately 50% of the total leaf thickness. Spongy mesophyll cells are irregular in shape with wide intercellular spaces occurring sporadically between cells. Secretory cells enclosed by a ring of parenchyma cells occur throughout the spongy mesophyll. Vascular bundles are collateral (xylem is on the adaxial side and phloem on the abaxial side) and surrounded by a bundle sheath of small parenchyma cells. Peridermal sections reveal vascular bundles with helical secondary xylem thickening.

#### Petiole

Transverse sections of the petiole are circular in shape (Plate 1, Fig. 9). Transverse sections of the uppermost portion of the petiole reveal that the lamina of the leaf-blade continues over the petiole (Plate 3, Figs. 1 - 2) and form wing-like extensions. The outermost area contains a single layer of elongated epidermal cells with straight anticlinal walls; the external walls are covered by cuticle. Epidermal cells tend to be slightly longer (5 – 25 µm; mean 12.2 µm) and wider (8 – 24 µm; mean 13.3 µm) in proximal areas compared to medial (length 2 – 17 µm, mean 9.6 µm; width 2 – 20 µm, mean 12.1 µm) and distal (length 7 – 20 µm, mean 11.5 µm; width 8 – 20 µm, mean 13.6 µm) regions (Table 1). Epidermal peels reveal epidermal cells form narrow, linear, parallel rows that are 16 -20 µm in width). Paracytic (rubiaceous) stomata are dispersed but are situated within the cell rows (Plate 1, Fig. 5); stomata ranged from 11 – 26 µm (mean 17.4 µm) in length; and 5 – 15 µm (mean 11.1 µm) in width. Two to three layers of lamellar collenchyma occur beneath the

epidermis (Plate 1, Fig. 8). Collenchyma cells in the medial section of the petiole are longer and wider (8 - 32 µm in length; 9 – 35 µm in width) compared to collenchyma cells associated with distal and proximal sections (Table 1). Several rows of round parenchymatous cells with large intercellular spaces (aerenchyma) are present below the collenchyma (Plate 1, Figs. 6, 9). The outermost layers of parenchyma (adjacent to the collenchyma) contain chloroplasts. Cortex parenchyma cells in distal regions of the petioles possess the greatest range in width (16 – 77 µm) compared to medial and proximal sections.

Throughout the parenchymatous cortex are numerous, circular (in cross-section) secretory ducts that may secrete volatile oils. Each secretory duct consists of a circular cavity (lumen) and is enclosed by 10 – 20 small thin-walled cells referred to as endodermis or boundary parenchyma (Plate 1, Fig. 9; Plate 2, Figs. 1-2). The lacuna part of each secretory duct varies from white to cream in color when neutral red dye is applied. Calcium oxalate prismatic crystals are also abundant in parenchyma cells that lack chloroplasts.

The petiole has an atypical eustele arrangement. Six or more amphivasal vascular bundles are widely spaced. Five vascular bundles form a ring-like arrangement below the cortical parenchyma (Plate 1, Fig. 9) with another vascular bundle occupying the center of the petiole. An endodermis ring surrounds each vascular bundle. The bundles are separated by aerenchyma or by elongated parenchymatous medullary rays (Plate 1, Figs. 6, 9). Longitudinal sections of vessels depict annular secondary thickening (Plate 1, Fig. 7).

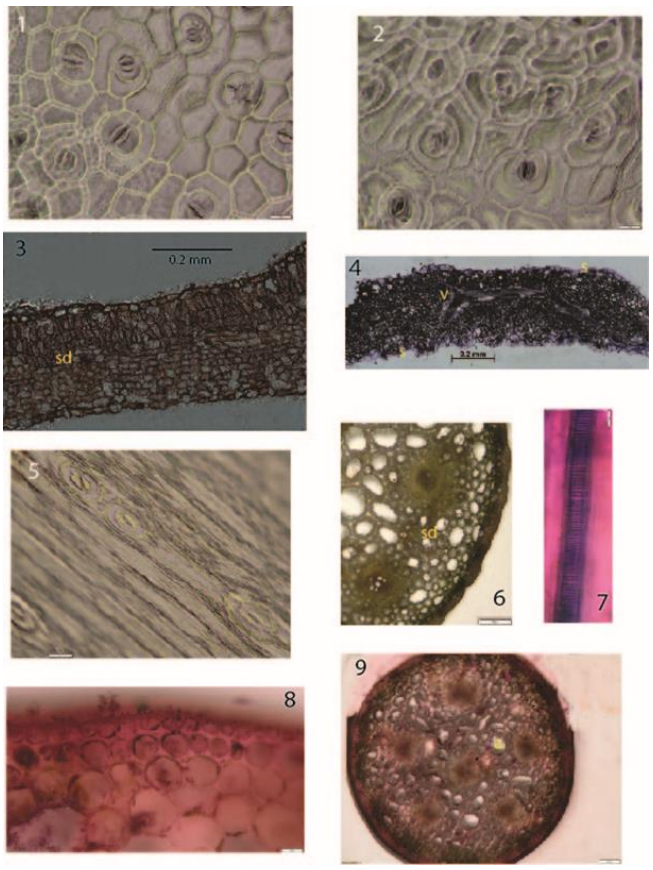


**Plate 1.** Figures 1-2. Nail-polish leaf peels of adaxial (upper) and abaxial (lower) epidermis surface respectively showing anisocytic stomata and normal epidermal cells distribution patterns (phase contrast). 3. Transverse section of *H. bonariensis* leaf lamina showing upper epidermis, multiple layers of abaxial palisade mesophyll, spongy mesophyll layers with vascular tissue, secretory ducts (sd), and lower epidermis (stained with safranin). 4. Transverse section of a leaf stained with toluidine blue; stoma (s), vein (v). 5. Parallel alignment of stomata in a leaf petiole (phase contrast). 6. Magnified view of the middle area of a middle petiole section (unstained). Note the secretory duct (sd) that is bounded by a ring of parenchyma cells. 7. A petiole longitudinal section showing a xylem vessel with helical secondary thickening (stained with neutral red). 8. Proximal petiole section depicting cuticle directly above the laminar collenchyma. 9. Transverse section of the upper part of a petiole at 40x magnification. Note the ring of vascular bundles and irregular to elongate shaped, aerenchyma (a) cells that encircle a central vascular bundle.

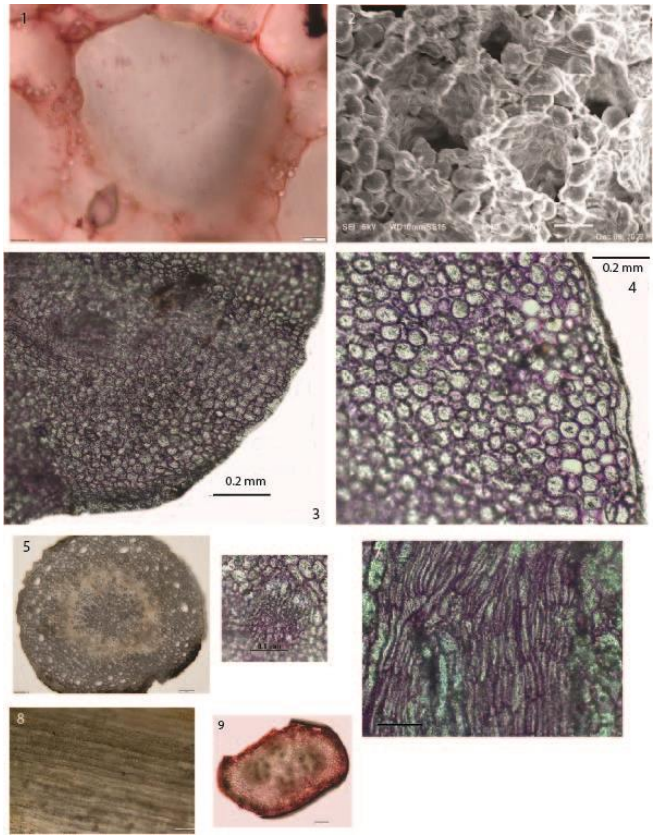


**Plate 2.** Figures 1. A boundary ring of parenchyma cells surrounds a lacuna in the ground tissue of a petiole (stained with neutral red). 2 A transverse scanning electron microscope section depicting part of a proximal end of a petiole. 3. Transverse section of a rhizome depicting the cortex (stained with toluidine blue). 4. Cortical parenchyma cells in a rhizome possessing calcium oxalate crystals (stained with toluidine blue). 5. Transverse cut of a rhizome. 6. An isolated collateral, vascular bundle in a rhizome (stained with toluidine blue). 7. Rhizome section depicting vascular tissue (stained with toluidine blue). 8. Longitudinal cut of a rhizome depicting xylem vessels with helical and annular thickening. 9. Peduncle, distal area, containing four vascular bundles (stained with neutral red).

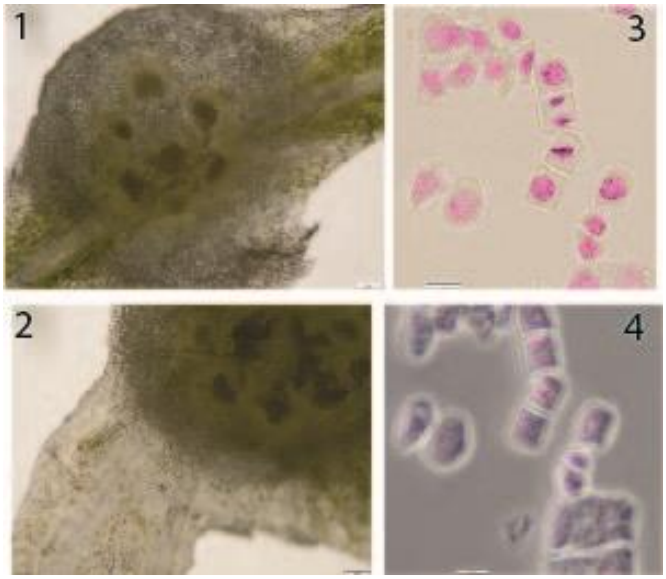


**Plate 3.** Figures 1 - 2. Transverse sections of the uppermost distal part of the petiole. Note the lamina of the leaf blade continues over the petiole and forms wing-like extensions. 3 - 4. Chromosomes found in cells from adventitious root tips. Figure 4 was taken using phase-contrast.

**Table 1. Measurements associated with leaves of *Hydrocotyle bonariensis*.**
All measurements are in micrometers (µm) except where indicated.

| Cell types | Mean | Median | Standard deviation | Range |
|---|---|---|---|---|
| **Blade** | | | | |
| Diameter of blade – length (cm) | 4.70 | 4.8 | 1.0 | 3.0 -7.4 |
| Diameter of blade – width (cm.) | 4.89 | 4.7 | 1.0 | 3.4 – 7.0 |
| Abaxial epidermis normal cells – length | 38.6 | 37 | 11.5 | 20 - 65 |
| Abaxial epidermis normal cells – width | 26.9 | 25 | 8.0 | 20 - 44 |
| Abaxial epidermis guard cells – length | 17.4 | 18 | 3.0 | 11 - 24 |
| Abaxial epidermis guard cells – width | 23.5 | 23 | 5.8 | 13 - 36 |
| Abaxial epidermis subsidiary cells – length | 33.6 | 31 | 10.8 | 12 - 62 |
| Abaxial epidermis subsidiary cells – width | 14.5 | 12 | 6.9 | 5 - 37 |
| Adaxial epidermis normal cells – length | 35.8 | 33 | 12.4 | 19 - 63 |
| Adaxial epidermis normal cells - width | 35.3 | 34 | 9.1 | 21 - 70 |
| Adaxial epidermis guard cells – length | 23.3 | 19 | 3.0 | 10 - 24 |
| Adaxial epidermis guard cells – width | 13.1 | 13 | 2.2 | 10 - 20 |
| Adaxial epidermis subsidiary cells – length | 31.9 | 32 | 12.5 | 16 - 45 |
| Adaxial epidermis subsidiary cells – width | 23.3 | 22 | 10.2 | 11 - 46 |
| **Petiole** | | | | |
| Epidermis distal part– length | 11.5 | 12 | 2.4 | 7- 20 |
| Epidermis distal part width | 13.6 | 14 | 3.1 | 8 - 20 |
| Epidermis medial part - length | 9.6 | 10 | 4.3 | 2 - 17 |
| Epidermis medial part -width | 12.1 | 14 | 5.8 | 2 - 20 |
| Epidermis proximal part -length | 12.2 | 11 | 4.0 | 5 - 25 |
| Epidermis proximal part - width | 13.3 | 13 | 3.6 | 8 - 24 |
| Stomata guard cells - length | 17.4 | 17 | 4.2 | 11-26 |
| Stomata guard cells – width | 11.1 | 11 | 2.2 | 5 -15 |
| Cortex collenchyma distal part - length | 16.3 | 17 | 4.3 | 9 - 24 |
| Cortex collenchyma distal part - width | 18.2 | 19 | 4.9 | 7 - 25 |
| Cortex collenchyma medial part – length | 17.1 | 16 | 5.8 | 8 - 32 |
| Cortex collenchyma medial part – width | 20.3 | 19 | 6.2 | 9 - 35 |
| Cortex collenchyma proximal part – length | 15.7 | 15 | 5.3 | 9 - 30 |
| Cortex collenchyma proximal part - width | 18.2 | 17 | 4.7 | 10 - 28 |
| Cortex parenchyma distal part – length | 41.1 | 40 | 13.5 | 18 - 73 |
| Cortex parenchyma distal part - width | 47.3 | 48 | 14.8 | 16 - 77 |
| Cortex parenchyma medial part - length | 44.6 | 44 | 11.2 | 22 - 66 |
| Cortex parenchyma medial part width | 46.6 | 48 | 12.1 | 22 - 71 |
| Cortex parenchyma proximal part - length | 44.1 | 46 | 47.1. | 25 - 60 |
| Cortex parenchyma proximal part - width | 47.2 | 45 | 11.2 | 22 - 75 |

**Rhizome**

The rhizome has an irregular circular outline and consists of an epidermis, cortex, endodermis, pericycle, vascular region, and a pith. It has a eustele pattern. The epidermis is thin and consists of a single layer of rectangular cells that are 7 – 29 µm (mean 15.9 µm) in length and 13 – 42 µm (mean 21.9 µm) in width (Table 1). The exterior of the epidermis is covered with a cuticle and is devoid of stomata. The cortex consists of 15 – 20 layers of parenchyma cells that range from 29 – 70 µm (mean 45.7 µm) in length and 20 – 81 µm (mean 44.5 µm) in width. Calcium oxalate crystals, starch granules, and tannins were observed in cortical parenchyma cells. Aerenchyma (Plate 2, Fig. 5; Plate 4, Figs. 1,4) and secretory ducts lined with boundary parenchyma/endodermis (Plate 4, Fig. 1) occur throughout the parenchymatous cortex region. An endodermis with a Casparian strip separates the cortex from the stele region. The endodermis is distinctive when safranin dye is applied (Plate 4, Fig. 1). The pericycle, situated directly below the endodermis, is sinuous and irregular in outline; it surrounds the vascular tissue region. Vascular bundles are collateral, separate, and are in a ring-like arrangement. Primary xylem vessels are evident (Plate 2, Fig. 6); longitudinal views depict xylem with annular and helical secondary thickening (Plate 2, Figs. 7-8). Phloem contains sieve tubes and companion cells (Plate 2, Fig. 6). Sclerenchyma fibers cap the phloem. A central pith composed of parenchyma cells occurs in the center of the rhizome (Plate 2, Fig. 5). Like the cortex, these parenchyma cells contain crystals, starch granules, and tannins. Pith parenchyma cells tend to be smaller in size compared to cortical parenchyma cells (Table 2), ranging from 18 – 52 µm (mean 36.8 µm) in length and 22 – 57 µm (mean 40.2 µm) in width. Lateral roots are well defined emerging through the rhizome and possess well-defined vascular tissue, ground tissue, and epidermis (Plate 4, Fig. 4).

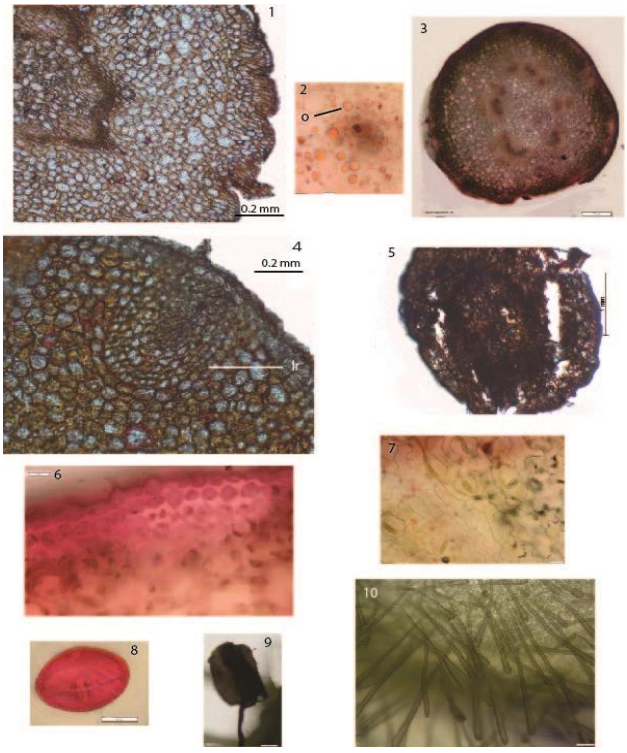


**Plate 4.**
Figures 1. Transverse section of a rhizome depicting epidermis, cortex, endodermis, vascular tissue, and pith (stained with safranin). 2. Yellow-orange oil drops (o) associated with an internode attached to verticil #1. 3. Transverse section of a medial part of an internode 1 attached to verticil #1 (stained with neutral red). Note the bicollateral vascular bundles are unevenly spaced in a ring arrangement. 4. Transverse section of a rhizome depicting an emerging lateral root (lr) penetrating through the cortex (stained with safranin). 5. Transverse section of a root (stained with safranin). 6. Lamellar collenchyma associated with the distal part of a peduncle (stained with neutral red). 7. Paracytic stomata associated with a flower petal. 8. Subprolate, ellipsoidal pollen. 9. Longitudinal view of a stamen. Anthers bear unicellular trichomes. 10. Abundant unicellular trichomes occurring at the base of a petal.

**Table 2. Measurements associated with rhizomes of *Hydrocotyle bonariensis*. All measurements are in micrometers (µm).**

| Cell types | Mean | Median | Standard deviation | Range |
|---|---|---|---|---|
| Epidermis- length | 15.9 | 15 | 5.9 | 7 - 29 |
| Epidermis- width | 21.4 | 20 | 6.9 | 13 - 42 |
| Cortex parenchyma - length | 45.7 | 40 | 12.5 | 29 - 70 |
| Cortex parenchyma - width | 44.5 | 40 | 12.0 | 20 - 81 |
| Pith parenchyma - length | 36.8 | 36 | 10.5 | 18 - 52 |
| Pith parenchyma - width | 40.2 | 40 | 10.0 | 22 - 57 |

## Roots

The roots are thin. Transverse sections became torn and difficult to study when making cuts with hand-held microtomes or with the American Optical Rotary Microtome. Cell measurements were not conducted on root sections. Partial transverse sections, however, depict that the roots are circular in outline (Plate 4, Fig. 5) and have an actinostele that is characteristic of other eudicotyledons. The epidermis consists of a single layer of elongated rectangular cells. Cortex parenchyma cells are round and contain calcium oxalate crystals and starch. The endodermis is distinct and is one cell layer thick. The vascular tissue is exarch and occurs in the center of the root. The xylem has a starch-shaped, tetrarch pattern with metaxylem occurring in the center and protoxylem at the periphery. The phloem is in between the xylem 'prongs of the star.' The xylem exhibits annular and helical secondary thickening in longitudinal sections.

Chromosomes are well defined in cells from adventitious root tips (Plate 3, Figs. 3 - 4). A chromosome count of 2n = 24 was noted in cells undergoing metaphase.

**Table 3. Measurements associated with the inflorescence of *Hydrocotyle bonariensis*.**
All measurements are in micrometers (µm) except where indicated.

| Cell types | Mean | Median | Standard deviation | Range |
|---|---|---|---|---|
| **First internode attached to the base of verticil #1 – proximal region** | | | | |
| Epidermis - length | 13.1 | 13 | 3.1 | 8 -20 |
| Epidermis - width | 15.7 | 16 | 3.3 | 8 - 22 |
| Cortex parenchyma - length | 33.6 | 34 | 6.0 | 20 - 53 |
| Cortex parenchyma- width | 35.9 | 35 | 5.9 | 20 - 51 |
| Pith parenchyma - length | 33.2 | 34 | 5.3 | 15 - 40 |
| Pith parenchyma - width | 32.5 | 33 | 5.5 | 8 - 45 |
| **First internode attached to the base of verticil #1 – medial region** | | | | |
| Epidermis - length | 11.6 | 11 | 1.7 | 8 - 16 |
| Epidermis - width | 13.7 | 13.5 | 3.0 | 10 - 20 |
| Cortex parenchyma - length | 39.1 | 40 | 6.9 | 25 - 55 |
| Cortex parenchyma- width | 39.6 | 37.5 | 7.2 | 29 - 57 |
| Pith parenchyma - length | 39.0 | 40 | 9.4 | 23 - 62 |
| Pith parenchyma - width | 37.7 | 36 | 9.5 | 24 - 74 |

| | | | | |
|---|---|---|---|---|
| **[1]Second internode attached to the base of verticil #2 - proximal region** | | | | |
| Epidermis - length | 12.6 | 12 | 2.0 | 9 - 17 |
| Epidermis – width | 14.2 | 13 | 3.3 | 10 - 25 |
| Cortex parenchyma – length | 35.2 | 35 | 6.4 | 25 - 50 |
| Cortex parenchyma – width | 37.2 | 36 | 6.1 | 27 - 50 |
| Pith parenchyma - length | 38.1 | 35 | 9.5 | 21 - 60 |
| Pith parenchyma - width | 37.1 | 35.5 | 9.6 | 22 - 60 |
| **Peduncle – distal region** | | | | |
| Epidermis - length | 14.9 | 15 | 3.4 | 8 - 22 |
| Epidermis - width | 17.6 | 18 | 4.0 | 11 - 26 |
| Collenchyma - length | 13.6 | 13 | 3.8 | 7 - 22 |
| Collenchyma - width | 16.2 | 16 | 2.9 | 10 - 22 |
| Cortical parenchyma - length | 34.2 | 32 | 8.5 | 20 - 55 |
| Cortical parenchyma - width | 39.5 | 38 | 9.9 | 22 - 59 |
| **Peduncle – medial region** | | | | |
| Epidermis - length | 10.6 | 11 | 3.0 | 3 - 16 |
| Epidermis - width | 13.5 | 13 | 3.1 | 5 - 20 |
| Collenchyma - length | 14.3 | 14 | 5.8 | 2 - 25 |
| Collenchyma - width | 14.9 | 15 | 5.0 | 2 - 23 |
| Cortical parenchyma - length | 41.9 | 40 | 13.9 | 9 - 65 |
| Cortical parenchyma - width | 46.0 | 48 | 15.4 | 15 - 80 |
| **Peduncle – proximal region** | | | | |
| Epidermis - length | 13.2 | 13 | 4.4 | 1 - 23 |
| Epidermis - width | 13.7 | 14 | 3.6 | 4 - 20 |
| Collenchyma - length | 17.9 | 19 | 5.3 | 7 - 28 |
| Collenchyma - width | 18.4 | 18 | 6.2 | 5 - 30 |
| Cortical parenchyma - length | 42.1 | 42 | 12.8 | 19 -72 |
| **Pollen – equatorial view** | | | | |
| Length | 23.0 | 23 | 2.9 | 17 - 29 |
| Width | 22.0 | 22 | 1.6 | 10 - 36 |
| **[2]Height of inflorescence** | | | | 0.7 - 8.2 |

Notes: [1]A total of twelve measurements were conducted for the second internode associated with verticil #2. [2] A total of six inflorescence heights were measured. Two had just a primary umbel, two had one verticil and one terminal umbel, two had two verticils and a terminal umbel, and one had three verticils and a terminal umbel.

## Peduncle

Peduncles are narrower compared to leaf petioles. Transverse sections are circular to elliptical in shape (Plate 2, Fig. 9). The outer boundary contains one row of axially elongated epidermal cells with straight anticlinal walls that are covered with a cuticle (Plate 4, Fig. 6). Small papillae project from the cuticle and are irregularly spaced. Epidermal cells associated with the distal area possess a greater range in length and width in the distal region compared to medial and proximal regions (Table 3). Two to three rows of lamellar collenchyma lie directly beneath the epidermis (Plate 4, Fig. 6) (Plate 2, Fig. 9). Collenchyma cells in the proximal transverse sections possess a greater range in length (7-25 μm, mean 17.86 μm) and width

(3-30 μm, mean 18.43 μm) compared to medial and distal areas. Six to nine rows of cortical parenchyma lie directly below the collenchyma; these cells are loosely packed, irregularly spherical, and contain starch granules. The cortical parenchyma in medial parts of the peduncle had the largest range in length (9 – 65 μm, mean 41.9 μm) and width 15 – 80 μm, mean 45 μm) compared to distal and proximal sections. Aerenchyma is absent in the cortex.

Vascular tissue has an eustele arrangement. Four separate, bicollateral (phloem surrounds the xylem) vascular bundles form a ring below the cortex (Plate 2, Fig. 9). The vascular region comprises about 50% of the peduncle area. A pith area, comprised of parenchyma cells, occurs in the center of the peduncle. Starch granules occur in pith parenchyma cells.

**Floral Structures**

**Internodes attached to verticils**

Internodes between verticils possess cell features that are typical of eudicotyledonous stems. An epidermis, cortex, vascular tissue, and a pith are present. Internode #1 is greater in width compared to other internodes that are associated with verticils that are more distal. The epidermis consists of a single layer. Epidermal cells are oval to rectangular in outline. In proximal sections, the epidermal cells are slightly longer (8 – 20 μm, mean 13.1 μm) and wider (8 – 22 μm, mean 15.7 μm) compared to epidermal cells associated with medial sections (Table 3). A thin cuticle overlies the outer surface of the epidermal cells. Two rows of lamellar collenchyma occur directly below the epidermis and eight to twelve rows or more of cortical parenchyma occur below the collenchyma (Plate 4, Fig. 3). Yellow round oil drops are abundant and starch granules are present in cortical parenchyma cells. Secretory ducts, lined with boundary parenchyma, are scattered throughout the cortical parenchyma (Plate 4, Fig. 3).

The vascular bundles (xylem between two areas of phloem) are bicollateral, unevenly distributed, and vary in size. Their primary xylem and phloem conform to a eustele arrangement; the vascular bundles form a single ring around the pith, which is internal to the vascular bundles. A few vascular bundles are adjacent to each other (Plate 4, Fig. 3). Parenchymatous tissue occurs in areas between vascular bundles.

Pith parenchyma cells are oval to polyhedral and are larger and wider compared to cortical parenchyma cells. Pith parenchyma in pedicel medial sections ranged from 23 – 62 μm (mean 39. 0 μm) in length and 24 – 74 μm (mean 37.7 μm) in width compared to 25 – 55 μm (mean 39.1 μm) in length and 25 – 57 μm (mean 39.6 μm) in width for cortical parenchyma. Pith parenchyma cells have larger dimensions in medial transverse sections compared to proximal transverse sections (Table 3).

**Flowers**

Flowers of *H. bonariensis* are small, complete, radially symmetrical, and five-merous. Flowers contain five green sepals, five white to creamy yellow to green petals, five stamens, two carpels, and an inferior ovary (Mazumdar et al. 2022). Involucre bracts occur below the umbel inflorescence. Anisocytic stomata are associated with sepals and paracytic (rubiaceous) stomata are associated with petals (Plate 4, Fig. 7). Numerous, elongated trichomes with a curved apex occur at the base of petals (Plate 4, Fig. 10). Stamens are free, dorsifixed, and comprised of a filament and an anther. Anthers are dithecal with longitudinal dehiscence and have unicellular trichomes along their exterior (Plate 4, Fig. 9). Pollen is yellow, subprolate, and tricolporate (Plate 4, Fig. 8). In equatorial view, pollen ranges

from 17 – 29 µm (mean 23.0 µm) in length and 10 – 36 µm (mean 22 µm) in width (Table 3). A slight thickening of the exine occurs at the poles.

## DISCUSSION

No species of *Hydrocotyle* contains a detailed anatomical account of vegetative and reproductive features, although partial anatomical descriptions are available for about half of the species (Appendix 1). Previous studies usually focused on one anatomical feature including leaf teeth associated with *H. asterias* Chem & Schtdl. and the epidermal leaf surface of *H. ramiflora* Maxim. (Appendix 1). Forty-eight species only have pollen and/ or fruit described by Tseng (1965). Metcalfe and Chalk (1950) recognized the resemblance between the Apiaceae and Araliaceae. Both families have peripheral collenchyma in young stems, thin-walled aqueous tissue in the stems, secretory canals in medullary vascular bundles, a eustele vascular structure arrangement in the petiole, and vessels with simple perforations.

Most of the anatomical features observed in *H. bonariensis* are apparent in other species of *Hydrocotyle.* For example, leaves are amphistomatic for *H. americana* L. (Holm, 1899; Theobald, 1967), *H. sibthorpioides* Lam. (Yang et al., 2015) and *H. umbellata* L. (Martins et al., 2008; Hamdy et al., 2018; Klapfer, 2018; Umroong et al., 2018) with more and larger stomata occurring in the abaxial epidermis. An endodermis was noted in rhizomes of *H. sibthorpioides* (Yang et al., 2015) and roots of *H. vulgaris* L. (Justin and Armstrong, 1987; Yang et al., 2015). Leaf petioles and lamina associated with *H. ranunculoides* L. f. (Seago 2020) and *H. umbellata* (Hamdy et al., 2018; Seago 2020) also have an endodermis that surrounds vascular bundles in the petiole. Petioles of *H. umbellata* (Hamdy et al., 2018) and *H. sibthorpioides* Lam. (Yang et al., 2015) possess a similar abnormal eustele arrangement of vascular bundles (a ring of vascular bundles below the cortex and one in the central area) like *H. bonariensis*. Aerenchyma occurs in petioles and rhizomes of *H. americana* (Holm, 1899), *H. umbellata* (Hamdy et al., 2018), and *H. vulgaris* (Justin and Armstrong, 1987). The size range of epidermal cells on adaxial and abaxial leaf surfaces of *H. umbellata* (41-75 µm in length, 33-50 µm in width; Hamdy et al., 2018) closely resembles the range for *H. bonariensis*.

Ergastic substances, including starch, volatile oils, tannins (phenolic compounds) and calcium oxalate crystals are reported for assorted species of *Hydrocotyle*. Oil ducts are found in petioles of *H. americana* (Holm, 1899), *H. javanica* Thunb. (Mittal, 1961), *H. umbellata* (Hamdy et al. 2018), the lamina and rhizomes of *H. umbellata* (Hamdy et al., 2018; Klapfer, 2018) as well as in other species within the Araliaceae (Holm, 1899). Tannins occur in rhizomes and leaves of *H. umbellata* (Hamdy et al., 2018), Solereder (1908) and Mital (1961) speculated that oil ducts associated with *Hydrocotyle* contain yellowish crystals, but the chemical compound is unknown, perhaps hesperidin; more research needs to be conducted about their chemical composition. Prisms and rosettes of aggregated calcium oxalate crystals occur in petioles of *H. umbellata* (Klapfer 2018).

Apparent anatomical differences are associated with the organization and arrangement of stomata in leaf lamina. Smith (1935) noted that stomata are regularly oriented where the epidermal cells are elongated over veins, but otherwise irregularly spaced. Ostroumova and Oskolski (2010) reported that paracytic and diacytic occur in *Hydrocotyle*. Other types of stomata arrangements, however, are present in species of *Hydrocotyle*. For example,

anisocytic occur in *H. bonariensis* (this study), *H. sibthorpioides* (Yang et al., 2015) and *H. umbellata* (Hamdy et al., 2018; Klapfer 2018). In contrast, *H. craibii* H. Eichler and *H. sibthorpioides* have anomocytic and hemiparacytic stomata (Ostroumova and Kljuykov, 2007), and *H. javanica* has allocytic (Mittal, 1961) and anomocytic stomata (Ostroumova and Kljuykov, 2007). Paracytic stomata are found in lamina and petioles of *H. umbellata* (Hamdy et al., 2018) and in petals and petioles of *H. bonariensis* (this study).

Several minor anatomical differences occur in species of *Hydrocotyle*. Characteristics include the shape of anticlinal walls (curved, wavy, straight) on leaf surfaces (Ostroumova and Oskolski, 2010), the stomata density associated with abaxial and adaxial leaf epidermal surfaces number, the configuration and number of vascular bundles in the petiole and rhizome, the number of apertures found in pollen grains, and the length and width of pollen in equatorial view. For example, *H. javanica* contains four vascular bundles in the nodal regions of the petiole (Mittal, 1961) compared to six in *H. bonariensis*. Four aperture pollen grains occur in *H. umbellata*, *H. dichondroide*s, and *H. javanica* compared to three apertures in *H. bonariensis*. *Hydrocotyle* species with the longest pollen include *H. bonariensis*, *H. acutifolia* Ruiz & Pav., and *H. batrachium* Hance (Tseng, 1965).

Environmental factors may affect the density, spacing, or removal of cell types associated with *H. bonariensis*. For example, Joesting et al. (2012) noted diurnal and seasonal changes of leaf orientation and the ratio of incident sunlight (photosynthetic photon flux density) that adaxial and abaxial (Ad/Ab) leaf surfaces receive influences the amount of palisade parenchyma. Leaves of *H. bonariensis* that possess an Ad/Ab value of 2.7-3.6 have a single layer of palisade parenchyma and more inclined leaves with an Ad/Ab value of 3.4 – 4.6 contain multiple layers of palisade parenchyma (Joesting et al., 2012). Specimens analyzed in this study were exposed to intense, open sunlight which may account for the presence of three well-developed layers of palisade parenchyma.

Additionally, the amount of aerenchyma in rhizomes and roots may correlate to flooding. Aerenchyma associated with submerged root systems enables gas exchange to take place in hypoxic conditions (Justin and Armstrong, 1987). It commonly forms in radial rows of cortical cells that possess cubic packing during development (Justin and Armstrong, 1987). Roots of *H. vulgaris*, a meadow wetland species (polyhygrob), originate from a highly aerenchymatous rhizome that may extend several centimeters below soil level (Justin and Armstrong, 1987). Species of *Hydrocotyle*, including H. bonariensis, have thin, short roots that do not rise in water (Iversen, 1949; Justin and Armstrong, 1987). The roots have a specific gravity > 1.0 (Holm, 1899; Iversen, 1949; Justin and Armstrong, 1987) and a low fractional root porosity (Justin and Armstrong, 1987).

Peduncles (flowering stems) of *H. bonariensis* exhibit pith autolysis. Carr et al. (1995) stated that individuals of *H. bonariensis* possess hollow stems that grow in sheltered, frontal dune regions in North Carolina. These plants tend to be tall (~36 cm). Carr et al., however, noted that individuals exposed to frontal coastal regions lack pith autolysis and are shorter (~14 cm) in height. Peduncles in this study all possessed a pith (Plate 2, Fig. 9), which may be the result of strong, occasional winds that occasionally occur in the Mississippi Delta.

Chromosome variation in the Araliaceae may be related to ploidy levels (Yi et al., 2004). Somatic chromosome counts,

associated with root tips and flower buds, suggest that *Hydrocotyle*, is an aneuploid (Yi et al., 2004). For example, chromosome counts are 2n = 144 for *H. hydrophila* Petrie (Webb & Benzenberg, 1987), 2n = 60 for *H. heteromeria* A. Rich (Webb & Benzenberg, 1987), and 2n = 18 for *H. rotundifolia* Roxb. (Subramanian, 1986). Yi et al. (2004) added that the predominance of x =12 occurs among species in *Hydrocotyle*. In this study, chromosome number 2n = 24 was observed by Dr. Katembe from adventitious root tips of *H. bonariensis*. Previously, n = 48 was reported for *H. bonariensis* by Constance et al. (1971).

Future research will investigate further the anatomy of pedicles, floral organs, internode regions of rhizomes that connect ramets, and fruit of *H. bonariensis*. Publications are lacking for these plant structures.

## ACKNOWLEDGMENTS

We thank Dr. Mac Alford at the University of Southern Mississippi for allowing us to make microtome sections of leaves, rhizomes, and stems and editorial comments regarding this manuscript. Thanks, are also given to Dr. Carol Hotton for describing the pollen morphology of *H. bonariensis*. Thanks also is given to Ms. Kim Huntzinger at the UDSA-ARS research center in Stoneville, MS, and Ms. Olivia Pharr, an Environmental Science student at Delta State University, for making edits to the manuscript. We also express appreciation to the McNair Research Scholar Program that provided partial financial support for this project. We also express gratitude to the Division of Ecology, Entomology, and Evolution Division of the Mississippi Academy of Sciences and to the Botanical Society of America for giving us the opportunity to present scientific posters on preliminary research about the anatomy of *H. bonariensis*.

## REFERENCES

Atlas of Florida Plants, Institute for Systematic Botany https://florida.plantatlas.usf.edu/plant.aspx?id=5 57

Anderson, L., M. Kocsis, and R. Eriksson. 2006. Relationships of the genus *Azorella* (Apiaceae) and other hydrocotyloids inferred from sequence variation in three plastid markers. *Taxon* 5(2): 270-280.

Carr, S. M., M. Seifert, B. Delbaere, and M. J. Jaffe. 1995. Pith autolysis in herbaceous dicotyledonous plants. A physiological ecological study of pith autolysis under native conditions with special attention to the wild plant *Impatiens capensis* Meerb. *Annals of Botany* 76: 177-189.

Constance, L., T. I. Chuang, and C. R. Bell. 1971. Chromosome numbers in Umbelliferae IV. *American Journal of Botany* 58: 577-587.

Courchet, L. 1884. Etude anatomique sur les Ombelliferes et sur les principales anomalies de structure que presentent leurs organes vegetatifs. *Annales des Sciences Naturelles Botanique* VI (7): 107-129.

Demarco C. F., T. F. Afonso, S. Pieniz, M. S. Quadro, F. A. O. Camargo, and R. Andreazza. 2018. In situ phytoremediation characterization of heavy metals promoted by *Hydrocotyle ranunculoides* at Santa Bárbara stream, an anthropogenic polluted site in southern of Brazil. *Environmental Science and Pollution Research International* 28: 28312-28321.

Drude, C. G. 0. 1897-98. Umbelliferae. *Die Natürlichen Pflanzenfamilien* 3(8): 63-128, 129-250.

Elpel, T. J. 2013. Botany in a day: the patterns method of plant identification: an herbal field guide to plant families of North America. HOPS Press, LLC.

Ernst, E. 2010. *Panax ginseng*: An overview of the clinical evidence. *Journal of Ginseng Research* 34(4): 259-263.

Evans, J. P. 1988. Nitrogen translocation in a clonal dune perennial, *Hydrocotyle bonariensis*. *Oecologia* 77: 64-68.

Evans, J. P. 1991. The effect of resource integration on fitness related traits in a clonal dune perennial, *Hydrocotyle bonariensis*. *Oecologia* 86: 268-275.

Evans, J. P. 1992. Seedling establishment and genet recruitment in a population of a clonal dune perennial, *Hydrocotyle bonariensis*. Barrier Island Ecology of the Mid-Atlantic Coast: *A Symposium Technical Report, Atlanta, GA* 75-84.

Evans, J. P., and S. Whitney. 1992. Clonal integration across a salt gradient by a nonhalophyte,

*Hydrocotyle bonariensis* (Apiaceae). *American Journal of Botany* 79: 1344-2147.

Goh, L. G. 2007. Effect of light intensity on the growth and chlorophyll content of pennywort (*Hydrocotyle bonariensis* Comm. ex. Lam.). Master thesis, University Putra Malaysia.

Hamdy, S. A., H. M. El Hefnawy, S. M. Azzam, and E. A. Aboutabl. 2018. Botanical and genetic characterization of *Hydrocotyle umbellate* L. cultivated in Egypt. *Bulletin of Faculty of Pharmacy, Cairo University* 56: 46-53.

Henwood M. J. 2014. *Hydrocotyle rivularis*: a new trifoliolate species from south-eastern Australia. *Telopea* 17: 217–221.

Holm, T. 1899. Notes on *Hydrocotyle americana* L. *Proceedings of the United States National Museum*.

Iverson, J. 1949. Determinations of the specific gravity of the roots of swamp, meadow, and dry soil. *Oikos* 1(1): 1-5.

Joesting, H. M., M. O. Sprague, and W. K. Smith. 2012. Seasonal and diurnal leaf orientation, bifacial sunlight incidence, and leaf structure in the sand dune herb *Hydrocotyle bonariensis*. *Environmental and Experimental Botany* 75: 195-203.

Joesting, H., J. Counts, J. Grier, and H. Z. Reilly. 2016. Leaf inclination in the coastal sand dune herb *Hydrocotyle bonariensis* Comm. ex Lam. *Flora* 224: 159-166.

Jurica, H. S. 1922. A morphological study of the Umbelliferae. *Botanical Gazette* 74(3): 292-307.

Justin, S. H. F. W. and W. Armstrong. 1987. The anatomical characteristics of roots and plant response to soil flooding. *New Phytologist* 106: 465-495.

Karuppusamy, S., M. A. Ali, K. M. Rajasekaran, J. Lee, S-Y Kim, A. K. Pandey, and F.M.A. Al-Hemaid. 2014. A new species of *Hydrocotyle* L. (Araliaceae) from India. Bangladesh J*ournal of Plant Taxonomy* 21(2): 167-173.

Khilji, S., and Firdaus-e-Bareen. 2008. Rhizofiltration of heavy metals from the tannery sludge by the anchored hydrophyte, *Hydrocotyle umbellata* L. *African Journal of Biotechnology* 7(20): 3711-3717.

Klapfer, V. 2018. Comparative Study on Morpho-anatomy and Histochemistry of Leaf, Fruit, Root, and Petiole of *Centella asiatica* (L.) Urb. and its Adulterant Plant *Hydrocotyle umbellata* L. Diploma thesis, University of Graz, Graz, Austria.

Lanning, F. C., and L. N. Eleuterius. 1983. Silica and ash in tissue of some coastal plants. *Annals of Botany* 51(6): 835-850.

Lemesle, R. 1925. Contribution a l'etude structurale des *Ombelliferes xerophiles*. Annales des Sciences. *Naturelles.Botanique Sér*. 10 (8): 1-138.

Martins, M. B. G., A. P. Marconi, A. J. Cavalheiro, and S. D. Rodrigues. 2008. Caracterização anatômica e química da folha e do sistema radicular de *Hydrocotyle umbellata* (Apiaceae). *Revista Brasileira de Farmacognosia* 18: 402-414.

Masoumian M, A. Arbakariya. A. Syahida and M. Maziah. 2011. Effect of precursors on flavonoid production by *Hydrocotyle bonariensis* callus tissues. *African Journal Biotechnology* 10: 32.

Mathias, M. E. 1936. The genus *Hydrocotyle* in northern South America. *Brittonia* 2: 201 237.

Mathias, M. E., and L. Constance. 1962. A revision of *Asteriscium* and some related Hydrocotyloid Umbelliferae. *The University of California Publications in Botany* 33: 99-134.

Mazumdar, P., N. S. M. Jalaluddin, I. Nair, T. T. Tian, N. A. B. Rejab, and A. Harikrishna. 2022. A review of *Hydrocotyle bonariensis*, a promising functional food and source of health-related phytochemicals. *Journal of Food Science and Technol*ogy. 60: 2503-2516.

Mendoza, J. M., and A. F. Fuentes. 2010. *Hydrocotyle apolobambensis* (Apiaceae) una especie nueva andina del noroeste de Bolivia. *Novon* 20: 303–306.

Mendoza, R. E., I. V. Garcia, L. de Cabo. C. F. Weigandt, and A. F. de Iorio. 2015. The interaction of heavy metals and nutrients present in soil and native plants with arbuscular mycorrhizae on the riverside in the Matanza-Riachuelo River Basin (Argentina). *Science of the Total Environment* 505: 555-564.

Metcalfe, C. R., and L. Chalk, 1950. Anatomy of the Dicotyledons I, Oxford University Press, Amen House, London.

Miao, L. H., Y. Y. Wang, D. D. Qiao, and M. C. Ji. 2018. Ecological adaptability of stolon and leaf anatomical structure of *Hydrocotyle vulgaris* to various water conditions. *Wetland Science and Management* 14: 45-49.

Mittal, S. P. 1961. Studies in the Umbellales. II. The vegetative anatomy. Research contribution No. 23 from the School of Plant Morphology, Meerut

College, Meerut.

Nesom, G. L., and G. A. Levin. In prep. *Hydrocotyle* (Araliaceae). For: Flora of North America Editorial Committee, eds. 1993+. Flora of North America North of Mexico. 24+ vols. New York and Oxford. Vol. 13.

Nery, E. E., M. E. Matchin-Viera, O. Camacho, M. K. Caddah, and P. Flaschi. 2020. Delimiting a constellation: integrative taxonomy of a star shaped *Hydrocotyle* species complex (Araliaceae) from the Brazilian Atlantic Forest. *Plant Systematics and Evolution* 306 (57): 1-17.

Nestel, A. 1905. Beitrage zur Kenntnis der Stengel- und Blattanatomie der Umbelliferen. *Mitteilungen aus dem Botanischen Museum der Universitat Zűrich* 24: 1-126.

Ostroumova, T. A. and E. V. Kljuykov. 2007. Stomatal types in Chinese and Himalayan Umbelliferae. *Feddes Repertorium* 118 (3-4): 84-102.

Ostroumova, T. A. and A. A. Oskoiski. 2010. Survey of the leaf anatomy of Araliaceae and some related taxa. *Plant Diversity and Evolution* 128 (3-4): 423-441.

Perkins, A. J. 2017. Rising from the ashes - *Hydrocotyle phoenix* (Araliaceae), a new annual species from south-western Australia. *Telopea* 20: 41–47.

Perkins, A. J. 2019. Molecular phylogenetics and species delimitation in annual species of *Hydrocotyle* (Araliaceae) from Southwestern Australia. *Molecular Phylogenetics and Evolution.* 134: 129-141.

Pimenov, M. G. and Leonov, M. V. 1993. The Genera of the Umbelliferae: A nomenclature. *Royal Botanic Gardens, Kew*, pp. 5-161.

Plunkett, G. M., and P. P. Lowry II. 2001. Relationships among "Ancient Araliads" and their significance for the systematics of Apiales. *Molecular Phylogenetics and Evolution* 19: 259-276.

Plunkett, G. M., and A. N. Nicolas. 2017. Assessing *Azorella* (Apiaceae) and its allies: Phylogenetics and a new classification. *Brittonia* 69: 31-61.

Reihani S. F.S., and M. E. Azhar (2012) Antioxidant activity and total phenolic content in aqueous extracts of selected traditional Malay salads (Ulam). *International Food Research Journal* 19: 1439–1444.

Rios, A. B. M., and V. C. Dalvi, 2020. Muito além de um dente: ocorrência de hidatódios nos dentes foliares de *Hydrocotyle asterias* Cham. & Schltdl. (Araliaceae Juss.). *Hoehnea 47*: 1-7.

Seago, J. L. 2020. Revisiting the occurrence and evidence of endodermis in angiosperm shoots. *Flora* 273: 1-19.

Simpson, M. G. 2019. Plant Systematics, Third Edition, Academic Press, Elsevier, Amsterdam.

Smith, G. E. 1935. On the orientation of stomata. *Annals of Botany* 49(195): 451-477.

Solereder, H. 1908.Systematic anatomy of the Dicotyledons, English edition, translated by L. A. Boodle and F. E. Fritsch. Oxford, 2 vols.

Subramanian, D. 1986. Cytotaxonomical studies in south Indian Apiaceae. *Cytologia* 51: 479-488.

Theobald, W. L. 1967. Anatomy and systematic position of *Uldinia* (Umbelliferae). *Brittonia* 19(2): 165-173.

Tseung, C. C. 1965. Anatomical and morphological studies of flowers and fruit in Hydrocotyloidea (Umbelliferae). University of California, Los Angeles, Ph.D. dissertation.

Umroong, P. 2018. Leaf anatomy and minimal structure in leaves of *Hydrocotyle umbellate* L., obtained from water stress, were examined under electron microscope and light microscope. *Microscopy and Microanalysis Research* 31(1): 29-33.

Webb, C. J. and E. J. Beuzenberg. 1987. Contributions to a chromosome atlas of the New Zealand flora - corrections and additions to number 21 Umbelliferae (*Hydrocotyle*). *New Zealand Journal of Botany* 25: 371-372.

Yang, C-D., S-F. Li, L. Yao, X-R. Ai, X-D. Cai, and X. Zhang. (2015). A study of anatomical structure and apoplastic barrier characteristics of *Hydrocotyle sibthorpioides*. *Acta Prataculturae Sinica* 24(7): 139-145.

Yi, T., P. P. Lowry II, G. M. Plunkett, and J. Wen. 2004. Chromosomal evolution in Araliaceae and close relatives. *Taxon* 53(4): 987-1005.

Yoon J, X. Cao, Q. Zhou, L. Q. Ma. 2006. Accumulation of Pb, Cu, and Zn in native plants growing on a contaminated Florida site. *Science of The Total Environment* 368: 456–64.

**Appendix 1. Former published anatomical studies on species of *Hydrocotyle*.**

| | Publications | Regions studied |
|---|---|---|
| *H. acutifolia* Ruiz & Pav. | Tseng, 1965 | Fruit, pollen |
| *H. acutiloba* (F. Muell.) N. A. Wakef. | Tseng, 1965 | Fruit, pollen |
| *H. americana* L. | Holm, 1899; Tseng, 1965 | Roots, stolon, tuber, fruit |
| *H. arbuscula* Schltr. | Lemesle, 1925 | Stem |
| *H. asterias* Cham. & Schltdl. | Rios, A. B. M., and V. C. Dalvi, 2020 | Leaf teeth (hydathodes) |
| *H. batrachium* Hance | Tseng, 1965 | Pollen |
| *H. barbarossa* Cham. & Schitdl. | Tseng, 1965 | Fruit |
| *H. benguetensis* Elm. | Tseng, 1965 | Pollen |
| *H. bonariensis* Comm. ex Lam. | Tseng, 1965; Carr et al., 1995; Joesting et al. 2012 | Blade, pith in stems, pollen |
| *H. bonplandi* A. Rich. | Tseng, 1965 | Fruit, pollen |
| *H. bowlesioides* Mathias & Constance | Tseng, 1965 | Fruit |
| *H. callicarpa* Bunge | Tseng, 1965 | Fruit |
| *H. callicephala* Cham. | Tseng, 1965 | Fruit |
| *H. capillaris* F. Muell. | Tseng, 1965 | Fruit |
| *H. chamaemorus* Cham. & Schltd. | Tseng, 1965 | Fruit |
| *H. craibii* H. Eichler | Ostroumova & Kljuykov, 2007 | Epidermal leaf surface |
| *H. dichondroides* Makino | Tseng, 1965 | Fruit, pollen |
| *H. elongata* A. Cunn. ex Hook. f. | Tseng, 1965 | Fruit |
| *H. exigua* (Urb.) Malme | Tseng, 1965 | Fruit |
| *H. filpes Mathias* | Tseng, 1965 | Fruit |
| *H. formosana* Masam. | Tseng, 1965 | Fruit, pollen |
| *H. globiflora* Ruiz & Pav. | Tseng, 1965 | Fruit |
| *H. grossulariifolia* Rusby | Tseng, 1965 | Fruit |
| *H. gunnerifolia* Wedd. | Tseng, 1965 | Fruit |
| *H. hederacea Mathias* | Tseng, 1965 | Fruit, pollen |
| *H. hitchcockii* Rose ex Mathias | Tseng, 1965 | Fruit |
| *H. hirsuta* Sw. | Tseng, 1965 | Fruit |
| *H. hirta* A. Rich. ex R. Br. | Tseng, 1965 | Fruit |
| *H. humboldtii* A. Rich | Tseng, 1965 | Fruit |
| *H. humboldtii* var. *pubescens* Mathias | Tseng, 1965 | Pollen |
| *H. incrassata* Ruiz & Pav | Tseng, 1965 | Pollen |
| *H. javanica* Thunb. | Mittal, 1961; Tseng, 1965; Ostroumova & Kljuykov, 2007 | Nodal anatomy of petiole; epidermal leaf surface, fruit, |

| | | |
|---|---|---|
| | | pollen |
| *H. keelungensis* Tang S. Liu, C. Y. Chao & T. I. Chuang. | Tseng, 1965 | Fruit, pollen |
| *H.* l*angsdorffii* DC | Tseng, 1965 | Fruit |
| *H. laxiflora* DC | Tseng, 1965 | Fruit |
| *H. lehmannii* Mathias | Tseng, 1965 | Fruit, pollen |
| *H. leucocephala* Cham. & Schltdl. | Tseng, 1965 | Fruit, pollen |
| *H. marchantioides* Clos | Tseng, 1965 | Fruit |
| *H. mexicana* Schltdl. & Cham. | Tseng, 1965 | Fruit, pollen |
| *H. modesta* Cham. & Schltdl | Tseng, 1965 | Fruit |
| *H. moschata* G. Forst. | Tseng, 1965 | Fruit |
| *H. multifida* A. Rich. | Tseng, 1965 | Fruit |
| *H. nixoides* Mathias & Constance | Tseng, 1965 | Fruit, pollen |
| *H. novae-zeelandiae* DC | Tseng, 1965 | Fruit |
| *H. pedicellosa* F. Muell. ex Benth. | Tseng, 1965 | Fruit, pollen |
| *H. peruviana* H. Wolff. | Tseng, 1965 | Fruit, pollen |
| *H. poeppigii DC.* | Tseng, 1965 | Fruit |
| *H. pusilla* A. Rich. | Tseng, 1965 | Fruit |
| *H. quinqueloba* Ruiz & Pav. var. *stella* (Pobl.) Urban | Tseng, 1965 | Fruit |
| *H. quinqueloba* Ruiz & Pav. var. *asterias* (Cham.) Urban | Tseng, 1965 | Fruit |
| *H. ramiflora* Maxim. | Tseng, 1965; Ostroumova and Oskolski, 2010 | Epidermal leaf surface, pollen |
| *H. ranunculifolia* Ohwi | Tseng, 1965 | Fruit, pollen |
| *H. ranunculoides* L. f. | Seago, 2020 | Blade, petiole, stem |
| *H. ribifolia* Rose & Standl. | Tseng, 1965 | Pollen |
| *H. setulosa* Hayata | Tseng, 1965 | Fruit, pollen |
| *H.* s*ibthorpioides* Lam. | Tseng, 1965; Ostroumova & Kljuykov, 2007; Yang et al., 2015 | Adventitious root, blade, petiole, pedicel, pollen, stolon |
| *H. tambalomaensis* H. Wolff | Tseng, 1965 | Fruit, pollen |
| *H. torresiana* Rose & Standl. | Tseng, 1965 | Fruit |
| *H. tripartita* R. Br. | Tseng, 1965 | Fruit |
| *H. umbellata* L. | Tseng, 1965; Martins et al., 2008; Hamdy et al., 2018; Klapfer, 2018, Umroong, 2018; Seago, 2020 | Fruit, leaf, petiole, rhizome, root, pollen |
| *H. verticillata* Thunb. | Lemesle, 1925; Tseng, 1965 | Stem, pollen |
| *H. vulgaris* L. | Courchet, 1884; Drude, 1897; Nestel, 1905; Tseng,1965; Justin and Armstrong, 1987; Miao et al., 2018 | Leaf, stolon, root, fruit |

# A Plant Anatomical Investigation of Viola sororia Willd

YaeEun Yun, Nina Baghai-Riding and William Katembe

Delta State University, Cleveland, MS

**Corresponding Author:** Nina Baghai-Riding
**Email:** nbaghai@deltastate.edu
**Doi:**10.34107/CTJP1687

## ABSTRACT

*Viola sororia* Willd. (blue violet/common meadow violet) is native to eastern and central North America. This herbaceous species thrives in the Mississippi Delta and blooms throughout the early spring. It occurs in woodlands, shady banks, sandy substrates, and forest edges. It has dull green, unlobed, ovate to orbicular leaves with a cordate base and crenate or serrate margins, a thick rhizome, and chasmogamous and cleistogamous flowers. In this study, roots, stems, leaf blades, petioles, peduncles, and floral features are investigated. Clear nail-polish peels were made to analyze surface sections of leaves and petioles. Transverse and longitudinal anatomical sections were made manually using commercial single-edged razor blades or with hand-held microtomes. Measurements of cell features were made using a micrometer. Thirty-five measurements were made on starch grains, parenchyma cells, collenchyma cells, and vessel elements in rhizomes; collenchyma, parenchyma, and guard cells in petioles; and guard cells and regular epidermal cells in leaves. Interesting anatomical characters include the presence of anisocytic stomata on leaf blades, the distal end of petioles possessing two lateral wings, the presence of calcium-oxalate crystals occurring in the pith of rhizomes, oil droplets in peduncles and petioles, the center of the peduncle containing two crescent-shaped vascular bundles associated with chasmogamous flowers compared to four vascular bundles in the medium of the peduncle associated with cleistogamous flowers, collateral vascular bundles in petioles and peduncles, and more. The combination of plant anatomical characters is unlike other described species associated with this genus. Significant range variation was noted for petiole stomata which ranged 10-50 µm (mean 24.5 µm) in length and 5-30 µm (mean 13.5 µm) in width and cortex rhizome parenchyma cells which ranged 10-60 µm (mean 31.1 µm) in length and 10-50 µm (mean 21.9 µm) in width. Range for other cell types investigated was less variable.

**KEYWORDS:** *Viola sororia*, Violaceae, plant anatomy, Mississippi Delta

## INTRODUCTION

The Violaceae are a relatively large family of angiosperms (Simpson, 2019) consisting of 34 genera and more than 985 species. Three genera, *Viola*, *Rinorea* and *Hybanthus,* include 98% of the species and are widely distributed in both hemispheres (Wahlert et al. 2014). The family consists of perennial, rarely annual, herbs, trees, and vines (Dinç and Yıldırımlı 2007, Dinç 2009) and bloom in early to late spring in the Northern Hemisphere (Dinç 2009). Many species occur in temperate regions (Bağci et al. 2008; Dinç 2009). The family, however, is cosmopolitan. Species are reported from diverse habitats: boreal areas (Havran et al. 2009), dry and mesic forests (Havran et al. 2009; Bölöni 2017), tropical rainforest (Hekking 1988), coastlines (Thiele and Prober 2006), bogs (Tilley et al. 2022), crevices and fissures of cliffs (Youssef and Véla 2019), floodplains (Eckstein et al. 2006), ruderal habitats (e.g., lawns), and more.

*Viola* L., which includes violets and pansies, is the largest genus in the Violaceae, consisting of 525 – 600 species (Ballard et al.1999; 2023; Dinç and Yıldırımlı 2007, Dinç 2009; Chen and Yang 2009) and is one of the largest angiosperm genera (Marcussen

et al. 2022). Species of *Viola* may freely hybridize making species differentiation difficult (Gil and Kim 2016; Małobęcki 2016). Species of *Viola* occur commonly in damp woods and meadows in temperate climates although some species have other ecological specializations (Metcalfe and Chalk 1950). Some species are endemic to specific regions, have narrow distributions (Bağci et al. 2008), and are endangered. The genus has economic pharmacological properties (Chandra et al. 2015) and has been used as an anticancer agent as well as in traditional medicine to cure coughs, colds, flu, and malaria. Additionally, *V. macedonica* Boiss. and Heldr., *V. allcharensis* G. Beck, and *Viola arsenica* G. Beck are known to accumulate heavy metals such as arsenic, stibnite, and titanium from contaminated soils (Bačeva et al. 2014). *Viola odorata* is a widely cultivated as an ornamental plant; young leaves and flower buds are edible (Lust 1986). The genus had its origins in the southern hemisphere (Ballard et al. 1998; Marcussen et al. 2011; Shahrestani et al. 2014). Centers of morphological and taxonomic diversity occurred in the northern hemisphere following dispersal in the early Miocene 18 million years ago based on fossil seed morphotypes from Eurasia (Nikitin, 2007; Marcussen et al. 2011; Shahrestani et al. 2014).

Flowers of *Viola* are typically bilateral, consist of five petals with distinct purple veins, and have a superior, three-carpellate ovary with parietal placentation. Inflorescences are mainly axillary and emerge from rhizomes in acaulescent species (Flora of North America, 2015). Most species possess both chasmogamous and cleistogamous flowers (Ballard et al. 2023). Chasmogamous flowers have well-developed petals and are pollinated by insects but are commonly sterile; cleistogamous flowers lack petals and are self-pollinated (Ballard et al. 2023). Seeds range from 6-75 per capsule, are spherical or ovoid, glabrous, and are often arillate with an elaiosome. Leaves are normally simple, and may be petiolate, deltate, ovate, orbiculate, reinform, linear spatulate, or lanceolate (Flora of North America 2015). Many species have an acute apex. Rhizomes may be in the form of a caudex and are shallow or deep-seated (Flora of North America 2015).

Twenty-one native species of Viola are referenced in SouthEast Regional Network of Expertise and Collections (SERNEC) website from Mississippi: V. affinis Leconte, V. a*mpliata* Greene, V. bicolor Pursh, V. *canadensis* L., V. *cucullata* Aiton, V. *hirsutula* Brainerd, V. *lanceolata* L., V. *missouriensis* Greene, V. *pallens* (Banks ex Ging.) Brainerd, V. *palmata* L., V. *papilionacea* Pursh, V. *pedata* L., V. *primulifolia* L., V. *rafinesquei* Greene, V. *rosacea* Brainerd, V. *sagittata* Aiton, V. *sororia* Willd., V. tricolor L., V. t*riloba* Schwein., V. tripartita Elliott, and V. *walteri* House. Two species, V. bicolor and V. sororia occur natively in Bolivar Co., Mississippi. *Viola bicolor* is a caulescent, annual plant and has simple, alternate, glabrous leaves with entire margins. The lower three petals are lemon-yellow on both surfaces and the upper two are brown with purple veins. In contrast, *V. sororia*, known as the common blue violet or woolly blue violet, is an acaulescent, perennial violet with simple, alternate, often glabrous leaves with toothed margins that grow 5 to 50 cm in height (Flora of North America 2015). It is the state flower of Illinois, New Jersey, and Rhode Island (Marcussen et al 2022).

*Viola sororia* is included in the endemic North America lineage sect. *Nosphinium* subsect. *Borealiamericanae* (Marcussen et al. 2022). The center of origin for this lineage is the Appalachian Mountain range and adjacent uplands (Marcussen et al. 2022). It

has a rosulate habit and a perennial, cream color, vertical, fleshy (approximately 10 mm thick) rhizome. Each rhizome possesses 3 – 15 erect petioles; impressions of withered petioles occur on their outer surfaces. Shallow taproots and thin stolons develop from the rhizomes (Flora of North America 2015). Leaf blades are dull green; unlobed; ovate, deltate, reniform, or orbiculate in shape; with crenate or serrate margins; and a shallow to deeply cordate base (Flora of North America 2015; Marcussen et al. 2022). The leaves are erect or suberect. Individual plants measured 4 - 16 cm in height. Venation is palmate with camptodromous veins. The angle of divergence between the secondary veins is acute. Petioles are green but may have a purple tinge at the base, lack pubescence, and range from 3.0 – 16 cm in length. Leaf blades range from 3.5 – 11 cm in length to 3.5 – 14 cm in width. Peduncles are unjointed and glabrous. Chasmogamous flower petals are light to dark blue or dark purple violet to reddish purple with often conspicuous white throats. The style is trilobate, and the ovary is superior. Cleistogamous flowers occur on ascending short peduncles. Fruits are a three-chambered ovoid to ellipsoid capsule containing 6 – 75 spherical to ovoid seeds (Flora of North America 2015). In Bolivar County, Mississippi, this species blooms in mid-March – late April and occurs in woods, lawns, disturbed areas, and stream banks.

Weakley and the Southeastern Flora Team (2022) have identified three different varieties of *V. sororia*. The foliage of *V. sororia* var. *sororia* (at least the petiole and the undersurface of the blade) is hirsute and the calyx is ciliate; *Viola sororia* var. 1 ["*glabrous*" variant] and *Viola sororia* var. 2 ["*hirsutula*-like" variant] have essentially glabrous foliage and eciliate calyxes. Variant 1 has foliage that is medium green. The leaf blade apex is obtuse to abruptly acute and leaf margins are incurved-serrate. In comparison, variant 2 has crenate leaf margins. The midrib is purple on the upper surface of the leaf blade and the lower surface of the leaf blades, petioles, and peduncles are flushed with purple. The form discussed in this report does not conform to these variants since it has essentially glabrous leaves, ciliated sepals, and a purple tinge at the base of the petioles.

## Previous Work

Approximately 6% of the species in *Viola* have published anatomical studies (Appendix 1). These studies contain information about vegetative structures (blade, petiole, peduncle, rhizome, and lateral roots), reproductive structures (sepals, petals, ovary, pollen, and seeds), or both. Recent studies focus on species from Argentina (Pilberg 2016), China (Chen and Yang, 2008), Europe (Colombo et al. 2007; Toiu et al. 2010, Kuta et al. 2012, Mehrvarz et al. 2013, Mereacre et al. 2014), Iran (Yousefi et al. 2012; Mehrvarz et al. 2013; Shahrestan et al. 2014), North America (Rubin and Paolillo 1978; Hayden and Clough 1990; Marcussen et al. 2011), Pakistan (Dastagir et al. 2023), and Turkey (Akarsu 1989, Dinç and Yildirimli 2007, Dinç et al. 2007; Bağci et al. 2008; Dinç 2009). Measurements of assorted cell types are provided in only a few publications (e.g., Colombo et al. 2007, Dinç and Yıldırımlı 2007; Bağci et al. 2008, Dinç 2009, Toiu et al. 2010; Mereacre et al. 2014; Shahrestani et al. 2014; Dastagir et al. 2023). There are no published reports regarding anatomical features of *Viola* species from the Southeastern United States. This paper provides a description of anatomical features of the rhizome, leaves, peduncles, roots, flowers, fruits, and seeds of individual specimens of *V. sororia*.

## MATERIALS and METHODS

Fresh living specimens from lawns and yards in Cleveland, Mississippi, were

collected from March 2021 – July 2022. Herbarium specimens were collected, dried, mounted, and stored in the Delta State University Herbarium with other specimens of the same species Voucher DSC115143 is illustrated as Figure 1. Two other voucher specimens (DSC116031, DSC116032) were collected at the same time in June 2021.

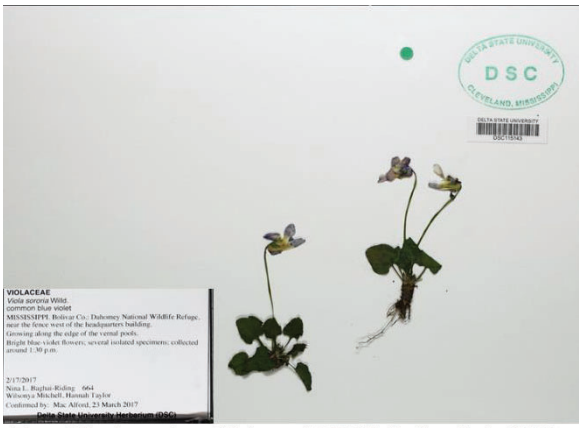

Figure 1. Voucher specimen of *Viola sororia* DSC115143 collected in April 2014.

Transverse and longitudinal anatomical sections were made manually using commercial single-edged razor blades or with hand-held microtomes. Anatomical features studied include mature roots, rhizomes, leaf lamina, petioles, peduncles, flower petals, and young ovules inside capsules. The upper, middle, and lower parts of petioles and peduncles were examined to determine variation in ground and vascular tissue. Paradermal cuts of leaves were prepared to observe details of leaf mesophyll, veins, and stomata. Methylene blue or neutral red was applied to stain transverse and longitudinal sections of rhizomes. Clear nail polish peels were made of adaxial and abaxial epidermal surface of leaves to determine size of guard cells, subsidiary cells, trichomes, and more. Digital photographs were taken under 40×, 100× and 400× magnifications with an Olympus Q-Color 3 camera attached to an Olympus BX43 compound light microscope (Plates 1-3). A phase-contrast condenser aided in observing unstained transparent features such as guard cells on leaf epidermal peels. An Olympus CX31 Polarizing microscope facilitated examining calcium oxalate crystals in the rhizome pith and cortex.

About ten mature roots and leaves were fixed in FAA and then transferred to 70 – 100% alcohol solutions for three days because longitudinal cuts of the leaves and roots are difficult to acquire from fresh specimens. The fixed specimens were transferred to a 1:1 ratio of xylene and embedding paraffin wax and were put overnight in a THELCO: Model 19 oven at 60° C. Afterwards, specimens were cooled and placed in ice water for 10 minutes to harden the wax prior to being sectioned with a microtome.

General morphological observations were made on live and fixed specimens. Measurements include the length and width of cell types in adventitious roots, leaf blades, petioles, peduncles, rhizomes, ovules, pollen, immature seeds, and more (Tables 1-3). Thirty-five measurements for each specified anatomical feature were captured for statistical purposes. To reduce bias, two to six microscope slides, from different individual plant specimens, were scanned. Data were recorded in an Excel spreadsheet for conducting statistical values: mean, standard deviation, median, and range.

Chromosome counts were conducted on fresh adventitious root tip meristems generated by rhizomes. Root tips were fixed in alcohol/acetic acid 3:1 v/v, hydrolyzed in 1N HCL at 60 ºC for 10 min, incubated in Schiff's Reagent for 40 min., then rinsed three times in a beaching solution (5 mL 1N HCL, 5 mL 10% potassium metabisulfite ($K_2S_2O_5$), and 90 mL $dH_2O$) to remove background dye. Stained root tips were cut and placed on a clean microscope slide with one drop of 45% acetic acid and broken into tiny fragments before placement of a cover

slip (tapping with the rubber end of a standard pencil aided in breaking apart the root cells). Slides were placed on folded paper towels and a gentle thumping pressure applied to help break apart the cells and spread chromosomes. Chromosomes were seen using Olympus BX32 compound light microscopes.

## RESULTS

### Leaves

### Lamina/blade

Leaves are dorsiventral, bifacial, and amphistomatic. Nail-polish epidermal leaf peels depict that the blades have a thin, sometimes striated cuticular layer on both the adaxial and abaxial lamina surfaces (Plate 1, Fig. 3). The epidermal surfaces consist of a single layer of rectangular, squarish, to ovoid cells (Plate 1, Figs. 8-9). The length and width of epidermal cells on the upper surface (Table 1) is greater (length 20 – 50 µm, mean 34.9 µm; width 20 – 70 µm, mean 32.3 µm) compared to epidermal cells on the lower epidermal surface (length 15 – 50 µm, mean 29.1 µm; width 10 – 60 µm, mean width 28.3 µm). Abundant chloroplasts occur in upper epidermal cells (Plate 1, Fig. 8). Stomata are anisocytic (cruciferous) and are in the same plane as the epidermal cells (Plate 1, Figs. 3, 9). The length of the stomata on both surfaces possesses the same size range (10 – 30 µm), but the stomata on the abaxial epidermis surface appear to be more abundant and are wider (mean 14.5 µm) compared to stomata on the adaxial surface (mean 10.8 µm). Chloroplasts occur in the guard cells on the upper epidermis (Plate 1, Fig. 9). Unicellular, simple trichomes are widely scattered on both epidermal surfaces (Plate 1, Fig. 6). Paradermal sections reveal vascular bundles with helical secondary xylem thickening (Plate 1, Fig. 5).

### Petiole

Petiole colors vary from green at the distal end to a reddish purple near the base, where it attaches to the rhizome. Transverse anatomical sections of petioles are semi-circular to cordate. The distal end has two lateral, adaxial wings (Plate 1, Fig. 1), rudiments of the leaf blade (Yousefi et al. 2012). Lateral wings are asymmetrical (vary in length) ranging from 250 – 1500 µm in length and 100 – 300 µm in width. Lateral wings are reduced in mid sections and absent in basal sections (Plate 1, Fig. 2). In transverse sections, the petiole epidermis is composed of elongate to ovoidal cells that are cutinized. The cuticle surface varies from 0 –5 µm in thickness. The epidermal cells decrease in length from the distal end of the petiole (range 5 – 100 µm, mean 29 µm) to the basal end (5- 45 µm, mean 21 µm). Simple, widely scattered, one-celled hairs occur on epidermal cells (Plate 1, Fig. 4). Epidermal nail-polish peels portrayed that chloroplasts and stomata occur on the upper parts of the petiole surface. Stomata range from 10-50 µm (mean 24.5 µm) in length to 5-30 µm (mean 13.5 µm) in width and tend to be longer than those observed on the leaf blades.

Two to three layers of lamellar collenchyma occur beneath the epidermis (Plate 1, Fig. 4); in the ‘wings’ the collenchyma consists of 3 – 5 layers of cells. Collenchyma cells are spherical to elongate and range from 10 – 30 µm (mean 16.9 µm) in length to 10-25 µm (mean 15.6 µm) in width (Table 2). Parenchymatous cortex is present under collenchyma, and its cells are loosely packed, irregularly spherical, and range from 10 – 50 µm (mean 28.3 µm) in length to 10 – 40 µm (mean 29.3 µm) in width (Table 2). Occasionally large cortical parenchyma cells are near the center of the cortex whereas the smaller cells are either adjacent to the collenchyma or border the

vascular tissue. Starch grains and calcium oxalate crystals occur in parenchyma cells. A few oil bodies occur in groups among some parenchyma cells (Plate 1, Fig. 4). In the basal portion of the petiole, some parenchyma cells adjacent to the collenchyma possess a red pigment (Plate 1, Fig. 2).

A prominent, single, crescent-shaped vascular bundle is in the upper central region of the petiole (Plate 1, Fig. 1); a smaller vascular bundle occurs in each lateral wing. Only one crescent-shaped closed vascular cylinder, open on the abaxial side, occurs in the center of the petiole in basal sections (Plate 1, Fig. 2). The placement of the xylem is adaxial, and the phloem is abaxial. All three vascular bundles are collateral and are surrounded by a parenchymatous bundle sheath. Some mid-transverse sections of the middle petiole contain a hollow pith and lack a large central vascular bundle (Plate 1, Fig. 7).

**Table 1. Measurements associated with leaves of *Viola sororia*. All measurements are in micrometers.**

| Cell types | Mean | Median | Standard deviation | Range |
|---|---|---|---|---|
| **Blade** | | | | |
| lower epidermis normal cells - length | 29.1 | 30 | 10.0 | 15 - 50 |
| lower epidermis normal cells - width | 28.3 | 30 | 9.8 | 10 - 60 |
| lower epidermis stomata - length | 22.0 | 20 | 4.9 | 10 - 30 |
| lower epidermis stomata - width | 14.5 | 15 | 4.2 | 7 - 20 |
| upper epidermis normal cells - length | 34.9 | 30 | 7.0 | 20 - 50 |
| upper epidermis normal cells - width | 32.3 | 30 | 13.0 | 20 - 70 |
| upper epidermis stomata - length | 18.5 | 20 | 5.4 | 10 - 30 |
| upper epidermis stomata - width | 10.8 | 10 | 3.2 | 5 - 20 |
| **Petiole** | | | | |
| stomata – length | 24.5 | 27.5 | 9.4 | 10 - 50 |
| stomata – width | 13.5 | 10.0 | 6.1 | 5 - 30 |
| epidermis distal part - length | 29.0 | 25.0 | 21.8 | 5 - 100 |
| epidermis distal part – width | 26.1 | 25.0 | 14.0 | 5 - 50 |
| epidermis middle part – length | 22.6 | 25.0 | 9.5 | 5 - 50 |
| epidermis middle part – width | 19.9 | 20.0 | 8.8 | 5 - 50 |
| epidermis basal part – length | 21.0 | 20.0 | 8.4 | 5 - 45 |
| epidermis basal part – width | 15.4 | 15.0 | 7.6 | 5 - 35 |
| cortex collenchyma - length | 16.9 | 15.0 | 5.5 | 10 - 30 |
| cortex collenchyma - width | 15.6 | 15.0 | 5.3 | 10 - 25 |
| cortex parenchyma - length | 28.3 | 30.0 | 10.0 | 10 - 50 |
| cortex parenchyma - width | 29.3 | 20.0 | 8.0 | 10 - 40 |
| pith parenchyma - length | 23.7 | 20.0 | 9.4 | 10 - 40 |
| pith parenchyma - width | 24.7 | 20.0 | 9.8 | 10 - 50 |
| phloem - length | 8.5 | 10.0 | 2.4 | 5 - 10 |
| phloem - width | 6.5 | 5.0 | 2.4 | 5- 10 |

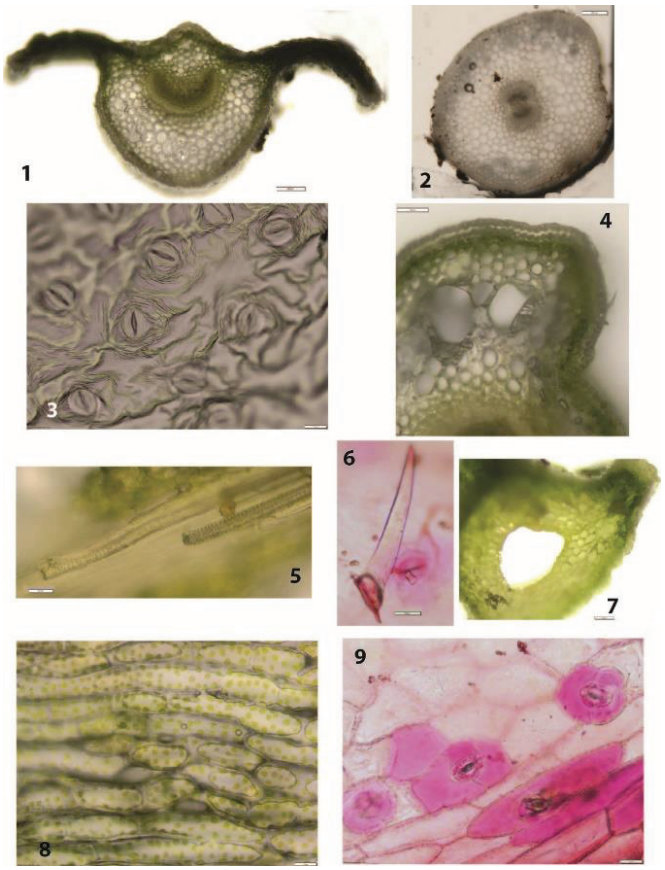


Plate 1. Figures. 1. Transverse section of the upper part of a leaf petiole depicting lateral 'wings', 2. basal petiole transverse section, 3. abaxial leaf epidermis surface; 4. petiole transverse cut depicting lamellar collenchyma and cortical parenchyma, 5. helical secondary xylem thickening in leaf lamina, 6. a unicellular trichome on a leaf lamina, 7. Mid transverse section of a petiole with a hollow pith, 8. adaxial leaf epidermal surface depicting chloroplasts in epidermal cells, 9. adaxial leaf epidermal section depicting guard cells with chloroplasts.

**Rhizome**

In transverse sections, the rhizome has a thin layer of rectangular epidermal cells (Plate 2, Figs. 1-2). Two or three layers of lamellar cortex collenchyma occur below the epidermal cells (Plate 2, Fig. 2). Numerous layers of cortical parenchyma cells form a relatively thick layer beneath the collenchyma. Starch grains in cortical parenchyma cells range from 1 – 15 µm (mean 6.2 µm) in length and 1-10 µm (mean 5.5 µm) in width (Table 2). An endodermis separates the well-developed cortex from the vascular tissue and stained red when neutral red dye was applied (Plate 2, Figs. 3-4). A pericycle layer occurs directly underneath the endodermis. Lateral roots formed in the pericycle emerge out through the epidermis (Plate 2, Fig. 4). Secondary phloem and xylem occur within the pericycle. The secondary phloem forms a closed ring and contains sieve tubes, companion cells, and rays of parenchyma cells. The secondary xylem contains vessels, libriform fibers, and parenchyma (Plate 2, Fig. 3). The vessel elements form irregular clusters and are narrow, ranging from 5-10 µm (mean 7.9 µm) in diameter (Table 2). Longitudinal sections depict vessels with helical, annular, and scalariform secondary thickening and simple perforation plates (Plate 2, Fig. 5). The pith is solid and contains thin walled, amyliferous parenchyma cells with abundant clusters of calcium oxalate crystals.

**Root**

Transverse sections of the root have a circular shape (Plate 2, Fig. 8). The epidermis represents the outer layer and is one cell layer in thickness. Underneath the epidermis is a parenchymatous cortex that contains large air spaces. A prominent endodermis occurs below the cortex. A vascular cylinder

occupies the center of the root; the xylem area is in the center and contains vessels; a thin ring of phloem cells surrounds the xylem core. Calcium oxalate crystals were not observed in the roots. Lateral sections depicted vessel elements with annular and helical thickening. Chromosome counts of *2n* = 12 were obtained from lateral root cells (Plate 3, Fig. 7) that developed from the rhizome pericycle and root apical meristems

.

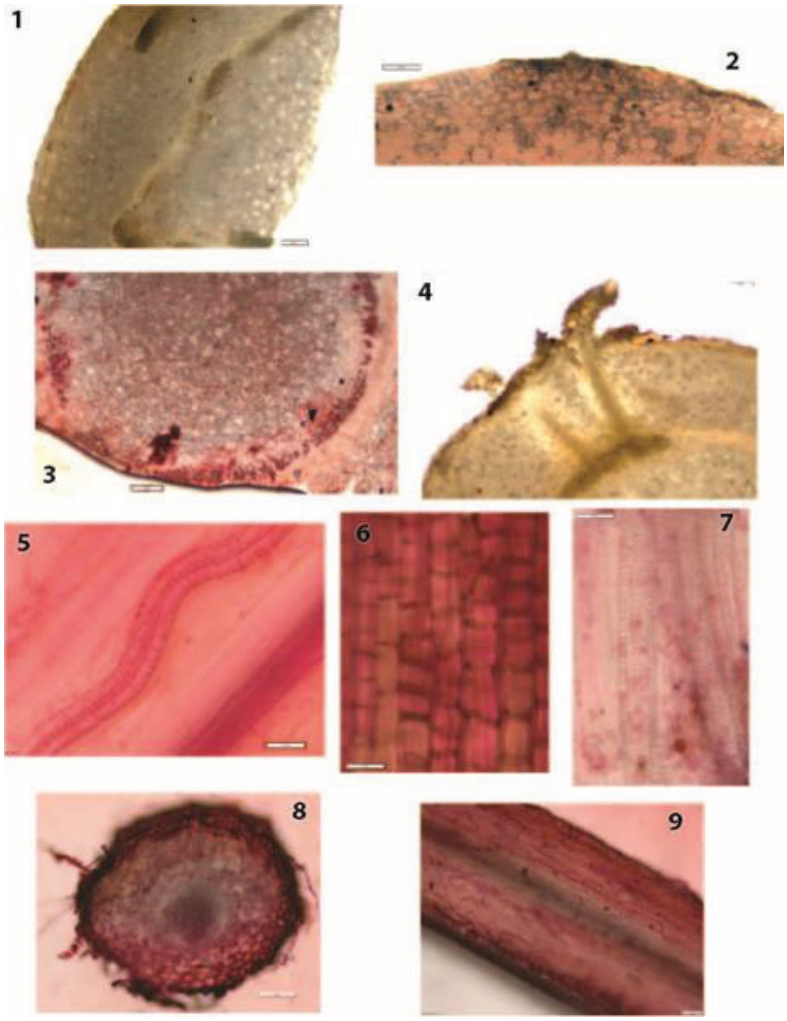


Figures. 1-4 - Transverse sections of rhizomes. 1 Partial section of the epidermis to pith 2. Close-up of lamellar collenchyma, 3. Central pith with starch and calcium oxalate crystals, bordering the pith are phloem with rays, sieve cells and companion cells, xylem vessels, fibers and parenchyma cells 4. Lateral roots emerging from the pericycle and protruding through the endodermis, cortex, and epidermis.

Figures 5-6 - Longitudinal cut of rhizomes: 5. Helical secondary xylem thickening, 6. Stained surface view of epidermal cells,

Figures 7-9 - Lateral root sections (stained): 7. Longitudinal cut of a root depicting helical secondary xylem thickening, 8. Transverse section of a lateral root 9. view of a lateral root showing epidermal, ground, and vascular tissues.

**Table 2. Measurements associated with rhizomes of Viola *sororia*. All measurements are in micrometers.**

| Cell types | Mean | Median | Standard deviation | Range |
|---|---|---|---|---|
| Collenchyma - length | 28.9 | 30 | 10.0 | 10 - 54.2 |
| Collenchyma - width | 16.7 | 15 | 6.0 | 10 - 29.2 |
| cortex parenchyma - length | 31.1 | 30 | 14.9 | 10 – 60 |
| cortex parenchyma - width | 21.9 | 20 | 9.6 | 10 - 50 |
| cortex parenchyma starch grains - length | 6.2 | 5 | 4.0 | 1 - 15 |
| cortex parenchyma starch grains - width | 5.5 | 5 | 3.2 | 1 - 10 |
| pith parenchyma - length | 23.7 | 20 | 7.7 | 10 - 40 |
| pith parenchyma - width | 24.3 | 20 | 10.1 | 10 - 60 |
| vessel elements (transverse view) - length | 7.9 | 19 | 2.6 | 5 - 10 |
| vessel elements (transverse view) – width | 7.9 | 10 | 2.6 | 5 - 10 |
| adventitious root parenchyma cells - length (longitudinal cut) | 182.9 | 200 | 29.6 | 150 - 250 |
| adventitious root parenchyma cells - length (longitudinal cut) | 52.9 | 50 | 11.8 | 50 - 100 |

**Flower parts**

**Peduncle**

Peduncles are circular to somewhat quadrangular in shape. Peduncles of cleistogamous flowers are shorter than those of chasmogamous flowers. The epidermis consists of a single layer of small, thin-walled, ovoid to rectangular cells that contain chloroplasts. Occasional trichomes are attached to the epidermal cells. Collenchyma, consisting of 1-2 layers of cells, is under the epidermis. Collenchyma cells range from 10 -30 µm in length (mean 15.1 µm) to 10-40 µm (mean 14 µm) in width (Table 3). Parenchymatous cortex cells are below collenchyma. Parenchyma cells range from 10 – 40 µm (mean 23.1 µm) in length and 10-40 µm (mean 22.6 µm) in width (Table 3). Intercellular spaces occur between most parenchyma cells. Parenchyma cells that border the collenchyma often contain a red pigment, possibly due to anthocyanins (Plate 3, Figs. 5. 9). Oil droplets occur on the surface of some parenchyma cells in fresh cut transverse sections which obscure cell details.

An endodermis surrounds the conductive tissue. Two collateral vascular bundles usually are in the median region of the peduncle associated with chasmogamous flowers (Plate 3, Fig. 8). The two bundles are directly opposite and form a circular/oval arrangement; prosenchymatous elements exist between the two vascular bundles. Xylem forms towards the inside and the phloem forms towards the outside. Spherical parenchyma cells, 3-4 layers thick, appear between the two vascular bundles. Some cleistogamous peduncles possess four vascular bundles in the median area that are situated in a circular arrangement. A pith consisting of spherical parenchyma cells is in the center (Plate 3, Fig. 5), Longitudinal sections of the xylem possess helical secondary thickening (Plate 3, Fig. 6).

**Flowers**

The chasmogamous flowers are zygomorphic and have five sepals and petals. Sepals are green, elongated, and ciliate along the margin (Plate 3, Fig. 1). The petals vary in color

depending on the plant, ranging from deep violet to lavender to almost white. Petals are bearded proximally and contain numerous straight hairs ranging from 250 – 1300 µm (mean 601 µm) in length and 100 µm in width (Table 3). Petals possess a thin epidermal layer on both surfaces. Veins approximately 100 µm in width are spaced 600 – 700 µm apart and form parallel rows consisting of three to four layers (Plate 3, Fig. 4). The external surface of the ovary and style are green. The ovary is superior and exhibits parietal placentation (Plate 3, Fig. 2). Ovules in cleistogamous flowers are anatropous, beige in color, oval, have a prominent calaza, and a micropyle pointed toward the base. Faint polyhedric sculpturing is evident on the surface (Plate 3, Fig. 2). The number of ovules observed in transverse sections of the ovary range from 8 – 16. Ovules range from 500 – 1350 µm (mean 783 µm) in length to 300 – 800 µm (mean 450 µm) in width. Seed capsules are oval to round, compressed at the apex, have a glabrous outer surface, and are green to brown in color. They form in the late spring and summer and contain three chambers. Immature seeds within the capsule range from 500 – 1350 µm (mean 783 µm) in length and 300 - 800 µm (mean 500 µm) in width. Pollen is syncolporate with three apertures, suboblate, and ranges from 40 – 42 µm in length (mean 40.5 µm) and 35-40 µm in width (mean 38.3 µm) in equatorial view; in polar view, grains are oval to subtriangular. Exine is 2 µm thick and has psilate-perforate ornamentation.

**Table 3. Measurements associated with flora parts and immature seeds of *Viola sororia*. All measurements are in micrometers.**

| Cell types | Mean | Median | Standard deviation | Range |
|---|---|---|---|---|
| **Chasmogamous peduncle basal section** | | | | |
| collenchyma - length | 15.1 | 10 | 5.6 | 10 – 30 |
| collenchyma - width | 14 | 10 | 5 | 10 – 20 |
| cortex parenchyma - length | 23.1 | 20 | 6.8 | 10 – 40 |
| cortex parenchyma - width | 22.6 | 20 | 8.5 | 10 - 40 |
| **Flower structures** | | | | |
| pollen - length | 40.5 | 40 | 1.0 | 40 - 42 |
| pollen - width | 38.3 | 39 | 2.4 | 35 - 40 |
| trichomes at base of petals - length | 601.4 | 600 | 270.5 | 250 – 1300 |
| trichomes at base of petals - width | 100 | 100 | 0 | 100 |
| ovules inside the ovary – length | 280 | 300 | 47.3 | 200 – 400 |
| ovules inside the ovary – width | 182.9 | 200 | 38.2 | 100 - 200 |
| **Immature seeds within a cleistogamous flower capsule** | | | | |
| length | 783 | 675 | 318.5 | 500 - 1350 |
| width | 500 | 450 | 187.9 | 300 - 800 |

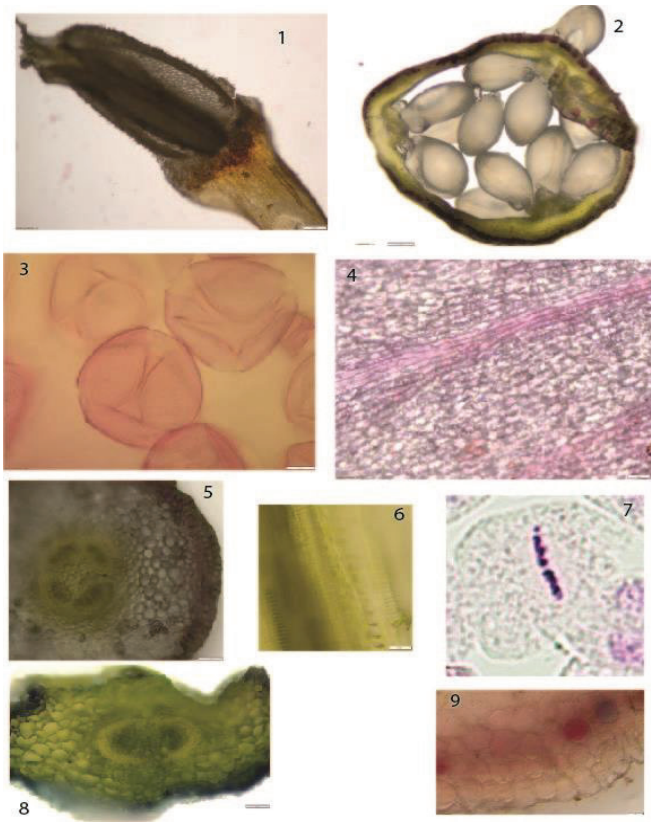


Plate 3. Figures. 1. Flower bud with trichomes along the outer edge of sepals, 2. Anatropous oval ovules with micropyles pointed toward the base. The ovules have a distinct elaiosome and raphe. 3. Syncolporate pollen, 4. A surface view of a petal showing epidermal cells and veins. The veins form parallel rows and are represented by darker bands of cells; 5. Transverse section of a chasmogamous peduncle transverse section depicting four central vascular bundles; 6. Longitudinal cut of a peduncle depicting vessels with helical and annular secondary wall thickening; 7. Root cell with chromosomes in metaphase. 8. Transverse section of a cleistogamous peduncle depicting two vascular bundles in the center. 9. Transverse section of a cleistogamous peduncle that depicts red pigment in parenchyma cells that border collenchyma cells.

## DISCUSSION

Anatomical sections have been used to delineate related sections, subsections, and species within Viola (Yousefi et al. 2012; Jura et al 2019; Dastagir et al 2023). Anatomical features also reveal ecological and evolutionary significances (Dastagir et al. 2023). The presence of a pith in root transverse sections and the number of vascular bundles in aerial stems as well as the layers of collenchyma, presence or absence of trichomes and lateral wings, crystal storage associated with petioles, and papillate epidermis on petals are established as important characters in distinguishing some species in Viola (Colombo et al. 2007; Bağci, et al. 2008; Yousefi et al. 2012)]. Many of the plant anatomical and morphological characters observed for V. sororia are like those found in other species of Viola: amphistomatic leaves, anisocytic stomata, one-celled trichomes, collateral vascular bundles, prosenchymatous elements existing between the two vascular bundles in peduncles, presence of collenchyma and parenchyma in petioles and peduncles, syncolporate pollen, and more. Metcalfe and Chalk (1950) mentioned that the pith is hollow in some herbaceous species which is apparent in some mid-sections of the petiole of *V. sororia*. *Viola sororia,* however, lacks aerial runners that occur in *V. odorata* and aerial stems that occur in *V. arvensis* and *V. kitaibeliana*. The peduncles and petioles of *V. sororia* are directly produced from the rhizome. The rhizome has secondary xylem and phloem, lateral roots emerging from the pericycle and calcium oxalate crystals like *V. hirta* and *V. odorata* described by Mereacre et al. (2014). Calcium oxalate crystals were not observed in lateral roots which is like *Viola* sect. *Sclerosium* described by Shahrestani et al. (2014). The leaf petiole possessing two lateral-adaxial wings and three vascular bundles occurs in species of *V. elatior*, *V. hirta*, *V. hymettia, V. odorata*, *V.*

kitaibeliana, and more. The peduncle, containing two collateral vascular bundles, is not documented; four collateral bundles are noted in V. alba subsp. alba (Yousefi et al. 2012), V. kizildaghensis (Dinç et al. 2007), V. stocksii (Shahrestani et al. 2014), and V. odorata (Yousefi et al 2012; Dastagir et al. 2023).

Oil droplets have not been reported previously from petioles and peduncles in Viola. Methyl salicylate (an oil of wintergreen), however, occurs in roots of V. arvensis and V. rafinesquei, which may serve as a protection from pathogens or herbivory (Hayden and Clough 1990). Dastagir et al. (2023) noted that oil in seeds of V. odorata is used as a diuretic, expectorant, for heart, in gout, spleen disorders, headaches, AIDS, and dizziness.

Most measurements conducted in this study are not documented in other published accounts. The stomata length and width had a greater range for petioles compared to stomata on leaf epidermal surfaces. Epidermal cells on the distal part of the petioles were significantly greater range in length (5 – 100 µm) compared to the range of epidermal cells observed in mid (5 – 50 µm) and basal (5 – 45 µm) sections of the petiole. The size of the stomata on the leaf blades are within the size range of V. kizildaghensis discussed by Dinç et al. (2007). Stomata size is smaller compared to those of V. ucriana and V. tineorum (Colombo et al. 2007) and V. odorata (Bağci et al. 2008) The stomata on the lower epidermis of V. sororia also are not as wide compared to V. yildirimlii (Bagci et al. 2008) and V. kizildaghensis (Dinç et al. 2007).

Additionally, the Flora of North America (2015) and Marcussen et al. (2022) states that the chromosome count is 2n=54 and not 2n=12 for V. sororia. The discrepancy could be from hybridization as well as intra- and interindividual variability. Slomka et al. (2014) noted that some evolutionary young species of *Viola* are karyologically unstable. Only chromosome counts were analyzed from root tips in this study. Marcussen et al. (2022) stated that there are limited numbers of chromosome counts for *Viola* and that two counts in the subg. *Neoandinium* show 2*n*=14. Marcussen et al. (2022) added that for subg. *Viola* x =6 was assumed for a long time because 2*n* = 12 was shared by diploid sections *Chamaemelanium* and sect. *Rubellium*. The reduction of x = 7 from x = 6 may be a synapomorphy for the most recent common ancestors but more counts from South American lineages are needed.

## ACKNOWLEDGMENTS

We wish to thank Dr. Mac Alford for assisting with questions regarding plant anatomical features and to Mr. Kevin England for helping us identify morphological features. Thanks are also given to Dr. Carol Hotton for describing pollen morphology.

## REFERENCES

Akarsu, F. 1989a. Batı Anadolu ' da Doğal Yayılış Gösteren *Viola* L.(Syn: subgen. *Nomimium* Ging.) Alt Cinsi Üzerinde Morfolojik ve Anatomik Araştırmalar I *Viola odorata* L. – Doğa Turkish Journal of Botany Dergisi 13: 522 – 529.

Bačeva, K., T. Stafilov, and V. Matevski. 2014. Bioaccumulation of heavy metals by endemic *Viola* species from the soil in the vicinity of the As-Sb-Tl mine "Allchar", Republic of Macedonia. *International Journal of Phytoremediation* 16(4), 347-365.

Bağci, Y., M. Dinç, and M. Ozturk. 2008. Morphological, anatomical, and ecological study of Turkish endemic *Viola yildirimlii* M. Dinç and Y. Bağci. *International Journal of Natural and Engineering Sciences* 2(3): 1-5.

Ballard, H. E. Jr., Sytama, K. J., and R. R. Kowal.

1999. Shrinking the violets: phylogenetic relationships of infrageneric groups. In *Viola* (Violaceae) based on internal transcribed spacer DNA sequences. *Systematic Bot*any 23:430-458.

Ballard, H. E. Jr, J. T. Kartesz, and M. Nishino 2023. A taxonomic treatment of the violets (Violaceae) of the northeastern United States and adjacent Canada. *The Journal of the Torrey Botanical Society*, 150(1), 3-266.

Bölöni, J., P. Ódor, R. Ádám, W. S. Keeton, and R. Aszalós. 2017. Quantity and dynamics of dead wood in managed and unmanaged dry-mesic oak forests in the Hungarian Carpathians. *Forest Ecology and Management* 399: 120-131.

Chandra, D., G. Kohli, K. Prasad, G. Bisht, V. D. Punetha, K. S. Khetwal, and H. K. Pandey. 2015. Phytochemical and ethnomedicinal uses of family Violaceae. *Current Research in Chemistry* 7: 44-52.

Chen, Y.S. and Q. E. Yang, 2009. Two new stoloniferous species of *Viola* (Violaceae) from China. *Botanical Journal of the Linnean Society* 159: 349-356.

Colombo, P., V. Spadaro and F. M. Raimondo. 2007. Morpho-anatomical analysis of *Viola tineorum* and *V. ucriana* (Violaceae) endemic to the mountains around Palermo (NW-Sicily). *Bocconea* 21: 233-247.

Dastagir, G., S. Bibi, N. U. Uza, R. W. Bussmann, I. Ahmad, and Samiuliah. 2023. Microscopic evaluation, ethnobotanical and phytochemical profiling of a traditional drug *Viola odorata* L. from Pakistan. Ethnobotany Research and Applications 25:4.

Dinç, M. 2009. Comparative morphological and palynological study on poorly known *Viola sandrasea* and its closest relative *V. kizildaghensis*. *Biologia* 64(1): 81-87.

Dinç, M., Y. Badci, and M. Öztűrk. 2007. Anatomical and ecological study on Turkish endemic *Viola kizildaghensis* M. Dinç and S. Yildirimli. *American-Russian Journal of Scientific Research* 2(1): 05-12.

Dinç, M., and S. Yıldırımlı. 2007. Anatomical and ecological study on Turkish endemic *Viola kizildaghensis*. *American-Eurasian Journal of Scientific Research* 2: 5–12

Eckstein, R. L., N. Hòlzel, and J. Danihelka. 2016. Biological flora of Central Europe: *Viola elatior*, *V. pumila* and *V. stagnina*. Plant Ecology Evolution and Systematics 8:45-66.

Flora of North America. 2015. Family list, FNA Vol. 6, www.eFloras.org.

Gil, H. Y., and S. C. Kim. 2016. *Viola woosanensis*, a recurrent spontaneous hybrid between *V. ulleungdoensis* and *V. chaerophylloides* (Violaceae) endemic to Ulleung Island, Korea. *Journal of Plant Research*129: 807-822.

Havran, J. C., K. J. Sytsma, and H. E. Ballard, Jr. 2009. Evolutionary relationships, interisland biogeography, and molecular evolution in the Hawaiian violets (*Viola*: Violaceae). *American Journal of Botany* 96(11), 2087-2099.

Hayden, W. J., and J. Clough. 1990. Methyl salicylate secretory cells in roots of *Viola arvensis* and *V. rafinesquii* (Violaceae). *Castanea* 55(1): 65-70.

Hekking, W. H. A. (1988). Violaceae Part I: Rinorea and Rinoreocarpus. *Flora Neotropica*, *46*, 1–207.

Kuta E., J. Bohdanowicz, A. Słomka, M. Pilarska, and H. Bothe. 2012. Floral structure and pollen morphology of two zinc violets (*Viola lutea* ssp. *calaminaria* and *V. lutea* ssp. *westfalica*) indicate their taxonomic affinity to *Viola lutea*. *Plant Systematics and Evolution*, 298: 445-455.

Jurca T.Ü., A. Pallag, E. Marian, M.A. Eugenia MA. 2019. The histo-anatomical investigation and the polyphenolic profile of antioxidant complex active ingredients from three *Viola* species. Farmer Journal 67:634-40.

Lust, J. 1986. The Herb Book,16th imprint. Bantam, Sun Valley, California.

Małobęcki, A., T. Marcussen, J. Bohdanowicz,

G. Migdałek, A. Słomka, and E. Kuta. 2016. Cleistogamy and phylogenetic position of *Viola uliginosa* (Violaceae) re-examined. *Botanical Journal of the Linnean Society* 182(1):180-194.

Marcussen, T., H. E. Ballard, J. Danihelka, A. R. Flores, M. V. Nicola, and J. M. Watson. 2022. A revised phylogenetic classification for *Viola* (Violaceae). *Plants* 11(17), 2224.

Marcussen, T., K. Blaxland, M.D. Windham, K. E. Haskins, and F. Armstrong. 2011. Establishing the phylogenetic origin, history, and age of the narrow endemic *Viola guadalupensis* (Violaceae). *American Journal of Botany* 98(12): 1978-1988.

Mehrvarz, S. S., M. Vafi, and T. Marcussen. 2013. Taxonomic and anatomical notes on *Viola* sect. *Viola* (Violaceae) in Iran. *Wulfenia* 20:73-79.

Mereacre, A., A. Toniuc, C. Toma. 2014. Histo-anatomical observations regarding *Viola* L. species in the Gârboavele Reserve (County of Galati). *Analele Stiintifice ale Universitatii" Al. I. Cuza" din Iasi*, 60(1), 13-24.

Metcalfe, C. R. and L. Chalk, 1950. Anatomy of the Dicotyledons I, Oxford University Press, Amen House, London.

Nikitin, V.P. 2007. Paleogene and Neogene strata in Northeastern Asia: paleo carpological background. *Russian Geology and Geophysics* 48:675-682.

Pilberg, C., M. V. Ricco, and M. A. Alvarez. 2016. Foliar anatomy of *Viola maculata* growing in Parque Nacional Los Alerces, Chubut, Patagonia, Argentina. *Revista Brasileira de Farmacognosia,* 26: 459-463.

Rubin, G., and D. J. Paolilo. 1978. Vascular and general anatomy of the rootstocks of three stemless *Viola* species. *Annuals of Botany* 42:981-988.

Shahrestani, M. M. S. S. Mehrvarz, T. Marcussen, and N. Yousefi. 2014. Taxonomy and comparative anatomical studies of *Viola* sect. Sclerosium (Violaceae) in Iran. *Acta Botanica Gallica* 161(4): 343-353.

Simpson, M. G. 2019. Plant Systematics, Third Edition, Academic Press, Elsevier, Amsterdam, 781 pgs.

Slomka, A., E. Wolny, and E. Kuta. *Viola tricolor* (Violaceae) is a karyologically unstable species. *Plant Biosystems* 148(4): 602-608.

Thiele, K. R., and S. M. Prober. 2006. *Viola silicestris*, a new species in *Viola* section *Erpetion* from Australia. *Telopea* 11(2): 99–104.

Tilley, D., J. Spencer, and M. Wolf. 2022. Seed production and propagation of northern bog violet (*Viola nephrophylla*) for Nokomis fritillary (*Speyeria nokomis*) butterfly habitat restoration. *Native Plants Journal* 23(1): 130-138.

Toiu, A. I. Oniga, M. Tămaş. 2010. Morphological and anatomical research on *Viola arvensis* Murray (Violaceae). Farmacia 58(5): 654-659.

Trusov, N. A. 2014. Aril morpho-anatomical structure and development of *Viola odorata* L. (Violaceae). *Modern Phytomorphology* 6:141-142.

Wahlert, G. A., T. Marcussen; J, de Paula-Souza, M. Feng, H. E. Ballard. 2014. A Phylogeny of the Violaceae (Malpighiales) inferred from plastid DNA sequences: Implications for Generic Diversity and Intrafamilial classification. *Systematic Botany*. 39 (1): 239- 252.

Yousefi, N., S. S. Mehrvarz, and T. Marcussen. 2012. Anatomical studies on selected species of *Viola* (Violaceae). *Nordic Journal of Botany*,30:461-469.

Youssef, S., and E. Véla 2019. *Viola pachyrrhiza*. *The IUCN Red List of Threatened Species. International Union for Conservation of Nature and Natural Resources*.

## Appendix 1. Plant anatomical studies conducted on species of *Viola*.

| | |
|---|---|
| *Viola alba* Bess. subsp. *alba* | Yousefi et al. 2012; Mehrvarz 2013 |
| *Viola arvensis* Murray | Hayde and Clough 1990; Yousefi et al. 2012; Mereacre et al. 2014 |
| *Viola behboudiana* Rech.f. and Esfand. | Shahrestani et al. 2014 |
| *Viola caspia* (Rupr.) Freyn | Yousefi et al. 2012, Mehrvarz 2013 |
| *Viola cinerea* Boiss. | Shahrestani et al. 2014 |
| *Viola cucullata* Aiton | Rubin and Paolillo 1978 |
| *Viola cunninghamii* Hook. f. | Metcalfe and Chalk 1950 |
| *Viola elatior* Fr. | Mereacre et al. 2014 |
| *Viola hirta* L. | Mereacre et al. 2014 |
| *Viola kauaiensis* A. Gray | Metcalfe and Chalk 1950 |
| *Viola kitaibeliana* Schult. | Yousefi et al. 2012; Mereacre et al. 2014 |
| *Viola kizildaghensis* Dinç and Yıld. | Dinç 2009; Dinç et al. 2007; Dinç and Yıldırımlı 2007 |
| *Viola luciae* Skottsbert | Metcalfe and Chalk 1950 |
| *Viola lutea* ssp. *calaminaria* (Gingins) Nauenb. | Kuta et al. 2012 |
| *Viola lutea* ssp. *westfalica* | Kuta et al. 2012 |
| *Viola maculata* Cav. | Pilberg et al. 2016 |
| *Viola mauiensis* Mann. | Metcalfe and Chalk 1950 |
| *Viola muscoides* Philippi | Metcalfe and Chalk 1950 |
| *Viola occulta* Lehm. | Yousefi et al. 2012 |
| *Viola odorata* L. | Yousefi et al. 2012; Rubin and Paolillo 1978, Bağci 2008; Mereacre et al. 2014, Mehrvarz 2013; Tpycob 2014; Dastagir et al. 2023 |
| *Viola rafinesquei* Greene | Hayden and Clough 1990 |
| *Viola reichenbachiana* Jord. ex Bor. | Yousefi et al. 2012; Mehrvarz 2013 |
| *Viola robusta* Hillebr. | Skottsberg 1940, Metcalfe and Chalk 1950 |
| *Viola rotundifolia* Michx. | Rubin and Paolillo 1978 |
| *Viola rupestris* F. W. Schmidt | Yousefi et al. 2012; Mehrvarz 2013 |
| *Viola sandrasea* Melch. | Dinç 2009 |
| *Viola sintenisii* W. Becker | Yousefi et al. 2012; Mehrvarz 2013 |
| *Viola somchetica* C. Koch | Yousefi et al. 2012 |
| *Viola spathulata* Willd. | Yousefi et al. 2012 |
| *Viola stocksii* Boiss. | Metcalfe and Chalk 1950; Shahrestani et al. 2014 |
| *Viola tineorum* Erben & Raimondo | Colombo et al. 2007 |
| *Viola tricolor* L. | Yousefi et al. 2012 |
| *Viola tridentata* Menz. | Metcalfe and Chalk, 1950 |
| *Viola ucriana* Erben & Raimondo | Colombo et al. 2007 |
| *Viola yildirimlii* Dinç and Bağcı | Bağci et al. 2008 |

# 89th Annual MAS Meeting

## MISSISSIPPI GULCOAST CONVENTION CENTER
## BILOXI, MS

## MARCH 20 - 21, 2025

https://msacad.org/

# CALL FOR ABSTRACTS

Due November 15, 2024

https://event.fourwaves.com/716f4aac-7f43-4779-b028-54525ad32843/pages

**Make sure to Register to receive Complimentary Membership**

**Can also be done on-line at : http://msacad.org/**

**Membership/Registration opens September 1, 2024**

**Renew and join early to avoid late fees**

# Author Guidelines

**Editorial Policy.** The Editorial Board publishes articles on all aspects of science that are of general interest to the scientific community. General articles include short reviews of general interest, reports of recent advances in a particular area of science, current events of interest to researchers and science educators, etc. Research papers of sufficiently broad scope to be of interest to most Academy members are also considered. Articles of particular interest in Mississippi are especially encouraged.

Research papers are reports of original research. Submission of a manuscript implies that the paper has not been published and is currently at the time of submission being considered for publication elsewhere. At least one of the authors must be a member of the Academy, and all authors are encouraged to join.

**Manuscripts.** Submit the manuscript electronically to the Mississippi Academy of Sciences under your profile in the member location of the website. Please also provide a cover letter to the Editor of the Journal. The cover letter should authorize publication: give the full names, contact information, for all authors; and indicate to whom the proofs and correspondence should be sent. Please notify the Editor on any changes prior to publication.

**Manuscripts must adhere to the following format:**

- One inch margins on 8.5 x 11 inch paper;
- Text should be left-justified using twelve point type;
- Double spaced throughout, including the title and abstract;
- Arabic numerals should be used in preference to words when the number designates anything that can be counted or measured (7 samples, 43 species) with 2 exceptions:
- To begin a sentence (Twenty-one species were found in…)
- When 2 numeric expressions are adjacent in a sentence. The number easiest to express in words should be spelled out and the other left in numeric form (The sections were divided into eight 4-acre plots.).
- Measurements and physical symbols or units shall follow the International System of Units (SI *Le Système international d'unités*) with metric units stated first, optionally followed by United States units in parentheses. *E.g.*: xx grams (xx ounces); and
- Avoid personal pronouns.

---

**Format**

**Abstract.** In 250 or fewer words summarize any new methods or procedures critical to the results of the study and state the results and conclusions.

**Introduction.** Describe the knowledge and literature that gave rise to the question examined by, or the hypothesis posed for the research.

**Materials and methods.** This section should describe the research design, the methods and materials used in the research (subjects, their selection, equipment, laboratory or field procedures), and how the findings were analyzed.

**Results.** The text of the results should be a descriptive narrative of the main findings, of the reported study. This section should not list tabulated data in text form. Reference to tables and figures included in this section should be made parenthetically in the text.

**Discussion.** In this section compare and contrast the data collected in the study with that previously reported in the literature. Unless there are specific reasons to combine the two, as explained by the author in the letter of transmittal, Results and Discussion should be two separate sections.

**Acknowledgments.** Colleagues and/or sources of financial support to whom thanks are due for assistance rendered in completion of the research or preparation of the manuscript should be recognized in this section rather than in the body of the text.

---

**Literature cited.** List references alphabetically. Cite references in the text by author and year of publication (e.g., Smith, 1975; Black and Benghuzzi, 2011; Smith et al., 2010; Smith, 2011a, 2011b). The following examples illustrate the style to be used in the literature list.

Black DA, Lindley S, Tucci M, Lawyer T, Benghuzzi H. A new model for the repair of the Achilles tendon in the rat. J Invest Surg. 2011; 24(5): 217-221.

Pearson HA, Sahukhal GS, **Elasri** MO, Urban MW. Phage-bacterium war on polymeric surfaces: can surface-anchored bacteriophages eliminate microbial infections? Biomacromolecules. 2013 May 13;14(5):1257-61.

Bold, H.C., C.J. Alexopoulos, and T. Delevoryas. 1980. Morpholgy of plants and fungi, 4th ed. Harper and Row, New York. 819 pp

Web-page

- name of author(s) -if known
- title of the work - in quotes, if known
- title of the Web page - in italics, if applicable
- date of last revision
- URL
- Date accessed

**Example:**
Ackermann, Ernest. "Writing Your Own Web Pages." *Creating Web Pages.* 23 Oct. 1996. http://people.umw.edu/~ernie/writeweb/writeweb.html 10 Feb. 1997.

**File available by anonymous FTP**

- name of author(s) -if known
- title of the work - in quotes, if known
- date of last revision
- URL
- Date accessed

**Example:**
American Civil Liberties Union. "Briefing paper Number 5, Drug Testing in the Work Place." 19 Nov. 1992. ftp://ftp.eff.org/pub/Privacy/Medical/aclu_drug_testing_workplace.faq 13 Feb. 1997.

---

**Please Tables and Figures at the end of the manuscript submitted.**

**Tables.** Tables must be typed double spaced, one table to a page, numbered consecutively, and placed at the end of the manuscript. Since tables must be individually typeset, consolidation of data into the smallest number of tables is encouraged. A horizontal double underline should be made beneath the title of the table, and single underlines should be made the width of the table below the column headings and at the bottom of the table. Do not use vertical lines, and do not place horizontal lines in the interior of the table. Use footnotes, to clarify possible questions within the table, should be noted by asterisks, daggers, or other symbols to avoid confusion with numerical data. Tables should be referred to parenthetically in the text, for example (Table 1).

**Figures and illustrations.** Figures may be photographs, computer -generated drawings, or graphs and should be placed at the end of the manuscript and referenced in the appropriate place.. All illustrations are referred to as “Figures” and must be numbered consecutively. Illustrations other than those generated by the author(s) must include permission for use and credit to the originator. Each figure must have a complete legend that is typed, double-spaced, on a separate sheet which precedes the figures in the manuscript. Figures should be referred to parenthetically in the text, for example (Fig. 1).

---

**Footnotes**. Text footnotes **should not be used**

**Submission Preparation Checklist**

As part of the submission process, authors are required to check off their submission's compliance with all of the following items, and submissions may be returned to authors that do not adhere to these guidelines.

1. The submission has not been previously published, nor is it before another journal for consideration (or an explanation has been provided in Comments to the Editor).
2. The text adheres to the stylistic and bibliographic requirements outlined in the Author Guidelines.
3. I acknowledge that if my manuscript is peer-reviewed and accepted for publication, there will be a paper charge fee of $50/page for **non-Academy members**.
4. The manuscript file is in Microsoft Word format.

**Copyright Notice**

Authors who publish with this journal agree to the following terms:

1. Authors retain copyright and grant the journal right of first publication
2. Authors are able to enter into separate, additional contractual arrangements for the non-exclusive distribution of the journal's published version of the work (e.g., post it to an institutional repository or publish it in a book), with an acknowledgement of its initial publication in this journal.
3. Authors are permitted and encouraged to post their work online (e.g., in institutional repositories or on their website) prior to and during the submission process, as it can lead to productive exchanges, as well as earlier and greater citation of published

**Mississippi Academy of Sciences**
Post Office Box 55907
Jackson, MS 39296-5907

Nonprofit Organization
U. S. Postage
**PAID**
Jackson, MS
39216
Permit No. 305

**Coden: JMSS-A** **ISSN 0076-9436** **Volume 69, Numbers 2-3, April/July 2024**